Spring 1992

Characterization of a Novel Prostate Tumor-Associated Antigen

Grayson B. Lipford
Old Dominion University

CHARACTERIZATION OF A NOVEL PROSTATE TUMOR ASSOCIATED ANTIGEN

by

Grayson B. Lipford

B.S., May, 1984, Virginia Commonwealth University

A Dissertation Submitted to the Faculties of

Eastern Virginia Medical School

and Old Dominion University

in Partial Fulfillment of the Requirements for the Degree of

D O C T O R O F P H I L O S O P H Y

BIOMEDICAL SCIENCES

CANCER BIOLOGY/IMMUNOLOGY

EASTERN VIRGINIA MEDICAL SCHOOL

and

OLD DOMINION UNIVERSITY

April, 1992

Approved by:

George L. Wright, Jr., Ph.D. Kenneth D. Somers, Ph.D.

Gary F. Clark, Ph.D. Robert E. Ratzlaff, Ph.D.

Abstract

CHARACTERIZATION OF A NOVEL PROSTATE TUMOR ASSOCIATED TUMOR ANTIGEN

Grayson B. Lipford

Eastern Virginia Medical School

and

Old Dominion University

April, 1992

The murine monoclonal antibodies (MAb) TURP-27 and HNK-1 have been shown to detect antigens that are heavily expressed by benign prostatic hyperplasia (BPH) and carcinoma of the prostate (CaP). Western blot analysis of prostate extracts, showed that MAb TURP-27 and MAb HNK-1 bound glycoproteins of 180,140 120, 100, 90 and 69 kDa. Studies have shown that the HNK-1 carbohydrate epitope may be involved in cell adhesion and that it is a component of several characterized adhesion proteins. TURP-27 was found to bind at least three of these adhesion proteins: neural cell adhesion molecules (N-CAM), myelin-associated glycoprotein (MAG) and a second myelin glycoprotein, P_0. Western blot analysis of prostate extracts showed that an anti-N-CAM serum bound the 180 and 140 kDa proteins. On the basis of reciprocal blocking and chemical tests, it was determined that the TURP-27 and HNK-1 epitopes are not identical. These data imply that the TURP-27 epitope may be

a variant of the HNK-1 epitope or that the two epitopes are closely linked, and that the TURP-27 and HNK-1 epitopes on prostate cells are positioned on N-CAM like proteins.

DEDICATION

This work is dedicated with love and appreciation to my parents, who have always supported and stood beside me during the good and bad times.

ACKNOWLEDGEMENTS

I would like to thank and acknowledge Dr. George L. Wright, Jr. for his constant support, guidance and patience throughout my tenure as a graduate student. His professional and exemplary scientific conduct will always serve as a constant model.

I would also like to acknowledge Dr. K.D. Somers for keeping academic idealism at the heart of my training as a young scientist. His undying commitment to constructive criticism not only taught me how to evaluate myself but science in general. I would like to thank Dr. Gary Clark for endless discussions of my work and the possible avenues of study open to me.

I would also like to acknowledge all the teachers and professors who have shaped and influenced me throughout my educational experience. They are not a part of my final educational achievement but they are always in my thoughts.

Lastly, I would like to acknowledge my grandfather, Mashel Wilson, who at an early age instilled in me a sense of curiosity. This constant desire to know has made me who I am today.

TABLE OF CONTENTS

LIST OF TABLES

LIST OF FIGURES

Chapter I

Introduction

Review of Literature

Prostatic disease represents a major health-care problem in the United States. The prevalence of prostatic tumors is over 0.5 million diagnosed per year and consists of 400,000 cases of BPH and 120,000 cases of CaP (1). Surgery for BPH is the most common procedure performed on males and represents the second leading cost of Medicare reimbursements, exceeding one billion dollars per year (2). CaP is the most commonly diagnosed cancer in males and it accounted for an estimated 30,000 deaths in 1990, the second leading cause of cancer deaths in males surpassed only by lung cancer (3). Of all cancers in man, the incidence of clinical prostate cancer increases most rapidly with age (4). Because of the upward shift in the age distribution of the U.S. population, the number of new prostate carcinoma cases and the resultant deaths per year will continue to increase (5). Although prostate cancer is perceived as a cancer of the aged, one fifth of the diagnosed cancers are in men less than 65 and the average years of life lost is nine (6).

Based on autopsy studies, it is thought that 11 million U.S. males over the age 45 have histologically detectable

prostate cancer. However, the majority of these occult cancers do not manifest clinically and/or contribute to mortality in the lifetime of the host (7). Japanese men have the same prevalence of occult prostate cancer at autopsy as U.S. males. In a comparison of the two populations, there is a 15 to 20 fold higher prevalence in the age matched incidence of clinically manifested prostate cancer within the U.S. population. Moreover, when Japanese males immigrate to the U.S., their age adjusted incidence of clinical cancer increases although the prevalence of histological lesions remains the same. It is suggested that histological lesions found at autopsy are different biologically from clinical prostate cancer and that environmental factors enhance progression. Based on mathematical models it can be concluded that both histological and clinical cancers require multiple malignant events, but the progression from the latent to the aggressive phenotype (i.e. acquisition of the ability to invade, metastasize and grow in the absence of androgen) requires additional hits (7). The significance of this hypothesis should be stressed. With our present understanding of the natural history of prostate cancer it is not possible to predict which histological cancers will become clinically manifest. With changing demographics and the increased use of diagnostic tools, such as, transrectal ultrasound, needle biopsy and seroassays, like serum-PSA (prostate specific antigen), more lesions will be detected

(8). Because only 1 in 3-4 cases would be lethal if left untreated, gains through early detection could be offset by increased mortality and morbidity due to over zealous intervention as a consequence of incomplete differential diagnosis of latent versus lethal tumors (9). Therefore, an understanding and identification of morphological and phenotypic changes identifying the aggressive potential of prostate tumors is essential.

Several inquiries into phenotypic variation within the normal prostatic epithelium have focused on the presence of so-called neuroendocrine (NE) cells, also known as APUD (amine precursor uptake and decarboxylation) cells (10,11,12). Feyrter describe a system of clear cells dispersed in various organs and proposed that these cells constitute a diffuse endocrine organ with some cells being paracrine in nature (13). Pearse elaborated on the concept by further describing these cells as producing poly-peptide hormones and being of neuroectodermal origin (14). Organs containing these cells are pituitary, pancreas, adrenal, gastrointestine, lung, skin and, more recently reported, prostate and bladder (10). These cells can be distinguished with either histological stains which identify argentaffin or argyrophil cells, or immunohistochemically by staining for a variety of markers: neuron specific enolase, serotonin and chromogranin A, to name a few (10).

Within the prostate, NE cells are located in the epithelium of the acini and the ducts of all the different

parts of the gland, as well as in the urothelium of the prostatic part of the mucosa of the urethra (10,12). They are few (perhaps 1 in 50-100) and scattered singly with a patchy distribution in the columnar epithelium. None are located in the fibromuscular stroma. An observed difference between normal prostate and hyperplastic epithelium is an increase in the number of NE cells within the hyperplastic nodules (10). Similar relative increases in NE cell representation has also been noted in bronchopulmonary dysplasia of the lung (15).

Abrahamsson studied the incidence of NE manifestation during prostate tumor progression by means of repeated biopsies at intervals of a few years (16). Of the 25 cases studied, most underwent marked tumor progression, with the number of NE cells concomitantly increased in CaP relative to BPH samples. They concluded unequivocally that the more anaplastic the prostatic carcinoma the more numerous are the NE cells. DiSant'Agnese and DeMesyJensen support these observations and stress that these NE cells are not merely normal NE cells trapped within the tumor but are themselves malignant (11). They base this conclusion on the presence of NE cells with aberrant nuclei, prominent nucleoli, focal absence of the basal lamina and sheer quantity of NE cells present within CaP. The most intriguing observation is that NE cells occur in metastatic prostatic adenocarcinomas, tumors presumably of clonal origin.

A case report of a prostatic NE carcinoid tumor, demonstrated co-localization of PAP and PSA to cells expressing NE markers (17). Since PAP and certainly PSA are common markers restricted to prostatic epithelium, this implies that NE cells differentiate from a totipotential prostatic stem cell. This scenario would be similar to the hypothesis proposed for NE cell differentiation within lung and gastroenteropancreatic tissues (18). Multidirectional differentiation in malignant tumors is a common observation and neuroendocrine differentiation is common in carcinomas arising in organs that normally contain neuroendocrine cells, including the prostate (19).

Abrahamsson et.al. conclude that increasing NE differentiation in tumors seems to be a sign of decreasing maturity of the tumor cells and observed that prostatic carcinomas containing numerous NE cells are often aggressive neoplasias (16). Patients given hormone treatment (i.e. testosterone abatement) later presented with recurrent disease with high relative NE cell representation. A link between androgen independence and NE cell representation in the tumor was implied. A recent case study has indicated that two adenocarcinomas of the prostate with few NE cells recurred as NE carcinomas after hormonal therapy (20). The response and recurrence kinetics of hormonally treated prostatic carcinoma suggest that a subpopulation of cells exist which are androgen insensitive and of aggressive potential.

Prostate NE cells express serotonin, bombesin/gastrin releasing peptide and calcitonin, factors capable of autocrine and paracrine growth stimulation (11). The elaboration of these growth factors could replace the need for androgens within prostate tumors. The evidence suggests, that mature prostatic epithelium and cells expressing NE features are derived from the same progenitor stem cell and that dedifferentiation of the prostate to a less mature state appears to enhance the expression of NE markers. These changes might be a sign of androgen independence and more aggressive behavior. An understanding of NE-associated markers expressed during prostatic disease progression may therefore enhance the differential diagnosis of a tumor's aggressive potential.

A survey of cell surface markers common to NE cells reveals that the monoclonal antibody (MAb) HNK-1 (21) may be directed against a differentiation antigen associated with neuroectodermal cells. Immunohistochemical screening of normal and tumor tissues demonstrated that the HNK-1 antigen was expressed perhaps as an oncofetal antigen (22,23). MAb HNK-1 was reactive with tumors of the central and peripheral nervous system as well as tumors of neural crest origins including neuroblastoma, phaeochromo-cytomas and carcinoid tumors. It was also determined that MAb HNK-1 reacts with a marker on NE cells of endodermal origin (23). These included select cells within both adult and fetal gastrointestinal tract, pancreas and lung, and cells restricted to cortical

areas of fetal kidney. In an examination of fetal kidney, MAb HNK-1 reactivity was found to be developmentally regulated. At 10 weeks of gestation very few kidney cells are reactive with HNK-1 while an increasing proportion of kidney cortical tubules begin to react in the older fetus, approaching 50% of the cells at 25-30 weeks. Reactivity is progressively lost with the aging fetus and completely lost by adulthood. Thus in kidney, the HNK-1 antigen does behave as an oncofetal antigen, being expressed on some nephroblastomas and at precise stages of maturation on fetal tubules.

Our laboratory demonstrated that the HNK-1 antigen is a marker for prostate epithelial cells (24). Immunohistochemical staining of formalin-fixed normal prostate tissue revealed HNK-1 reactivity limited to scattered cells within the prostatic glandular epithelium, reminiscent of reported prostate NE cell staining patterns determined by NE peptide markers (10,11,12). More importantly, HNK-1 reacted extensively with the epithelial cells of BPH and CaP and within these tumors a very high percentage of the epithelial cells were stained. This is in contrast to the relatively low number of NE cells detected by other NE markers within prostate tumors. Therefore, HNK-1, a marker for neural crest tumors and endodermally derived NE tumors, is also reactive with an antigen widely expressed by prostate tumors but identifies many more cells than antibodies against NE peptide markers.

Concurrently, while evaluating other MAbs to prostate tumor-associated markers, a MAb, TURP-27, showed remarkable similarity to MAb HNK-1 in its reactivity to BPH and CaP (25). However, MAb TURP-27 has been found to be more restricted than HNK-1 in the number of scattered cells stained within normal prostate glands. Outside the prostate, MAb Turp-27 stains a population of large granular lymphocytes (LGL), chief cells of the stomach, adrenal medulla, and selected cells of the central and peripheral nervous system (26). Although these tissues are also reactive to MAb HNK-1, MAb TURP-27 reactivity is weaker and more limited in the number and types of cells stained. Furthermore, MAb TURP-27 is not reactive with normal pancreatic islet cells or any neuroendocrine derived malignancies tested thus far, whereas, MAb HNK-1 strongly binds these tissues (23). These data, as well as data described in this thesis, suggest that a similar but incomplete overlap in the immunohistochemical staining pattern exists between MAb HNK-1 and MAb TURP-27 and that the HNK-1 and TURP-27 epitopes may be a part of the same or very similar antigens within prostate.

Subsequent investigations have defined the antigenic determinant recognized by HNK-1 to be a carbohydrate which is present on at least two glycolipids and a variety of glycoproteins. The glycolipids, isolated from peripheral nerve, were characterized as sulfate-3-glucuronyl paragloboside and sulfate-3-glucuronyl neolactohexaosyl

ceramide within which the sulfate-3-glucuronyl moiety was essential for antibody binding (27,28,29). HNK-1 positive glycoproteins are cell adhesion proteins and include neural cell adhesion molecule (N-CAM), myelin-associated glycoprotein (MAG), cytotactin (tenascin), a neuroectoderm secreted fibronectin, brain chondroitin sulfate proteoglycans and others (30,31,32). The HNK-1 antigenic determinant, present on these glycoproteins, has not been fully characterized, although it is most likely a carbohydrate moiety.

Functional studies using MAb HNK-1 or its Fab fragments as blocking agents have directly implicated the HNK-1 epitope in cellular adhesion events (33,34). Evidence has been presented to show that the tetrasaccharide isolated from HNK-1 positive glycolipid interferes not only with cell-cell but also cell-substrate interactions (35). It also has been suggested that the differential expression of the HNK-1 epitope may modulate the functional character of its carrier proteins by enhancing or dampening adhesion (36).

The common denominator for all characterized HNK-1 carbohydrate carrying proteins is that they are involved in cell adhesion, and therefore, may be responsible for such processes as tissue morphogenesis, cell migration and cellular differentiation (37,30). Since TURP-27 shares similar immunohistochemical and immunoblotting characteristics with HNK-1, it is quite possible that the TURP-27 antigen, like HNK-1, is also related to adhesion

proteins. The demonstration that the HNK-1 epitope is involved in cell adhesion, primarily in neural tissues, may be significant with regard to carcinoma of the prostate. Villers et. al., in an examination of 78 stage B prostate carcinomas involving capsule penetration, concluded that penetration and spread outside the capsule depended almost entirely on the ability of the cancer to invade and travel along perineural spaces (38).

In summary, prostate cancer is a growing health care problem. The key to having an impact on this problem will be early diagnosis and defining those tumors that are most aggressive and therefore potentially lethal. NE cell involvement within prostate tumors has recently been suggested to be a sign of decreasing cell maturity, androgen independence and aggressive potential. The MAb HNK-1, which recognizes CAMs of presumed neural crest origin and tumors of NE origin, reacts with an antigen commonly expressed by prostate tumors. The MAb TURP-27, developed against prostatic tumors, shows tissue reactivity similar to HNK-1. However, TURP-27 is more restricted in its non-prostate tissue cross-reactivity and, therefore, may be more useful clinically. Preliminary data suggested a close relationship between the TURP-27 and HNK-1 epitopes. This thesis intends to examine the chemical nature of the TURP-27 epitope and its relationship to the HNK-1 epitope. CAMs play a key role in pattern formation during embryogenesis and histogenesis. Given the association of HNK-1 with neuroectoderm derived

adhesion proteins it would be of interest to determine if TURP-27 (a more restrictive prostate-associated antigen) is associated with these proteins. It is possible that these epitopes mark unknown adhesion proteins and/or NE differentiation markers restricted to the prostate which may be informative in determining the aggressive tumor phenotype. A better understanding of the TURP-27 and HNK-1 antigens could possibly facilitate a broader understanding of prostate cell differentiation, the natural history of prostatic neoplasia and the events important to prostate carcinogenesis and possibly organogenesis.

Chapter II

Materials and Methods

General Procedures

Antibodies

The production and tissue specificity of MAb TURP-27 (IgG_3) has been described previously (25). For this study, TURP-27 hybridoma culture supernatant or TURP-27 purified from ascites using the Affi-Gel Protein A MAPS II system (Bio-RAD, Richmond, CA) was used. The mouse-mouse hybridoma HNK-1 was purchased from American Type Culture Collection (ATCC, Rockville, MD). The MAb HNK-1 was also used as culture supernatant or purified from ascites using the Anti-Mouse IgM Affinity Isolation System (Hyclone, Logan, Utah). Polyclonal anti-N-CAM serum was a gift from Dr. Gerald Edelman (The Rockefeller University, New York, NY). The MAb B11F7 (39), generated against human central nervous system MAG, was a gift from Dr. Richard Quarles (NINCDS, National Institutes of Health, Bethesda, MD). The MAb UJ-13 was a gift from Cytogen Corporation. Murine isotyped matched control antibodies were purchased from Organon Teknika-Cappel (Malvern, PA). For some assays background or non-specific binding was assessed using sodium phosphate

buffered saline (PBS, 136 mM NaCl:2.7 mM KCl:8 mM Na_2HPO_4:0.9 mM $CaCl_2$:0.5 mM $MgCl_2$, pH 7.40) alone and/or supernatant from $P_3x63/Ag8$ (IgG_1K myeloma) as a negative control.

Tissue

Some primary prostate tumors as well as normal tissues were obtained at surgery from Sentara Norfolk General Hospital, (Norfolk, VA) while other primary, metastatic, and normal tissues were obtained at autopsy from the Cooperative Human Tissue Network, University of Alabama at Birmingham and the National Disease Research Interchange, Philadelphia, PA. Normal prostate tissues were obtained at autopsy from young males ages 19 to 26 from the above sources. Nude mouse xenografts were obtained from Centocor (Malvern, PA) which were produced by subcutaneous injection of the small cell lung carcinoma cell lines SW-105, OH-1 or GLC. Human semen was obtained from a random population of healthy males attending the infertility clinic of the Jones Institute for Reproductive Medicine, EVMS, Norfolk, VA. A pooled sample was centrifuged at 5,000 x g for 10 min, the supernatant was harvested, and is hereafter referred to as seminal plasma.

Membrane Preparation

Crude membrane preparations were prepared from autopsy or surgical specimens of human prostate or other tissues as previously described (25). Briefly, finely minced tissue was placed in 10 ml of 1.0 mM $NaHCO_3$ buffer containing 200 µl of a 50 x protease inhibitor cocktail (antipain 3.4 mg, pepstatin 10.0 mg, EDTA 0.372 g dissolved in 20 ml H_2O) for 20 min at 4°C. The tissue was then homogenized for five 15 s bursts at a setting #6 on a Polytron (Polytron, Brinkman Instruments, Westbury, NY) and dounced 10-20 times in a 15 ml Wheaton glass homogenizer. The homogenate was centrifuged at 2,000 x g for 5 min, and the supernatant was further centrifuged for 2 hr at 138,000 x g at 4°C. The resulting pellet was then resuspended in a minimum volume of PBS and stored at -70°C until use. Protein concentrations were determined using the BCA Protein Assay (Pierce, Rockford, IL). Purified N-CAM and MAG were a generous gift from Drs. Melitta Schachner and Brigitte Schmitz (University of Heidelberg, FRG). Myelin extracts were a gift from Dr. Steven Snyder (Veterans Medical Center, Memphis, TN).

Radiolabeling

Rabbit anti-mouse IgG (Jackson Immunoresearch Labs), MAb TURP-27 or MAb HNK-1 were labeled with ^{125}I sodium iodine (17 Ci/mg) using the chloramine-T method (40). Briefly, in a glass tube 10 µl of ^{125}I (approximately 250 µCi) was neutralized with 10 µl 0.01 N HCl. To this solution was

added 20 μl PBS and 122.5 μg rabbit anti-mouse IgG or 100 μg MAb in 50 μl PBS. The reaction was initiated with 21.6 μl of chloramine-T at 4 mg/ml prepared fresh and kept in the dark. The mixture was allowed to incubate at room temperature for 1 min with very gentle agitation. At this point sodium metabisulfite (90 μl) at 2.4 mg/ml was added to the mixture and incubated for 10 s. The reaction was quenched with 180 μl sodium iodide at 10 mg/ml. When monitored the efficiency of label incorporation was 59.7 +/- 1.7% with a specific activity of 1.13 +/- 0.1 μCi/μg protein (n=4), which is in good agreement with previous reports (40, 41).

The technique for separating protein bound from free ^{125}I by membrane ultrafiltration has been previously reported by Lipford et al. (42). Briefly, Ultrafree-MC filter units with a low binding PLGC membrane, nominal molecular weight limit 10,000, were used. These units are essentially a septum-capped 1.5 ml polypropylene conical microcentrifuge tube into which is inserted a 400 μl chamber with the membrane forming its bottom. The unit was prewashed by placing 400 μl of a solution containing 1.0% bovine serum albumin (BSA) and 1.0% sucrose in the upper chamber and spinning at 6,400 rpm (2,000 x g) for 20 min in a Millipore Personal Centrifuge. Both the filtrate and concentrate were removed. The iodination reaction mixture was transferred from the reaction vessel to the upper chamber of the filter unit and the tube centrifuged under the same conditions as

described above. The upper chamber was then transferred to a fresh microcentrifuge tube and the volume of the filtrate was determined. An aliquot of PBS equal to the filtrate volume was added to the concentrate to initiate the wash steps. Under these conditions between 240-260 µl of solution can be expected to move through to the filtrate. This procedure was repeated twice. After the final wash, the concentrate was measured for retained volume and transferred to a storage tube. Total activity as well as trichloroacetic acid (TCA) precipitable activity of the final concentrate were assayed in a gamma counter.

Electrophoresis

SDS-PAGE

Electrophoresis was carried out in polyacrylamide gels under reducing conditions according to the method of Laemmli (43). The gel apparatus was of the 15 x 17 cm or 7 x 9 cm minigel formats of Hoefer or Bio-Rad, respectively (Hoefer Scientific Instruments, San Francisco, CA; Bio-Rad, Richmond, CA). Gels were single percentage, i.e. 10 or 12.5%, or gradients ranging from 5-15% polyacrylamide. The quantity of protein loaded per lane varied depending on the complexity of the mixture. Purified proteins were of 1-5 µg while crude membrane preparations ranged from 75-100 µg. Protein sample aliquots were mixed with an equal volume of

2x Laemmli sample buffer (LSB) or ¼ volume 5x LSB, both containing 5% v/v 2ß-mercapto-ethanol. After electrophoresis the gels were either stained with Coomassie brilliant blue, silver stained according to Morresy (44), or used for Western blotting. Molecular weight estimates of the protein bands were made by simultaneously running Rainbow protein molecular weight markers (Amersham, Arlington Heights, IL). The distance of migration from the origin versus $\log_{10}$ of the known molecular weight was graphed and the resulting linear standard curve was used to extrapolate the distance of migration of the unknown protein bands to an approximate molecular weight.

Two dimensional gel electrophoresis was conducted using a Protean II system according to the manufacturers instructions (Bio-Rad, Richmond, CA). Briefly, 150 µg BPH extract was solublized in 9.5 M urea, 2.0% NP-40, 1.6% pH 5-7 ampholytes, 0.4% pH 3-10 ampholytes, and 5.0% 2β-mecaptoethanol (2-ME) and loaded onto a 5.0% tube gel made with the same ampholyte and urea concentrations. This gel was run at 400 v for 20 h (8,000 V/h). The gel was extruded and the basic end was markered with bromophenyl blue. The gel was equilibrated with 10% SDS, 5.0% 2-ME, and 0.0625 M Tris at pH 6.8 for 20 min. The tube gel was then attached to the top of a slab gel (gradient gel as described under SDS-Page) with 1.5% agrose and electrophoresed.

Western Blotting

Proteins separated by SDS-PAGE were transferred to Immobilon-P transfer membrane (Millipore, Bedford, MA) at 30V for 15 h according to the method of Towbins, et al. (45), with the exception that methanol was excluded from the transfer buffer. Following transfer of the proteins, the membrane was blocked with PBS, pH 7.2, containing 0.3% Tween 20 (polyoxethylene sorbitan monolaureate, (Sigma Chemical Co., St. Louis, MO) and 1% non-fat dry milk for 1.5 h at 37°C. The membrane was then incubated with test MAb or isotyped matched control antibody for 2 h at 25°C, washed 3 times with PBS-Tween, and subsequently incubated an additional 2 h with ^{125}I-labeled rabbit anti-mouse IgG at 1 x 10^7 cpm/50 ml. The membrane was then washed as above, air dried, and exposed to Kodak XAR X-ray film at -70°C for image development. The membrane was gently agitated during all incubation and wash steps using a platform rocker.

Radioimmunoassay

Antigen preparations were diluted with PBS, added to wells of 96-well polyvinyl chloride microtiter plates (Falcon Microtest III, Beckton Dickerson, Oxnard, CA) at 3 µg/well, dried overnight, fixed with glutaraldehyde or left unfixed, blocked by incubating plates with PBS containing 10% agammaglobulin serum and tested for MAb

binding. For the assay, 50 μl of MAb culture supernatant, 10 μg/ml pure MAb or a control antibody was added to test wells and incubated at 25°C for 1 h. Wells were then washed three times with 0.9% NaCl containing 1.0% serum and 0.2% NaN_3. Following the wash steps, wells were incubated for 1 h at 25°C with 25 μl of ^{125}I-labelled rabbit anti-mouse IgG at 100,000 cpm/well, washed four times , dried, cut, and counted in a gamma counter.

Biochemical Characterization

Epitope Sensitivity

Chemical Treatment

Membrane preparations (3 μg/well) were immobilized on 96-well plates, as described under RIA. Wells were then treated with sodium m-periodate, methanolic HCl or acid hydrolysis and followed immediately with RIA . Sodium periodate was added at concentrations varying between 0.1 to 50 mM in a 50mM acetate buffer, pH 4.5 for 60 min at 25°C in the dark. Wells were then washed with acetate buffer and the reaction was quenched with 100 mM glycine for 30 min (46) in order to prevent non-specific cross-linking of antibody to antigen. Mock treatment with acetate buffer alone served as the control. Acid hydrolysis was achieved with 0.05 M H_2SO_4 at 80°C for 30 min or 2.0 M acetic acid at 80°C for 0.5 to 3

h (47). Incubation with PBS, both at elevated temperature and 25°C, was used as the control. No degradation was noted with temperature alone, as assessed by antibody binding. Sulfate release was accomplished by incubation of antigen with 0.05 M HCl in methanol at 25°C for 5 h (28). Treatment with methanol alone served as the control.

Enzymatic Treatment

Some enzymatic treatments of the epitopes were accomplished by the same RIA format as for chemical treatment. Neuraminidase type X (Sigma Chemical Co., St. Louis, MO) at 0.1 unit/100 μl in 200 mM acetate buffer, pH 5.5 was incubated on the antigen plate for 30 min at 37°C, washed and followed by RIA. Mixed glycosidases (ICN Immmunobiological, Lisle, IL) at 10 mg/ml (48) were incubated with test wells for 40 h at 25°C, washed and followed by RIA. In both instances treatment with buffer alone served as the control. Protease digestion was conducted in a solution containing antigen and one unit pronase in 50 mM Tris-HCl, 2 mM $CaCl_2$, 3 mM 2-mercaptoethanol at pH 7.4 (49). Following digestion, the antigen preparations were diluted with PBS, added to the wells of microtiter plates, as described under RIA, and an RIA was performed. Reactions without pronase served as the control.

Physical Characterization

Blocking Assays

Antibody Reciprocal Blocking

MAbs TURP-27 and HNK-1 were radiolabeled with ^{125}I to a specific activity of ~3.0 $\mu Ci/\mu g$ by the method of Lipford et al., as briefly described above (42). Both unlabeled and labeled antibodies were titrated by a solid phase RIA, as described above (50). Three μg of prostate membrane protein preparation were fixed to 96 well microtiter plates and served as the target antigen. Heart membrane extracts were used as a negative control antigen to assess non-specific background binding. Labeled antibody binding was assayed directly, while unlabeled antibody binding was assayed indirectly using an ^{125}I-labeled rabbit anti-mouse secondary antibody. For the blocking assay, triplicate wells were incubated with PBS or saturating unlabeled MAbs TURP-27 or HNK-1 for 1 hr at 25°C and washed. They were then incubated with 50% maximal binding activity of either ^{125}I-labeled TURP-27 or ^{125}I-labeled HNK-1 for 1 hr at 25°C, washed and counted in a gamma counter. Wells in which like antibody had been sequentially incubated were taken to be background, i.e., unlabeled TURP-27 followed by ^{125}I-labeled TURP-27. Percent blocking was calculated as follows:

$$1-\left(\frac{\text{cpm antibody blocked wells - background}}{\text{cpm non-antibody blocked wells - background}}\right) \times 100$$

Lectin Blocking

Selective lectin blocking of antibody binding to prostate membrane preparations was conducted with lectins obtained from E.Y. Laboratories (San Mateo, CA) and included the following: peanut agglutinin (PNA), camel's foot tree (BPA), gorse (UEA), jackbean (ConA), soybean (SBA), wheat germ (WGA, suc-WGA), osage orange (MPA), horse gram (DBA), and Griffonia simpliciforia (GS-I, GS-II). The lectins were solubilized to a final concentration of 1 mg/ml in the appropriate buffer, as suggested by the manufacturer, for maximal activity. Target plates, consisting of membrane wells, as decribed above, were incubated for 1 h at 25 C with 50 µl of lectin that had been previously incubated with its competing sugar (48). All test wells were run in duplicate. An RIA was then immediately performed using one-half maximal binding titer of MAb culture supernatant as the primary antibody. Percent binding was calculated using the following formula:

$$\left(\frac{\text{mean cpm of the lectin treated wells}}{\text{mean cpm of the untreated wells}}\right) \times 100$$

Free Sugar Blocking

Competition with free mono- or di-saccharides was determined using the following carbohydrates obtained either from Sigma or E.Y. Labs and included D-galactose, D-mannose, maltose, N-acetyl-D-glucosamine, N-acetyl-D-galactosamine, and sialic acid. The carbohydrates were solubilized to 0.05 M or 0.1 M with PBS and incubated 1:1 with TURP-27 MAb for 1 h at 25 C. A 1:1 solution of PBS plus TURP-27 MAb was used as the control. Following incubation, these mixtures were centrifuged for 5 min in an Eppendorf centrifuge. Twenty-five microliters of each supernatant was used as the primary antibody for the RIA, again duplicate wells were assayed.

Glycolipid Analysis

Glycolipid Isolation

Peripheral nerve (6.5 mg/ml), brain (15.0 mg/ml) and BPH (8.9 mg/ml) membrane extracts, prepared as described above, were suspended in Tris buffer (20 mM Tris-HCl, pH 8.0, 10 mM CaCl2) to a final concentration of 5.0 mg protein in 1.5 ml buffer and 0.1% NP-40. The suspension was sonicated for 30 s and mixed with 0.5 ml of pronase (10 mg/ml) dissolved in Tris buffer. After 12 h at 50°C, another aliquot of the enzyme was added and the incubation continued for an additional 12 h.

The mixture was diluted with 3.6 ml methanol and 1.8 ml of chloroform to give a final reaction of 4:8:5.6 (v/v) in chloroform/methanol/buffer (a modified Folch partition) (51). After gentle mixing, both phases were resolved by centrifugation (1500 x g, 15 min). The upper phase was collected and saved. The lower chloroform phase was partitioned a second time. The upper aqueous fractions were pooled, dried under reduced pressure, and resuspended in methanol/water (1:1) (v/v) with brief sonication. The volume of the lower phase fraction was measured and gently mixed with two equal volumes of methanol. After centrifugation (1500 x g, 20 min), the insoluble material appearing at the interface between the two phases during the partitioning steps was precipitated. After collecting the supernatant containing the lower phase glycolipids, the contents of the insoluble pellet were resuspended in 1 ml chloroform/methanol (1:2) (v/v) and centrifuged again. The supernatant from this wash was combined with the lower phase glycolipids, dried under nitrogen, and resuspended in a small volume of chloroform/methanol (1:1) (v/v).

Reverse phase separation of glycosphingolipids was accomplished as follows. Water soluble compounds were separated from the upper layer glycolipids by reverse phase chromatography on Sep-Pak C_{18} cartridges (Waters Associates, Milford, MA) as described previously for the isolation of gangliosides (52). A final wash of the cartridge with 15 ml of chloroform/methanol/water (20:55:25)

(v/v) (afterwards to be designed CMW 20:55:25) was performed to insure complete removal of the glycosphingolipids. The two resultant fractions called upper layer aqueous and upper layer organic, as well as the lower layer glycolipid fraction from above, were subjected to RIA analysis. To achieve this fractions were dried onto 96-well plates and the RIA protocol as described above was conducted. Also tested by RIA was a mixed brain ganglioside preparation (Biocarb Inc.) suspended in methanol/water 1:1 before drying on 96-well plates.

DEAE cellulose chromatography of glycosphingo-lipids was accomplished as follows. One ml of DEAE cellulose (type DE-52 from Whatman, Maidstone, U.K.) was packed into a Pasteur pipet and washed with a minimum of five column volumes each of 2 N acetic acid, methanol, CMW 20:55:25, CMW 20:55:25 containing 1 M ammonium acetate and equilibrated with CMW 20:55:25. The upper layer organic glycolipids of brain, peripheral nerve and BPH were reconstituted in 1 ml CMW 20:55:25 and applied to the column. The column was washed 5 column volumes CMW 20:55:25 and eluted with 5 column volumes of CMW 20:55:25 1 M ammonium acetate. The wash and eluant were dried under reduced pressure, resuspended in methanol/water (1:1) and dried again.

Thin Layer Chromatography and Immunooverlay

Six millimeter lanes were marked off on a 7 cm x 10 cm aluminum backed silica gel 60 TLC sheet (Bodman Chemicals, Ashton Township, PA). Varying amounts of the different fractions were spotted and the plate was developed in a glass TLC tank containing chloroform/methanol/water (5:4:1). Once the solvent front approached the top of the plate it was removed from the tank and allowed to dry. The plate was either orcinol stained or immunostained with TURP-27 or HNK-1 (46,53, G. Clark, personal communication). For immunostaining, the plates were incubated in 0.2% polyisobutyl methacrylate in hexane for 30 s and allowed to air dry. They were then sprayed with PBS containing 1.0% bovine serum albumin (solution A) and soaked in the same solution for 10 min at 4° C. This blocking solution was removed and TURP-27 or HNK-1 at a concentration of 10 μg/ml in solution A was overlaid and incubated for 3 h at 4°C. The plates were washed by dipping four successive times in solution A and overlaid with ^{125}I-labeled rabbit anti-mouse at 1 x 10^6 cpm/ml solution A using 55 μl/cm^2. The plates were washed, dried and exposed to x-ray film at -70°C. Ganglioside standards were run in an adjacent lane cut from the plate before the immunostaining procedure and orcinol stained.

Purification

Antigen Solubilization

A pool of CaP tissues were mixed and a membrane extract was prepared as described above. Three one ml Eppendorf tubes containing 1.672 mg/ml total protein were centrifuged for 15 min at 4°C in a Eppendorf microfuge. The supernatants were removed, stored and referred to as the PBS soluble fraction. To each tube was added 1.0 ml PBS containing 4mM CHAPS (3(3-chloramidopropyl) dimethylammonio-1-propane-sulfonate; Sigma, St. Louis), 0.5% NP-40 (v/v) (Nonidet P-40; Sigma, St. Louis), or 1.0% NP-40 (v/v) (54). The mixtures were mildly agitated at 4°C for 1 hr and centrifuged for 15 min at 4°C in a microfuge. The supernatant was collected and the pellets were resuspended in their respective detergent solutions. For each fraction, protein concentration determinations were made using a Pierce BCA kit and dot blot style RIA was performed with MAb TURP-27 and MAb P3. All subsequent solubilizations were done in this fashion selecting one of the detergent solutions.

Seminal Plasma

Size Exclusion Chromatography

Within a Pharmacia C16 1.6 x 50 column, Sephadex G-200 (Pharmacia, Piscataway, NJ) was packed to a bed height of

approximately 34 cm. The column was equilibrated with PBS containing 0.5M NaCl at a flow rate of 1.5 ml/min. Following equilibration, 2.5 ml seminal plasma at 11.2 mg/ml was loaded on the column (28 mg) and elution initiated with the equilibration buffer at a flow rate of 1.5 ml/min. Fractions were collected at one min intervals. A BCA protein determination and MAb TURP-27 RIA was done on each fraction.

Ion Exchange Chromatography

Seminal plasma was fractionated on a DEAE column essentially as described by Wright et. al.(55,56). Briefly, seminal plasma was saturated to 30% ammonium sulfate at 4°C and centrifuged at 30,000 x g for 30 min. The supernatant was collected, saturated to 70% with ammonium sulfate at 4°C and centrifuged as before. The pellet was dissolved in 0.01M Tris-HCl, pH 7.8, and dialyzed at 4°C against the same buffer. After dialysis the sample was fractioned into pellet and supernatant by centrifuging at 30,000 x g for 1 h. The supernatant was loaded onto a DEAE-Sepharose CL-6B column, 30 cm x 1 cm (Pharmacia), preequilibrated with 0.01 M Tris-HCl. The column was washed with 250 ml of the same buffer and 5.0 ml fractions were collected. The elution conditions were as follows; 200 ml 0.01 M Tris-HCL, 0.08 M NaCl, then 200 ml 0.01 M Tris-HCL, with a 0.08 M to 0.2 M NaCl gradient, and finally 50 ml 0.01 M Tris-HCL, 1.0 M NaCl. Throughout 2.0 ml fractions were collected and assayed for

protein concentration by absorption at 280 nm. Selected fractions were assayed by indirect radioimmunoassay with antibodies directed against several prostate specific antigens, (PSA, PAP, TURP-27 and PSP).

In a second experiment seminal plasma was saturated directly to 70% and handled as described above. The resulting pellet from the 30,000 x g spin was resuspended in PBS, 0.5% NP-40 and agitated at 4°C for 1 hr. The material was centrifuged again at 30,000 x g and the supernatant was applied to the same DEAE column, as described above, and eluted in a similar fashion. Protein concentration was tracked by absorbance at 280 nm and selected fractions were assayed for MAb binding by RIA.

Fraction 595 from this column was concentrated, while performing a buffer exchange to 0.1 M Na_2SO_4 and 0.02 M NaH_2PO_4, using a Centriprep 30 concentrator (Amicon, Danvers, MA) (55) yielding a final concentration of 0.39 mg/ml. 50 μl were injected onto a Bio-Sil SEC-250 size exclusion column (Bio-Rad, Richmond, CA) eluted with 0.1 M Na_2SO_4 and 0.02 M NaH_2PO_4 at 1.0 ml/min. Molecular weights were estimated from the retention time of previously separated gel filtration standards. Protein was estimated by absorbance at 280 nm and selected fractions were analyzed by RIA with MAb TURP-27.

Because of the non-ionic and non-UV absorbing qualities of the detergent octyl-glucoside, it was used to solubilize seminal plasma components as described above under antigen

solubilization. Solubilization was followed by injecting a sample onto a DEAE-PW5 HPLC column (Bio-Rad) that had been washed and equilibrated with 50 mM $NaPO_4$ buffer pH 7.0 containing 3 mM octyl-glucoside. This buffer was continued for 10 min post injection at a flow rate of 0.5 ml/min followed by a linear gradient to 50 mM $NaPO_4$, 3 mM octyl-glucoside, 1.0 M NaCl in 100 min. Protein was monitored by 280 nm absorbance and selected fractions were collected and analyzed for antigen composition by RIA.

Affinity Chromatography

Purified MAb TURP-27, 3.02 mg, was coupled to 3.0 ml of Affi-Gel Hz according to manufacturers instructions (Bio-Rad, Richmond, CA). The matrix is agarose based and links via a hydrazine group to oxidized carbohydrates in the Fc region of the antibody. Coupling efficiency was 77% as judged by antibody loss in early washes.

Elution Buffer

An effective elution buffer which does not damage the antigen was determined by RIA. Triplicate wells of 96 well plates coated with a BPH membrane extract were incubated for 1 h at RT. The wells were washed and then incubated with one of eleven different elution buffers of various pHs and ionic strengths for 10 min and followed by washing. Then the RIA

was continued as normal with ^{125}I-labeled rabbit anti-mouse. Wells were counted and noted for decreases in CPMs. Antigen sensitivity to the eluants was tested by incubating the antigen plate first with the eluant for 10 min at RT followed by washing and then a normal RIA. Counts in the test wells were compared with a PBS control.

TURP-27 Affinity Chromatography

A BPH membrane extract, 6 mg in 300 ul, was centrifuged in a microfuge for 5 min and the supernatant and pellet were separated. The supernatant was diluted to 1 ml with PBS giving a total protein concentration of 1.39 mg/ml, and is referred to as the PBS soluble sample. To the pellet was added 1.0 ml PBS, 0.5% NP-40 for 1 h followed by centrifugation in a microfuge for 5 min. The supernatant was harvested and is referred to as the NP-40 sample.

Two independent column runs were performed one with the PBS soluble sample and one with the NP-40 sample. The column was equilibrated with PBS and loaded with the sample. For the NP-40 sample, 0.5% NP-40 was included in all buffers. PBS elution and washing was continued until the protein, as determined by absorbance at 280 nm, went to base line. Then the column was eluted with PBS brought to 1.0 M NaCl. Fractions were collected throughout. An RIA was performed with MAb TURP-27 on all fractions. In addition an RIA was performed on the TURP-27 positive fractions using HNK-1, a

polyclonal anti-N-CAM, HSP-2 (rat MAb to N-CAM) and PD-41 (a MAb specific for a mucin-liked prostate tumor associated antigen). For the NP-40 sample, 280 nm absorbance was not followed because NP-40 is UV absorbing.

Chapter III

Results

TURP-27 Antigen Characterization

Historical Perspective

Immunohistochemical results gathered before and during the time of this study implied a restricted binding pattern of TURP-27 to benign and malignant prostate tumors (25,26). It was suggested that this restricted binding pattern may have clinical utility for diagnosis and therapy of prostate carcinomas. Therefore, extensive study of the tissue distribution and antigen characterization was conducted. It was noted that the TURP-27 antigen could be found in a limited number of the 24 normal tissues tested by immunohistochemisty: these being, large granular lymphocytes present in sections of normal lymph node and spleen, scattered cells in the adrenal medulla, some normal breast (few luminal cells and secretions), kidney (intercalating cells), stomach (chief cells), brain and myelinated nerves. Fortuitously, a second antibody, HNK-1 was being evaluated for it prostate binding characteristics in this laboratory (24). The reported immunohistochemical staining pattern is

nearly identical to TURP-27 with the exception of a slightly broader range in normal tissues and its sporadic staining of neuroendocrine tumors (22,23,24). In unpublished data, Wahab et al. had conducted preliminary reciprocal blocking studies between the TURP-27 and HNK-1 antibodies and found their epitopes not to be the same (57). However, prior to this study no information had been collected on the biochemical nature of the TURP-27 antigen or the HNK-1 antigen within prostate. Concurrent with this study, biochemical analysis of the HNK-1 antigen within the central and peripheral nervous system was being conducted in several laboratories around the world, appearing in the literature in a fragmentary manner (28-36). With the goal of identifying the TURP-27 antigen in mind, it was believed that the tissue cross reactive pattern of MAb TURP-27 and similarities between the reactivity patterns of the HNK-1 and TURP-27 MAbs should not be ignored. Therefore, the following results are at times a direct comparisons between the TURP-27 and HNK-1 antigens and are guided by contemporaneous published observations about the HNK-1 antigen. This may be an unusual and limited approach but it is not unprecedented in antigen epitope characterization (27,28,58,59).

Western Blot Analysis

Preliminary Blots: Reducing and Non-Reducing

Initial Western blots were performed using 12.5% polyacrylamide gels according to Laemmli and blotting onto nitrocellulose using a Hoeffer wet transblot apparatus set at 100v for 1.5 h. The blots revealed that multiple bands in the 100-200 Kd molecular weight range, however, resolution, clarity and consistency were not satisfying (data not shown). The technique was modified to include protease inhibitors in the membrane isolation procedure, after which the absence of protease activity in the membrane preparations was confirmed using a fibrin based protease test kit (Boehringer Mannheim). To enhance band separation and clarity over a broad range of molecular weights, gradient gels ranging from 5-15% polyacrylamide with a stacking gel of 3.5% were used. To enhance the blotting procedure, a PVDF membrane with greater protein retention characteristics (Millipore, Immobilon Technical Protocol, TP007) was substituted for nitrocellulose membranes and the transblotting voltage was decreased to 30v for 12-15 h reducing the maximal force exerted on the proteins during transblotting. Towbin's buffer for transblotting includes 10-20% methanol which reportedly increases the protein binding characteristics of nitrocellulose. However, a price is paid because methanol reduces the porosity of the

polyacrylamide gels and apparently reduces the ability of large molecular weight proteins to escape the gel during transblotting (Millipore, Immobilon Technical Protocol, TP009, and personal communication). Methanol was observed to yield poor visibility of large molecular weight bands in the TURP-27 blots (not shown), therefore, it was omitted and clarity increased.

A representative TURP-27 blot is shown in figure 1 and the multibanding pattern can be appreciated immediately. The blot was conducted using a negative tissue control, lung carcinoma membranes in lanes 1 and 6, and a negative antibody control, the isotype matched (IgG3,k) MAb J606 raised by repeated mineral oil inoculations (Jackson Labs). The controls point out two important features that reoccurr in subsequent blots. First, the lung tissue is negative for protein banding with both TURP-27 and J606 indicating that Western blotting correlates with immuno-histochemisty and radioimmunoassay results (25) and that the positive banding is not artifactual. Second, the bands seen at 55 KD and 25 KD in lane 2,4,8 and 10 are proteins recognized by the polyclonal rabbit anti-mouse immunoglobulin because they are common to the same tissues on both the TURP-27 and J606 blots. These bands are most likely human immunoglobulin endogenous to the tissue preparation. The apparent molecular weights are what would be expected for reduced

Figure 1. Western blot analysis of MAb TURP-27 versus human tumor membrane preparations.

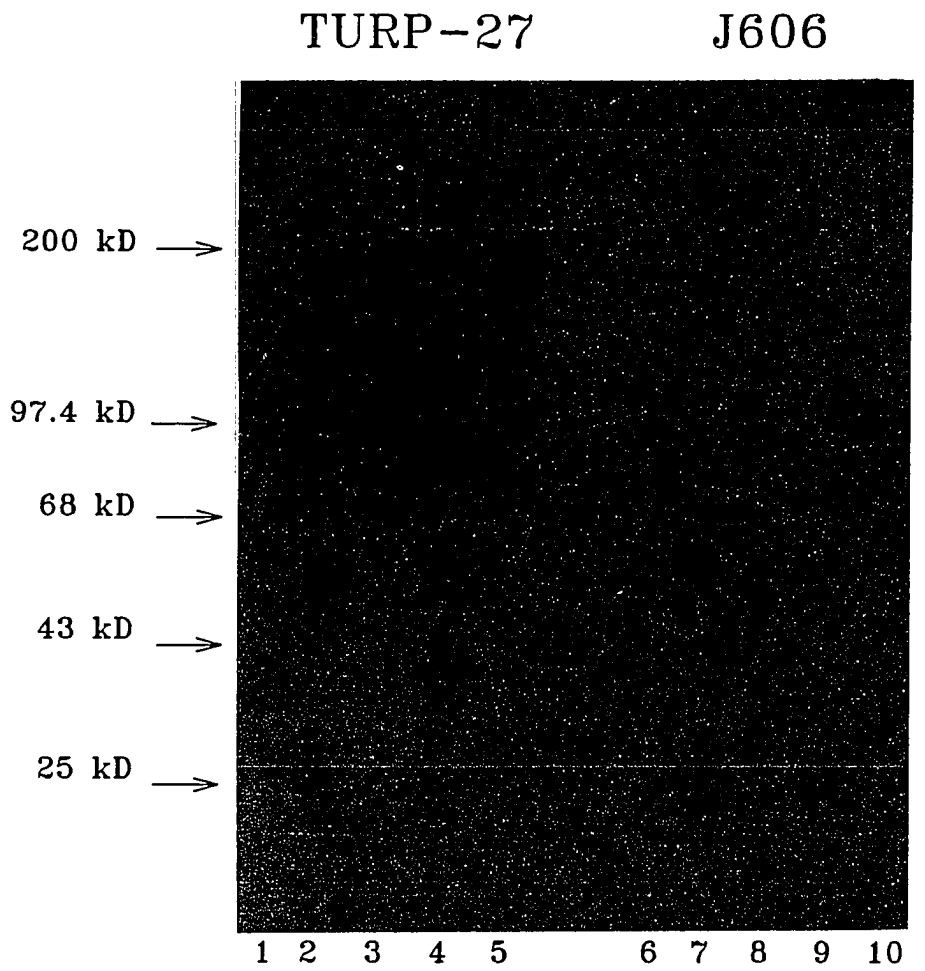

Lanes 1-5 are stained with MAb TURP-27 and lanes 6-10 are stained with negative control MAb J606. Lanes 1,6 are a lung carcinoma extract; lanes 2,7 are a BPH; lanes 3,4,8,9 are CaP; and lanes 5,10 are a small cell lung carcinoma cell line (SK-LC-2). The gel was a gradient of 5-15% run under reducing conditions.

heavy and light chain immunoglobulin. The BPH prep in lanes 2 gives bands at 180, 140, 120, 90, 55 and 25 KD. The two CaPs are similar with the addition of a band at greater than 200 KD. These patterns will be more fully described in Fig. 4. Included in lanes 5 and 11 is the only known cell line which is positive for TURP-27, SK-LC-2, a small cell lung carcinoma cell line. SK-LC banding with TURP-27 is also multiple in nature but does not directly correlate to the banding in prostate tissues.

Figure 2 shows the Western blot results of a non-reducing gel using the same tissues as in figure 1. The predominant bands in lanes 2, 3, 8, and 9, are present in both the TURP-27 and J606 panels and have an apparent molecular weight of 160 KD. These bands are considered to be endogenous human antibody in the extracts. The only specific bands visible are at 75 KD in lane 3 and bands near the origin of the running gel in lanes 3 and 4.

The panel of membrane extracts subjected to Western blot was expanded in number to determine if the number and relative mobility of TURP-27 proteins was consistent. Figure 3 shows a blot of several tissues. Brain reacts with TURP-27 in immunohisto-chemical assays(26) and in RIA. Lanes 2 and 3 are two independent brain extracts and show several bands in excess of 140 KD. This pattern is not fully representative of subsequent blots (see below Figs. 4 and 13). Lower molecular weight bands are not present and may represent incomplete reduction due to

Figure 2. Western blot analysis of MAb TURP-27 versus human tumor membrane preparations under non-reducing conditions.

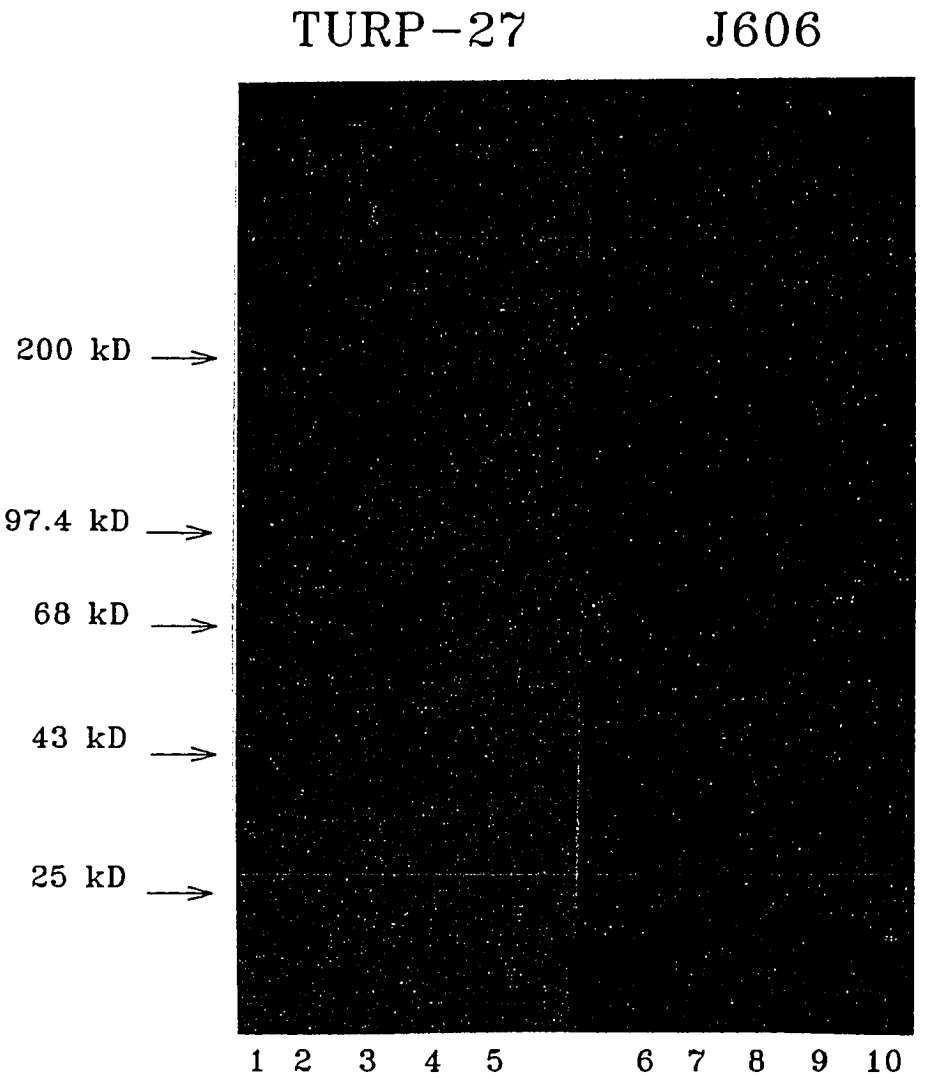

Lanes 1-5 are stained with MAb TURP-27 and lanes 6-10 are stained with negative control MAb J606. Lanes 1,6 are a lung carcinoma extract; lanes 2,7 are a BPH; lanes 3,4,8,9 are CaP; and lanes 5,10 are a small cell lung carcinoma cell line (SK-LC-2). The gel was a gradient of 5-15% run under non-reducing conditions.

Figure 3. Western blot analysis of several tissues with MAB TURP-27. Lane 1 and 11, normal seminal plasma; lanes 2 and 3, human brain extracts; lanes 4, 5 and 6, CaP extracts; lanes 7 and 8, BPH extracts; and lanes 9 and 10, normal prostate extracts. Elecrophoresis was on a 4-15% gel under reducing conditions and each lane was loaded with approximately 80μg total protein.

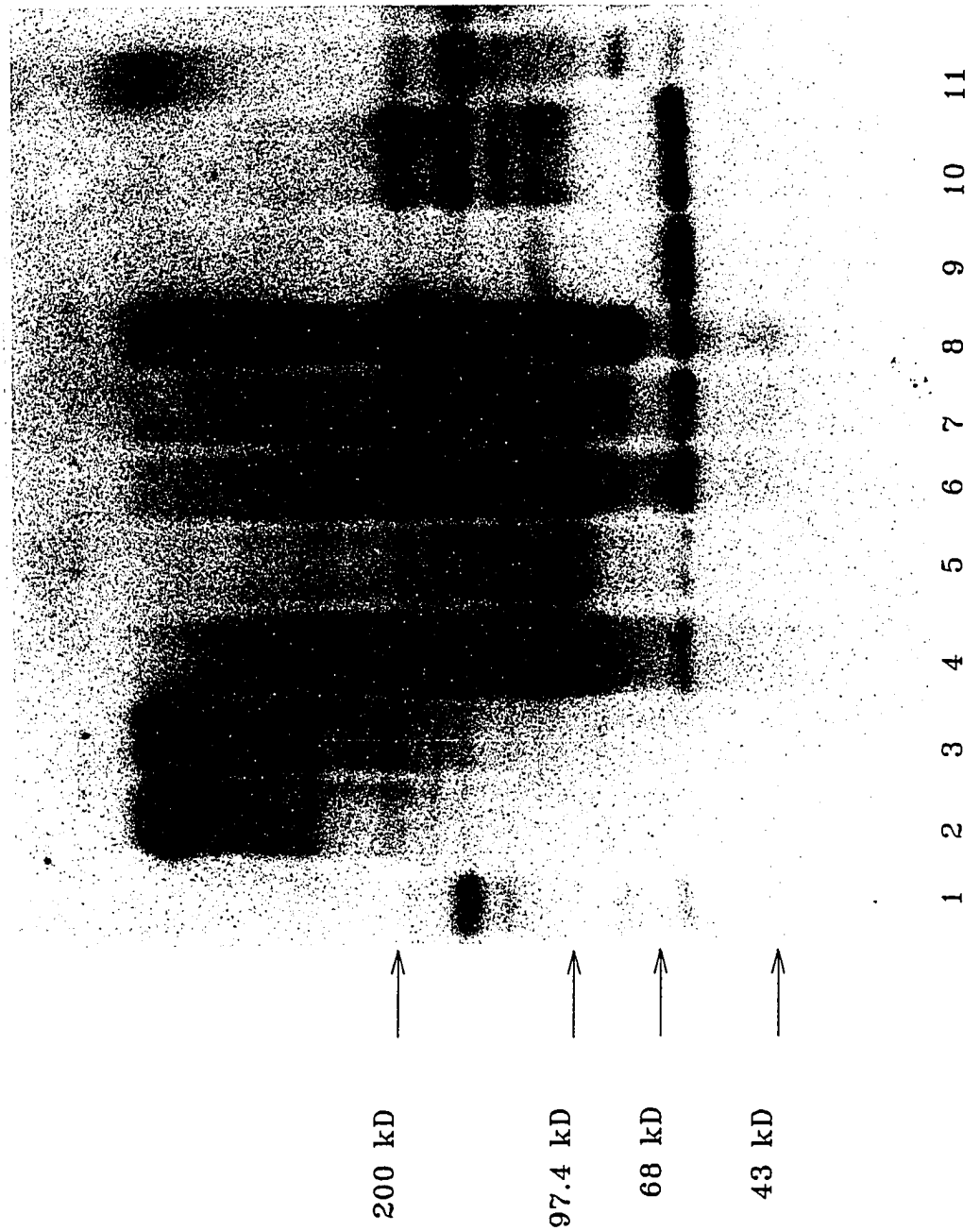

protein concentration of these two preparations. The two BPHs in lanes 7 and 8 can be used as references. Their banding is identical with the BPH in fig. 1, with the exception of a band at 69 KD. Lanes 4,5 and 6 are CaPs and show banding similar to the two CaPs in fig 1. However, it should be noted that they do not exactly align between all the five CaPs implying heterogeneity. Lanes 9 and 10 are normal prostate membranes prepared from autopsy material. The two lanes are different in staining, one is positive and the other essentially negative. This is consistent with variable expression of the antigen as seen in normal prostates (25,26). The normal prostate extract in lane 9 appears similar to BPH, however, with reduced intensity. Lanes 1 and 11 are two seminal plasma extracts and appear similar to the normal in lane 9, except the 180 KD band is faint as is the case in subsequent blots (see fig 4).

Figure 4 represents a similar blot to figure 3, however, the electrophoresis comb size was reduced from 15 to 10 lanes which increases clarity and a negative control breast tissue was included. The breast extract (lane 1) shows only a 55 KD band corresponding to endogenous human immunoglobulin heavy chain. This band is present in all the prostate samples and is the only band on blots using isotype matched control antibody (see fig. 1). Several TURP-27-reactive glycoproteins were identified in the brain membrane extract, lanes 2 and 3. The more prominent bands migrate

Figure 4. Western blot analysis of several tissues several tissue membrane preparations and seminal plasma reacted with MAb TURP-27. Lane 1, breast carcinoma extract (negative control tissue); lanes 2 and 3 normal brain extracts; lane 4, normal seminal plasma pool; lane 5, normal prostate extract; lane 6, BPH; lanes 7 and 8, prostate carcinoma extracts. Electrophoresis was on a 4-15% gel under reducing conditions using 75μg total protein per lane. Molecular weight bands recognized by TURP-27 are indicated by the arrows.

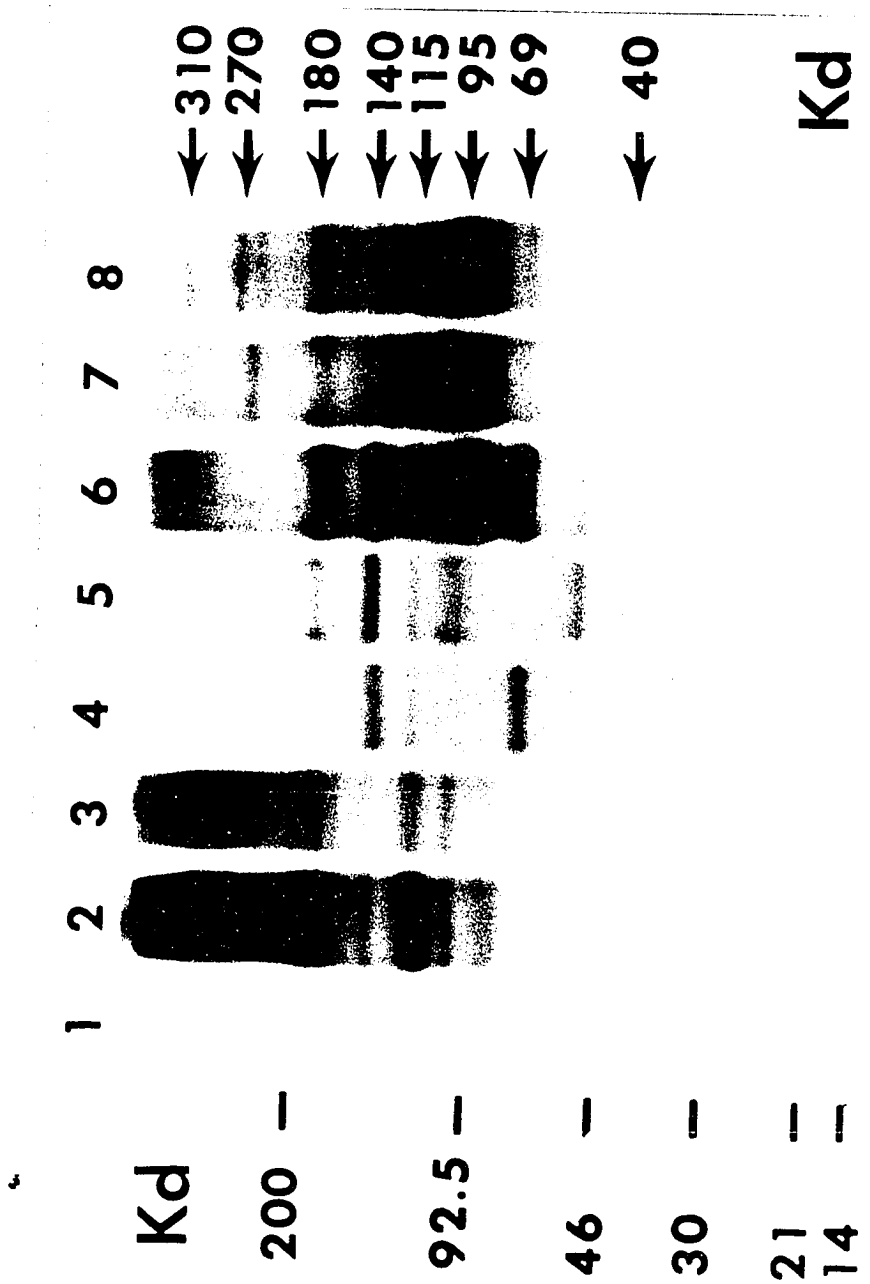

with apparent molecular weight of 310, 270, 180, 140, 115, 95, and 90 KD. These same bands are present in normal prostate (lane 5), with the exception of the 310, 270 and 90 KD bands. Normal seminal plasma (lane 4), reflects the pattern observed with the normal prostate extract except that the 180 KD band is missing and a prominent band at 69 KD is detected. BPH (lane 6) also yields a pattern similar to that of the normal prostate extract with the following exceptions: a prominent 90 KD band is now present along with the 69 KD band observed in normal seminal plasma as well as at least 2 bands migrating between 40 and 35 KD. The two prostate carcinomas (lanes 7 and 8) also show a pattern similar to normal prostate but more complex. Shifts in mobilities of bands between 350-310 KD and 270-250 KD were observed , whereas the 140 KD band evident in the brain, normal prostate and BPH membrane extracts was usually not detected or only weakly detected. A band migrating at 160 KD was weakly detected in all CaP specimens but not in any of the other tissue extracts tested. The 95-90 KD band was strongly detected, whereas the 69 KD band and the bands between 40 and 35 KD were weakly present. Although many of the higher molecular weight bands are also present in normal brain, the lower molecular weight bands, particularly the 69 KD band (normal prostate, seminal plasma, BPH, CaP), and bands with molecular weights between 40 and 35 KD (BPH, CaP) were only detected in the prostate extracts indicated.

In an attempt to identify an in-vivo mouse model tumor system for TURP-27 expression, membrane extracts of tumors which developed from the injection of in-vitro cultured small cell lung carcinoma cells were analyzed by Western blot. The blot was performed on extracts of three independent mouse tumors, OH-1, SW2-105 and GLC, and a BPH and Cap as shown in Figure 5. The figure shows that no specific protein staining was detected in the human-mouse xenografts. Only the apparent staining of mouse endogenous immunoglobulin detected by the rabbit-anti-mouse secondary.

Two Dimensional Blot

In order to extend the information on the TURP-27 antigen, two-dimensional gel electrophoresis followed by Western blotting was attempted. Figure 6 shows a blot of a BPH extract which had been subjected to isoelectric focusing in the first dimension and then PAGE under reducing conditions in the second dimension followed by blotting and staining with TURP-27. The blot is weak but it can be appreciated that the proteins run toward the acid end of the isoelectric focusing gel. The 180 and 69 KD proteins appear the most acidic. The 140 and possibly the 120 KD bands run somewhat less acidic and what may be the 55 KD antibody band remains to the more basic end.

Figure 5. Western blot analysis of MAb TURP-27 versus human-mouse xenograft tumor membrane preparations.

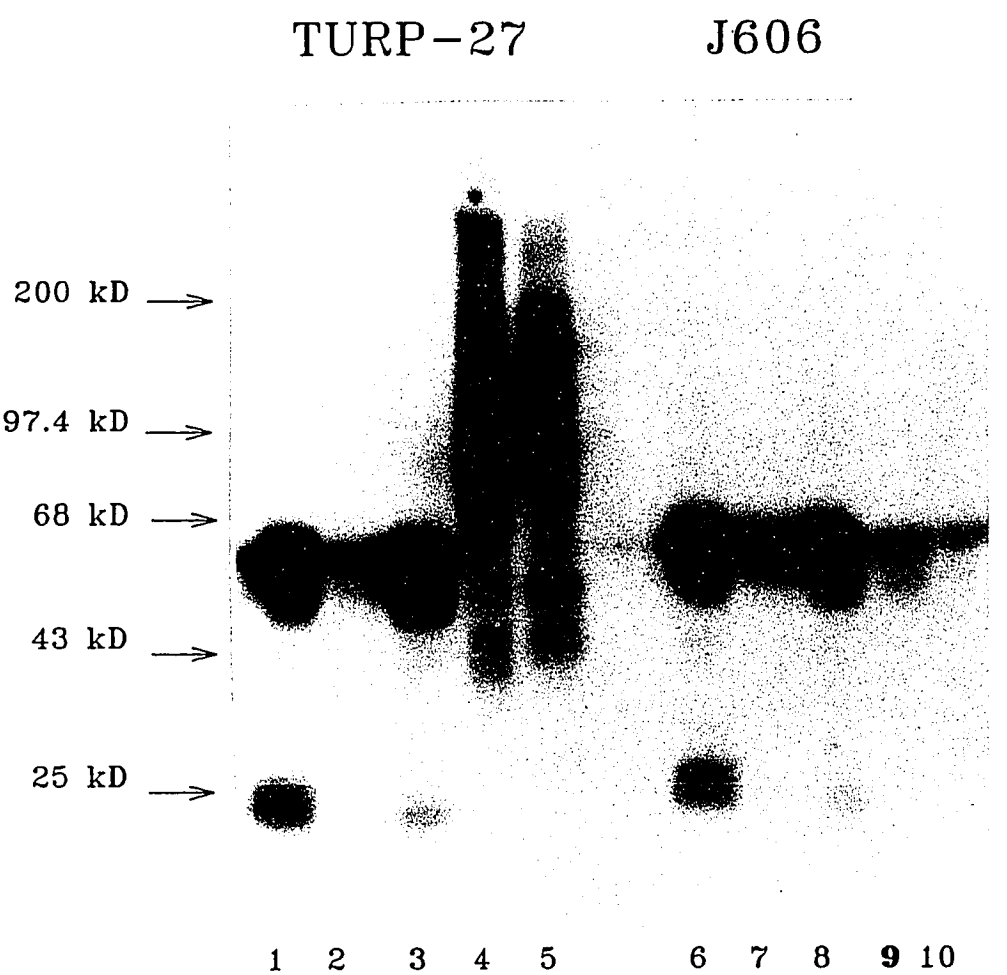

Lanes 1-5 are stained with MAb TURP-27 and lanes 6-10 are stained with negative control MAb J606. Lanes 1,6 are a OH-1 tumor extract; lanes 2,7 are a SW-105 extract; lanes 3,8 are a GLC tumor extract; and lanes 4,9 are a CaP; and lanes 5,10 are a BPH. The 10% gel was run under reducing conditions.

Figure 6. Two dimensional Western blot anlysis with MAb TURP-27.

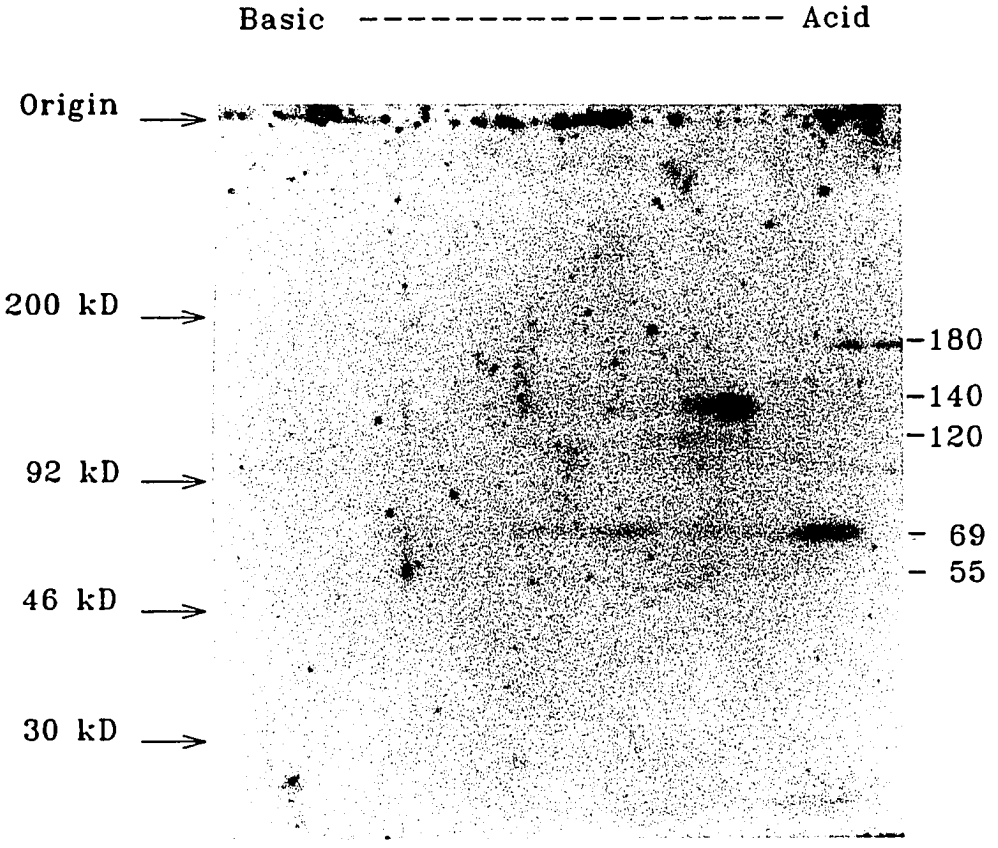

The tube isoelectic focusing gel was run with an ampholyte gradient ranging from pH 3-10. The second dimension gel was a 5-15% gradient run under reducing conditions. The sample is a BPH membrane preparation.

TURP-27 vs HNK-1 Comparison

Because of the similarity in immunohistochemical and RIA data when using Mab TURP-27 and HNK-1 and also because HNK-1 had been shown to bind to several glycoproteins, comparative Western blotting was pursued. Figure 7 shows a comparative blot between TURP-27 and HNK-1 using a normal seminal plasma (lane 1 and 4) and two seminal plasma preps from prostate carcinoma patients (lane 2,3 and 5,6). The two antibodies stain identical protein bands and the pattern is as described in Fig. 4 for normal seminal plasma. The similarity is to such an extent that the two patterns are indistinguishable. This is not due to artifact, other prostate antibodies i.e. PD-23, PD-7, PD-41, PSP and 7E-11 used within the course of this and other studies did not stain the prostate blots with the same pattern as TURP-27 and HNK-1 (55,60,61,62,data not shown).

Figure 8 shows a Western blot comparison of MAbs TURP-27 and HNK-1 using prostate and brain tissue extracts. Again the staining pattern is essentially the same with the pattern of staining in brain extracts somewhat stronger in intensity, although in this figure it is less obvious (see fig. 13).

Figure 7. Western blot analysis of normal and prostate carcinoma patient seminal plasma with MAb. TURP-27 and MAb HNK-1.

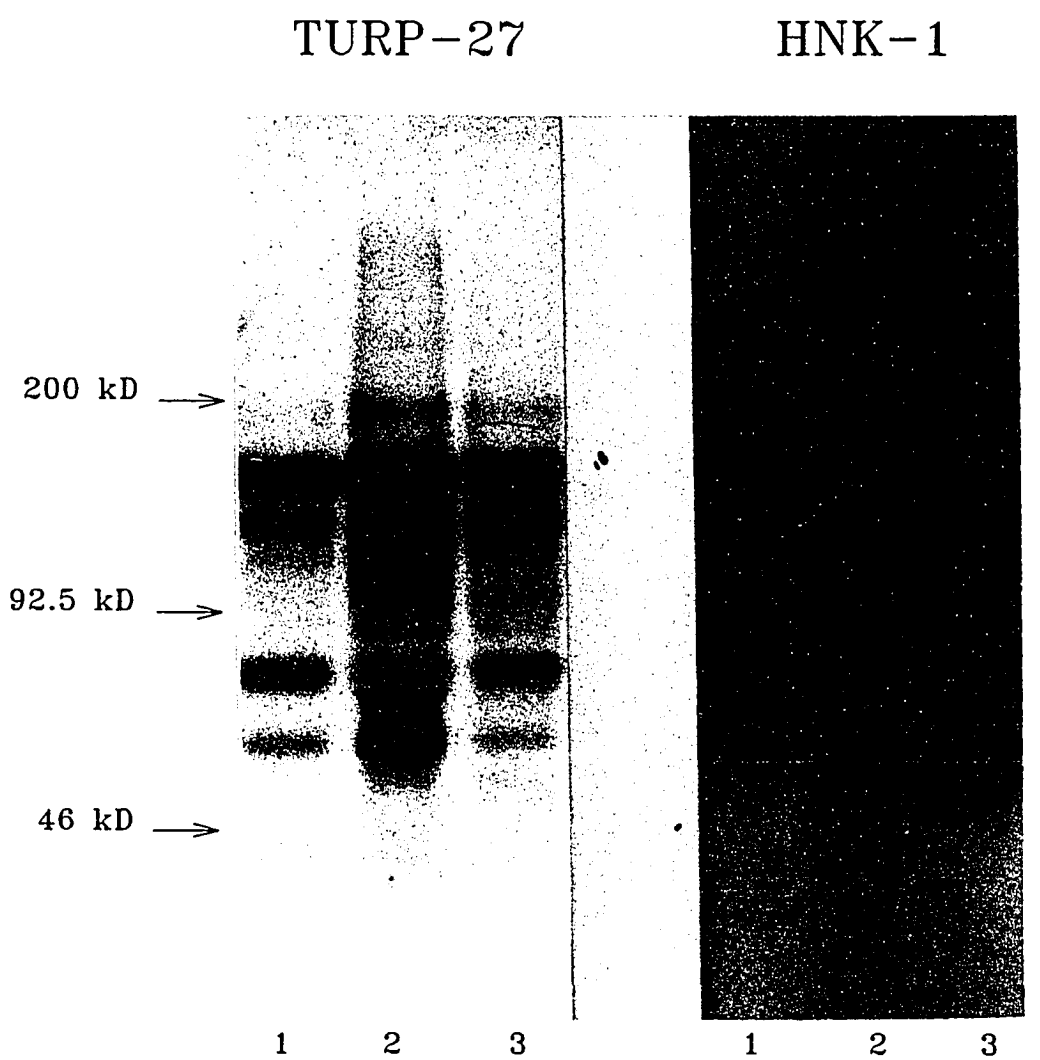

Lane 1, normal patient's seminal plasma; lanes 2 and 3, prostatic carcinoma patient's seminal plasma. Electrophoresis was a 5-15% gradient gel run under reducing conditions.

Figure 8. Western blot analysis of prostate and brain extracts reacted with TURP-27 or HNK-1. Panel A, extracts reacted with TURP-27; panel B, extracts reacted with HNK-1. Lane 1, normal prostate; lane 2, BPH; lane 3, CaP; lane 4, human brain. Total protein was 75μg per lane, and electrophoresis was on a 4-15% gradient gel under reducing conditions.

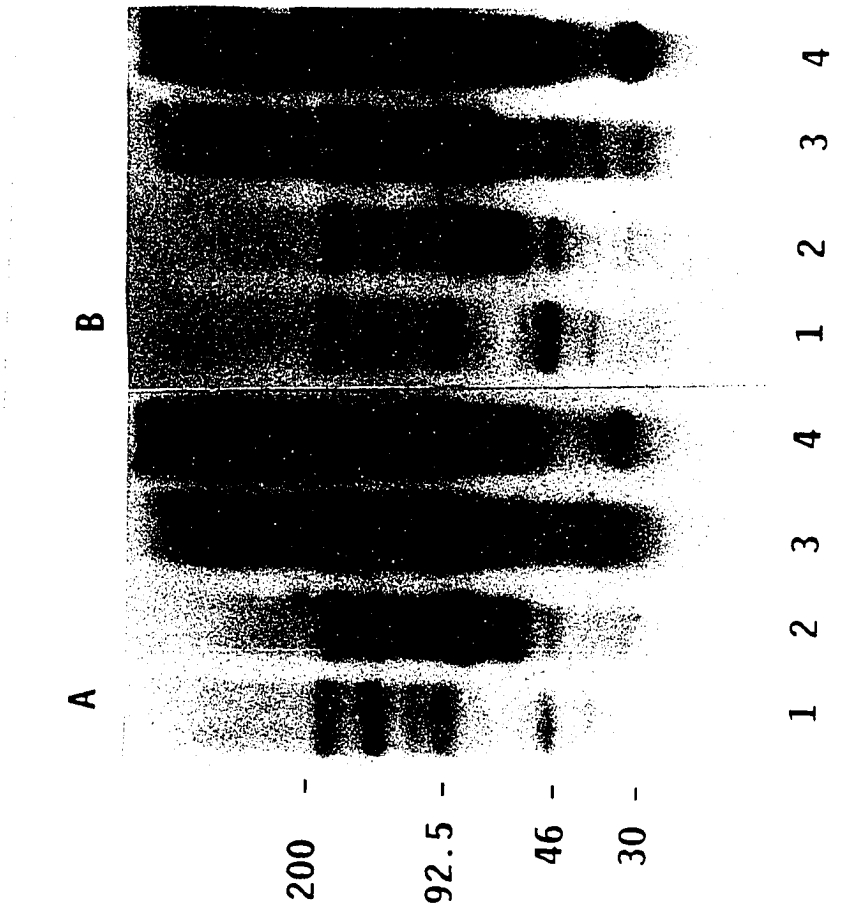

Epitope Characterization

Simultaneous with the current work, it was discovered that the HNK-1 epitope was carbohydrate in nature and may occupy an important posttranslational modification niche on several central and peripheral nervous system glycoproteins (33,34,35,36). In light of the multi-banding pattern displayed by MAb TURP-27 and its near identical reactivity in Western blot to MAb HNK-1 (figs. 7,8), two issues needed to be addressed. 1) Is the TURP-27 epitope carbohydrate in nature? 2) Are the TURP-27 and HNK-1 epitopes identical?

TURP-27 and HNK-1 Reciprocal Blocking

To explore further the relationship between the epitopes detected by TURP-27 and HNK-1, a reciprocal blocking assay was performed (Table 1). Although the TURP-27 and HNK-1 antibodies each completely block binding with the respective labeled antibody, the antibodies incompletely block binding by the heterologous labeled antibody. TURP-27 was able to block only 9.7% of the HNK-1 binding activity to its target antigen, while HNK-1 blocked 61.6% of the TURP-27 activity.

Lectin and Free Sugar Blocking

In order to address carbohydrate nature of the TURP-27 epitope, a lectin blocking assay and a free sugar

Table 1 MAb TURP-27 versus MAb HNK-1 reciprocal blocking assay.

Triplicate wells containing prostate membrane extract were incubated for 1 hr with saturating unlabeled MAb TURP-27 or MAb HNK-1, washed, and incubated with the indicated ^{125}I-labeled MAb. The ability of an antibody to block itself or the heterologous antibody is given as percent blocking. Variation between test wells did not exceed 2.0%.

	% of Blocking	
Unlabeled MAb	^{125}I-TURP-27	^{125}I-HNK-1
TURP-27	100	9.7
HNK-1	61.6	100

competition assay were used. A panel of eleven lectins were selected for a broad range of sugar specificities and preincubated for 1 h at room temperature with target prostate membrane preparations before RIA. The results are depicted in figure 9 and show that only wheat germ agglutinin (specificity NAc-glucosamine and sialic acid) blocks TURP-27 binding to prostate membrane extracts. This is apparently due to the competition for a sialic acid moiety because succinylated WGA (specificity NAc-glucosamine) did not block TURP-27 binding. Variation between test wells was less than 10%.

Next Mab TURP-27 was preincubated with free mono- and di-saccharides prior to performing RIA using prostate extracts. Sialic acid was found to be the only carbohydrate to inhibit (99%) the binding of TURP-27 to its target antigen (fig. 10). Variation between test wells was less than 10%.

Enzymatic and Chemical Epitope Dissection

In order to directly link TURP-27 binding to a carbohydrate moiety, several enzymatic and chemical treatments of prostate membrane extracts followed by RIA with TURP-27 were performed (fig. 11). TURP-27 antibody reactivity was lost after treatment of extracts with periodate, neuraminidase, or mixed glycosidases as evidenced by the percentage control binding of MAb TURP-27 to its

Figure 9. Lectin versus MAb TURP-27 competition assay.

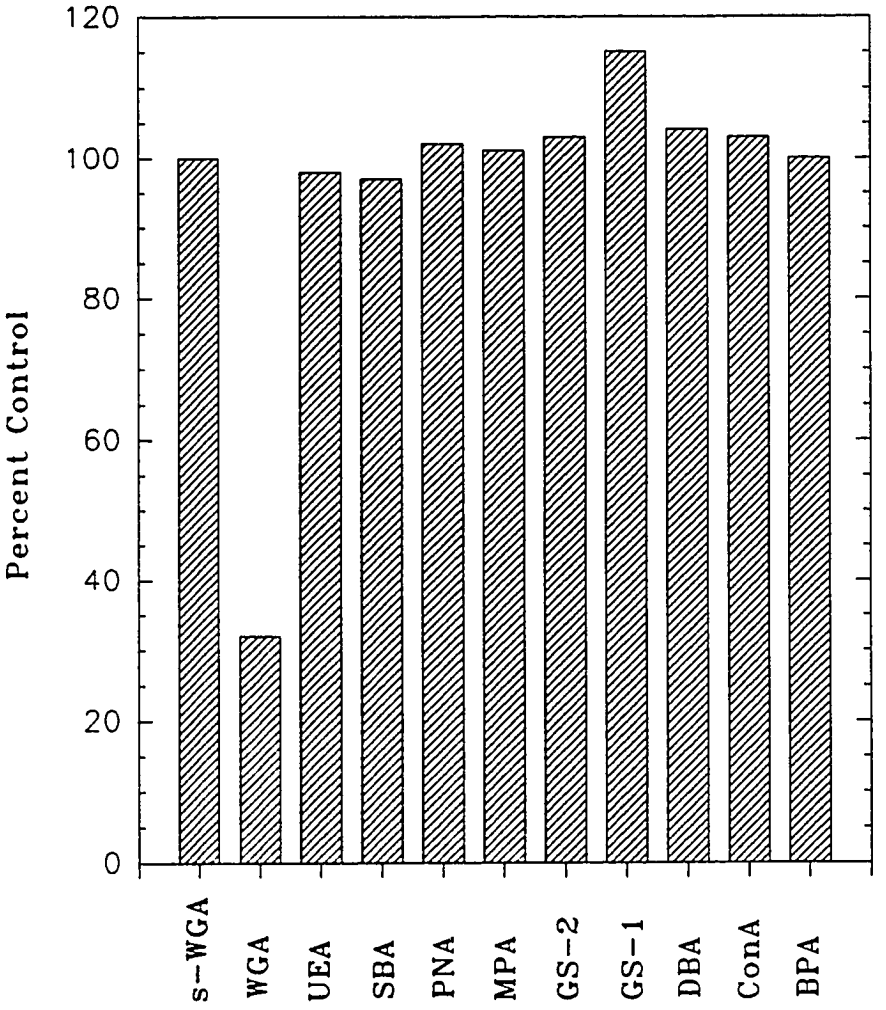

The percent binding of MAb TURP-27 following competition with various lectins of different carbohydrate specificities: D-galactose (PNA, MPA); N-acetylgalactosamine (BPA, DBA, SBA); fucose (UEA); mannose (ConA); N-acetylglucosamine, sialic acid (WGA); N-acetylglucosamine (s-WGA).

Figure 10. Free carbohydrate binding by MAb TURP-27.

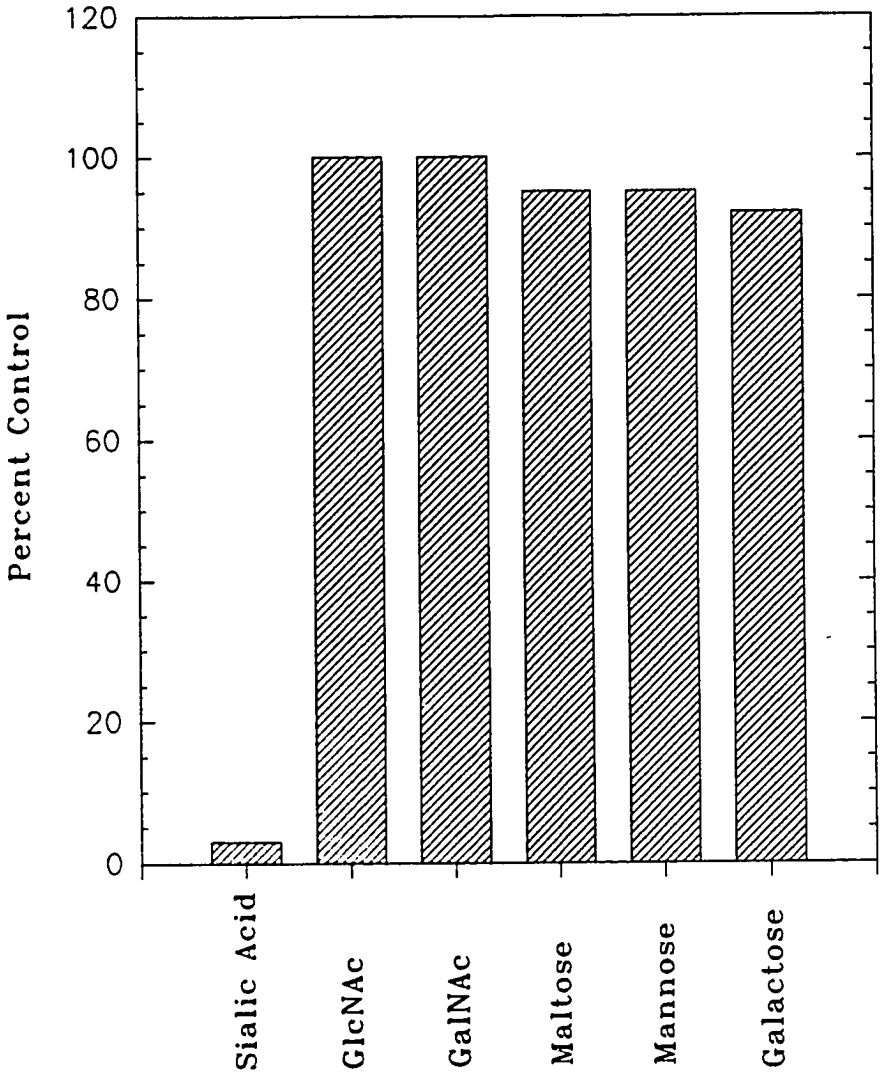

The competition of free mono- and di-saccharides with MAb TURP-27 binding to it's target antigen. GlcNAc, N-acetylglucosamine; GalNAc, N-acetyl-galactosamine.

Figure 11. Effect on MAb TURP-27 binding to its target antigen by chemical and enzymatic treatments.

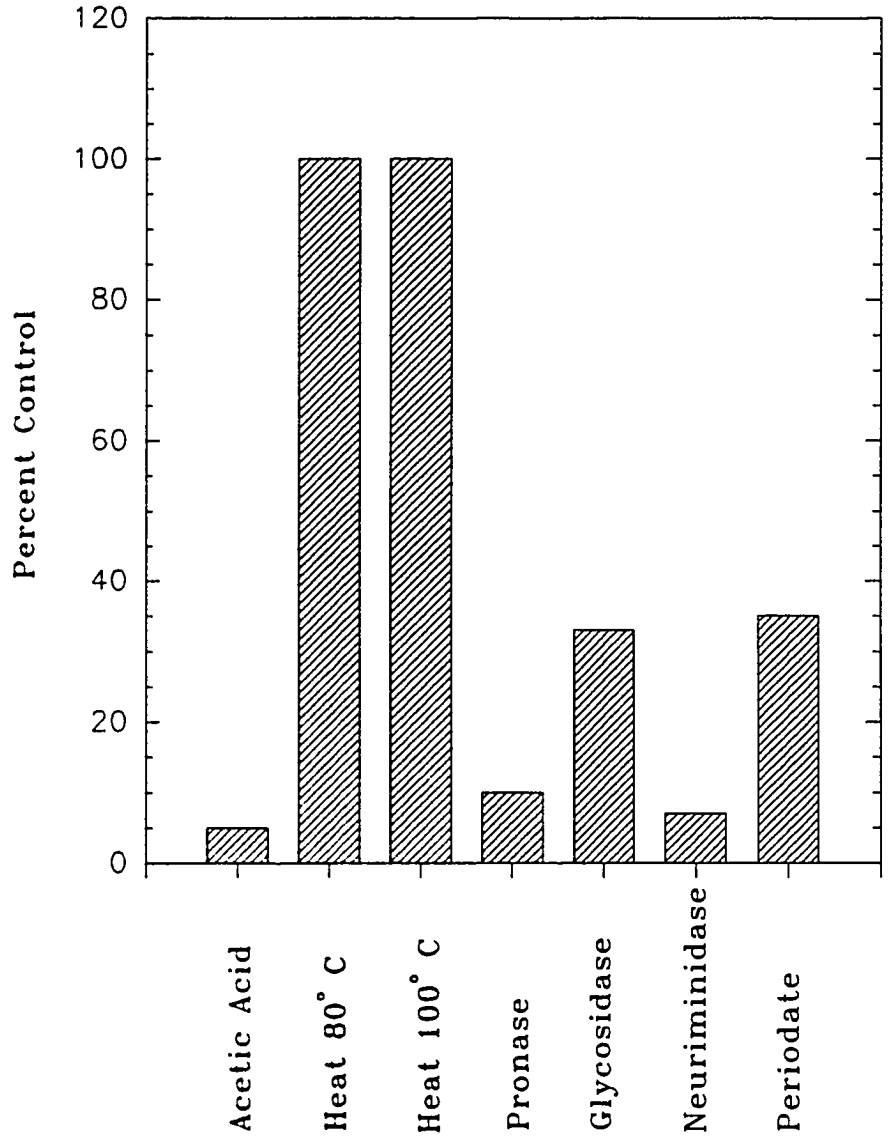

Binding of MAb TURP-27 to its target antigen after various enzymatic and chemical treatments.

target antigen. Treatment of the antigen with pronase or acetic acid also resulted in loss of binding by TURP-27, while heating the antigen resulted in no loss of antibody activity. Collectively, the data suggest that the integrity of the antigenic determinant is dependent on the presence of sialic acid supported by a protein backbone. Variation between test wells was less than 10%

To determine if the suggested conclusion of the above data could be verified by other means, a Western blot of a BPH extract previously treated with neuraminidase was performed. Figure 12 illustrates that MAb TURP-27 binding was completely abolished by loss of sialic acid residues (lane 3). This effect can not be attributed to the 24 h incubation at 37°C because the control, lane 2, appears nearly identical to the non-manipulated BPH extract in lane 1.

Turp-27 and HNK-1 Epitope Comparison

The binding of MAb HNK-1 to its antigenic determinant is reported to be dependent on a sulfated glucuronic acid moiety (27,28,29), and as shown above the MAb TURP-27 is dependent on a sialic acid moiety. Since the reciprocal blocking assay implied a possible close physical proximity of the two epitopes and the Western blot data implied the same carrier proteins, the sensitivities of TURP-27 and HNK-1 binding after sialic acid or sulfate hydrolysis were

Figure 12. Western blot analysis of MAb TURP-27 versus neuraminidase treated BPH extract.

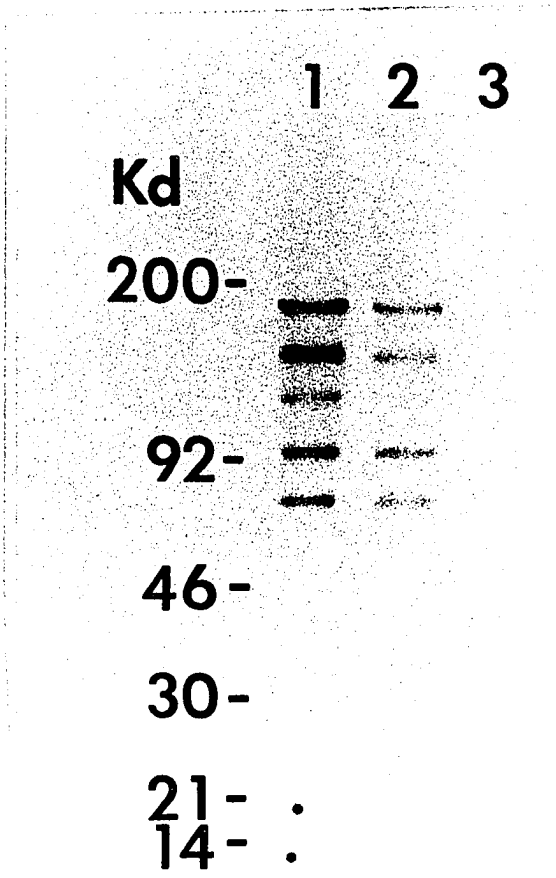

Lane 1, BPH extract no treatment; lane 2, BPH extract incubated for 24 h at 37°C in buffer without neuraminidase; lane 3, neuraminidase (0.25 units) treated for 24 h. Gel was a 4-15% gradient run under reducing conditions.

Table 2 Biochemical analysis of TURP-27 and HNK-1 epitopes expressed by prostate epithelium. Duplicate wells containing prostate membrane extracts were treated by enzymatic or chemical hydrolysis followed by RIA using MAb TURP-27 or MAb HNK-1. Values are given as percent control.

	% of Control Binding	
TREATMENT	TURP-27	HNK-1
NEURAMINIDASE	13.7[a]	137.5[a]
2M ACETIC ACID[b]	16.6[a]	125.2[a]
0.05M SULFURIC ACID	9.6[a]	121.0
0.05M HCl in MeOH	104.9	94.1

[a] Treatment mean significantly different from control mean ($P \leq 0.01$).

[b] Duplicate wells only.

compared (Table 2). Neuraminidase, 2 M acetic acid, and sulfuric acid treatments, all procedures which remove sialic acids from carbohydrates (47), reduced TURP-27 binding to prostate membrane extracts to approximately 10% of control levels. In contrast, HNK-1 binding was increased to approximately 125% of the control. To determine if a sulfate group masks the TURP-27 binding site, prostate extracts were desulfated by 0.05 M methanolic HCl hydrolysis, a treatment shown to remove the sulfate group from MAb HNK-1-reactive peripheral nerve glycolipids (27). The desulfation had little effect on the binding of either antibody to prostate extracts.

TURP-27 Expression on HNK-1 Epitope Carriers

Anti-NCAM, HNK-1 and TURP-27 Comparison

Because of the association of the HNK-1 epitope to N-CAMs, the reactivity of an anti-N-CAM serum, MAb HNK-1 and MAb TURP-27 against a brain extract was compared by Western blot analysis (Fig.13). The immunoblot obtained with the anti-N-CAM serum showed bands at 180, 140 and 120 KD (lane 1). This pattern is repeated by HNK-1 (lane 2) and TURP-27 (lane 3) with additional bands in the >200 KD range and the 90 KD range for both antibodies. Thus, both HNK-1 and TURP-27 react with proteins of 180, 140 and 120 KD bands on

Figure 13. Western blot of a brain extract reacted with anti-N-CAM, HNK-1, or TURP-27.

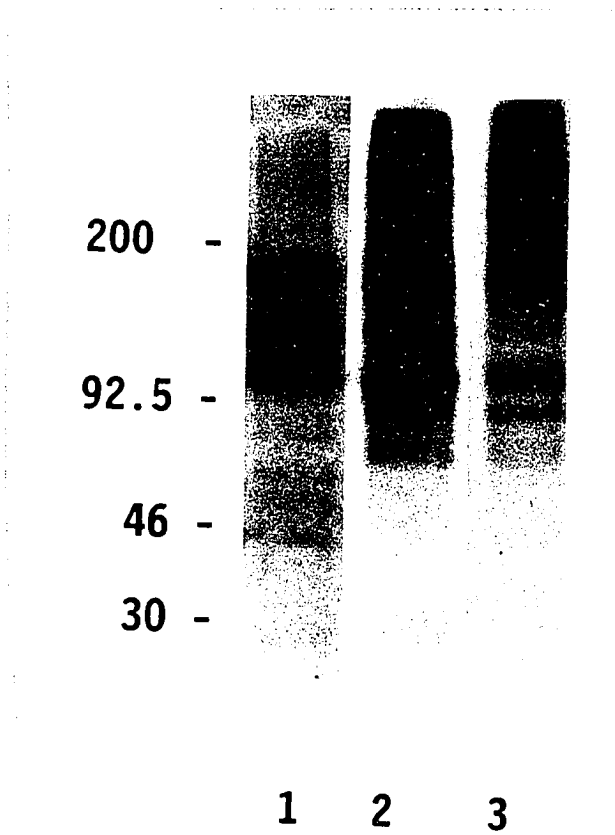

Each lane contained 75μg of brain membrane extract, and electrophoresis was on a 4-15% SDS-polyacrylamide gel run under reducing conditions. Lane 1, anti-N-CAM; lane 2, HNK-1; lane 3, TURP-27.

immunoblots of brain extracts, similar to the anti-N-CAM serum.

Western Blot of Pure HNK-1 Carrier Proteins

Given the ability of TURP-27 and HNK-1 to detect common proteins in brain extracts and the apparent correlation of the relative molecular weights to known central and peripheral nervous system antigens; nervous tissue HNK-1 epitope carrier proteins, purified by outside sources, were used in TURP-27 Western blots. Because this material was donated and difficult to obtain, a minimum of RIA and two Western blots were all that were performed.

Figure 14 is a blotted mini-gel; the mini-gel allowed conservation of material while serving as an initial source of data. Three panels are included: A, MAb TURP-27 stained; B, MAb HNK-1 stained (A and B are mirror images); and C, MAb UJ-13 (a monoclonal antibody developed against a fetal brain preparation reactive with some isoforms of N-CAM, primarily muscle N-CAM). Lanes 1 and 8 are a CaP extract and lanes 2 and 7 are a brain extract, the pattern for TURP-27 and HNK-1 are the same as described above. Lane 3 and 6 are purified N-CAM and both TURP-27 and HNK-1 show staining of the 180, 140 and 120 KD nervous tissue isoforms with lighter staining of an 90 KD band. This lower band may be a breakdown product or possibly a myelin associated glycoprotein (MAG) contaminant. Lane 4 and 5 are purified

Figure 14. Mini-immunoblot analysis of adhesion proteins reacted with TURP-27, HNK-1 and UJ-13. The panels were reacted with the indicated MAb. Lanes 1, 8 and 11, BPH; lanes 2, 7 and 12, human brain; lanes 3, 6 and 13, purified brain N-CAM; lanes 4, 5 and 14, purified peripheral nerve MAG, lanes 9 and 10, Rainbow molecular weight markers (non-specific staining of 200 kD 92.5 kD and 30 kD markers). Electrophoresis was on a 4-15% gradient gel under reducing conditions.

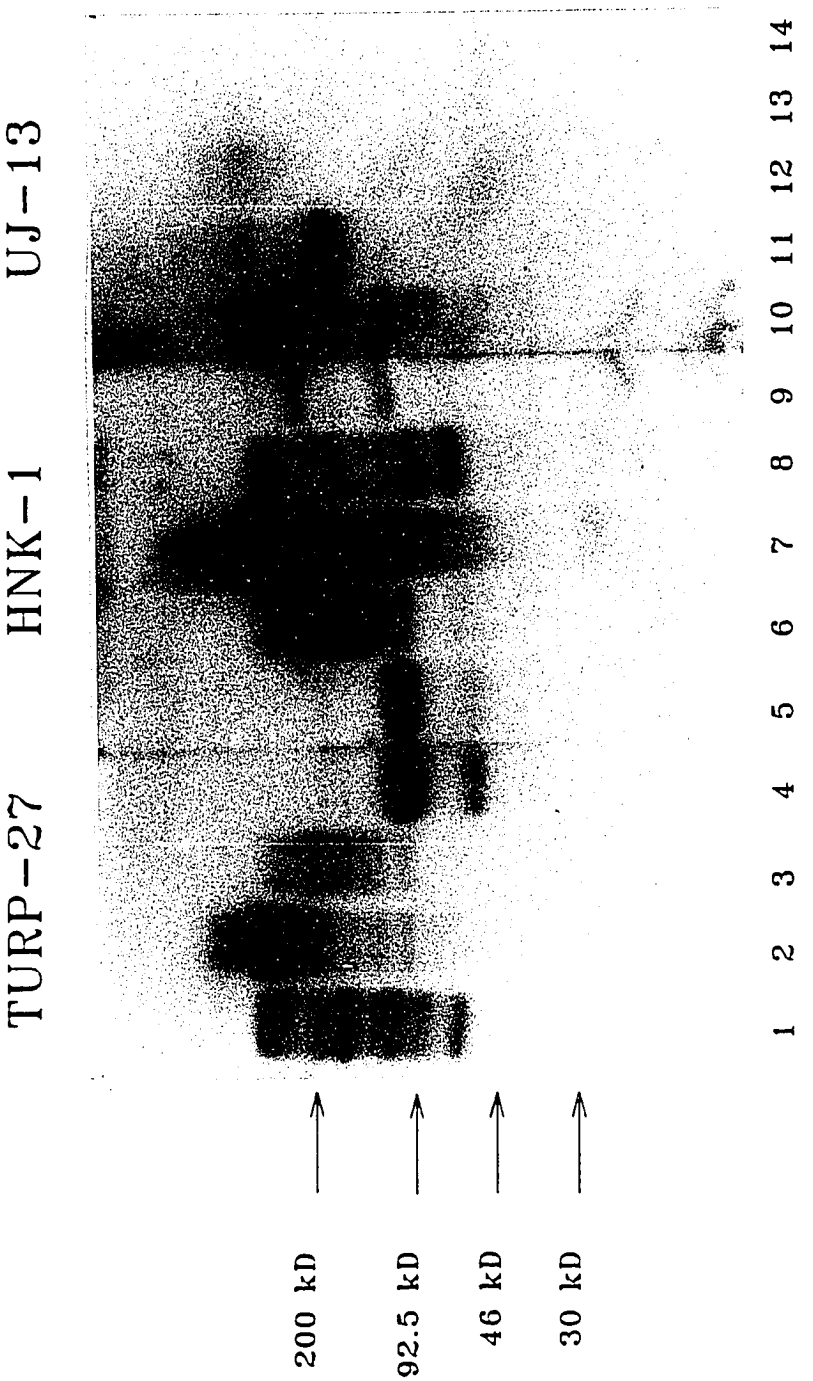

MAG staining with TURP-27 and HNK-1. The band is at 90 KD which is less than the 100 KD molecular weight reported for MAG on Western blot of myelin preparations (30), however this molecular weight is consistent with the weight of dMAG, a degradation product of full length MAG and typically isolated by some laboratories including the supplier of this sample (Dr. M. Schactner). In panel C MAb UJ-13 stained only a 145-150 KD band in lane 11, the CaP. This molecular weight is consistent with UJ-13's reactivity to muscle isoforms of N-CAM. The brain extract, purified brain N-CAM and purified MAG did not stain with UJ-13. In this instance the UJ-13 blot can serve as a negative control and the HNK-1 blot as a positive control clearly showing that the staining of brain N-CAM and MAG by MAb TURP-27 are specific and not artifactual. Secondarily, a muscle N-CAM isoform is expressed in prostate perhaps originating from membranes of the fibromuscularstroma.

In order to strengthen and extend the above observations pure preparations of N-CAM, MAG and peripheral nerve myelin were run in a larger gel format. TURP-27 reacts to purified N-CAM in a similar fashion to HNK-1 (Fig. 15, panel A and B, lane 1). MAG also was bound similarly by both TURP-27 and HNK-1 (Fig. 15, panel A and B, lane 2). When chicken and human myelin preparations were evaluated by immunoblotting with TURP-27, bands of 100, 28 and 22 KD were observed (Fig. 15, panel A, lanes 3 and 4). Similar molecular weight components were also observed on HNK-1

Figure 15. Western blot of adhesion proteins reacted with HNK-1, or TURP-27.

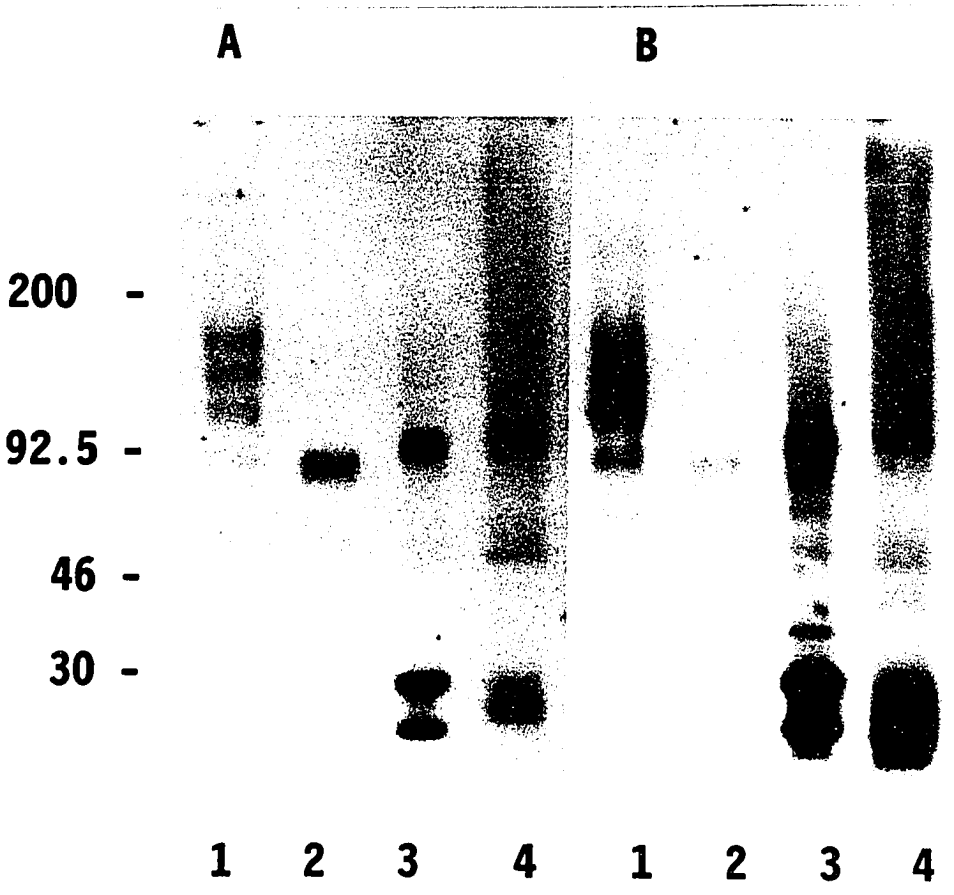

Panel A, MAb TURP-27; panel B, MAb HNK-1. Lane 1 5μg of purified N-CAM; lane 2, 1μg of purified MAG; lane 3, 20μg of chicken peripheral nerve myelin; lane 4, 20μg of human peripheral nerve myelin. Electrophoresis was on a 4-15% SDS-polyacrylamide gel.

immunoblots (Fig. 15, panel B, lanes 3 and 4). The 100 KD and 28 KD bands in these myelin preparations are MAG and the glycoprotein P_O, respectively (30,31). The 22 KD component has been reported to be HNK-1 positive but is as yet unidentified. Control antibody blots were negative for all of these proteins (see below).

The MAb UJ-13 was also used to stain a blot run in the larger gel format to investigate the staining of prostate extracts while at the same time serving as a control for the blotting of purified nervous tissue antigens. Figure 16 shows that the antibody only stains a 145 KD band in BPH and CaP. Brain and all purified nervous tissue antigens lanes are negative. One potentially important point to note is that in the normal prostate extract, lane 8, UJ-13 staining is absent. This does not appear to be due to error in the quantity of material loaded on the gel because the contaminating endogenous antibody band can be seen at 55 KD.

Neural Tissue Antigens in Prostate

To determine if the proteins recognized by TURP-27 and HNK-1 in prostate are N-CAM or MAG, Western blot analysis was performed against prostate membrane extracts using an anti-N-CAM serum or the MAb B11F7. Bands at 180 and 140 KD are clearly evident in the BPH extract blotted with anti-N-CAM (Fig. 17, panel B, lane 1), and are similar to the 180 and 140 KD bands detected by TURP-27 (Fig. 17, panel A, lane

Figure 16. Western blot analysis of adhesion proteins and prostate extracts with UJ-13.

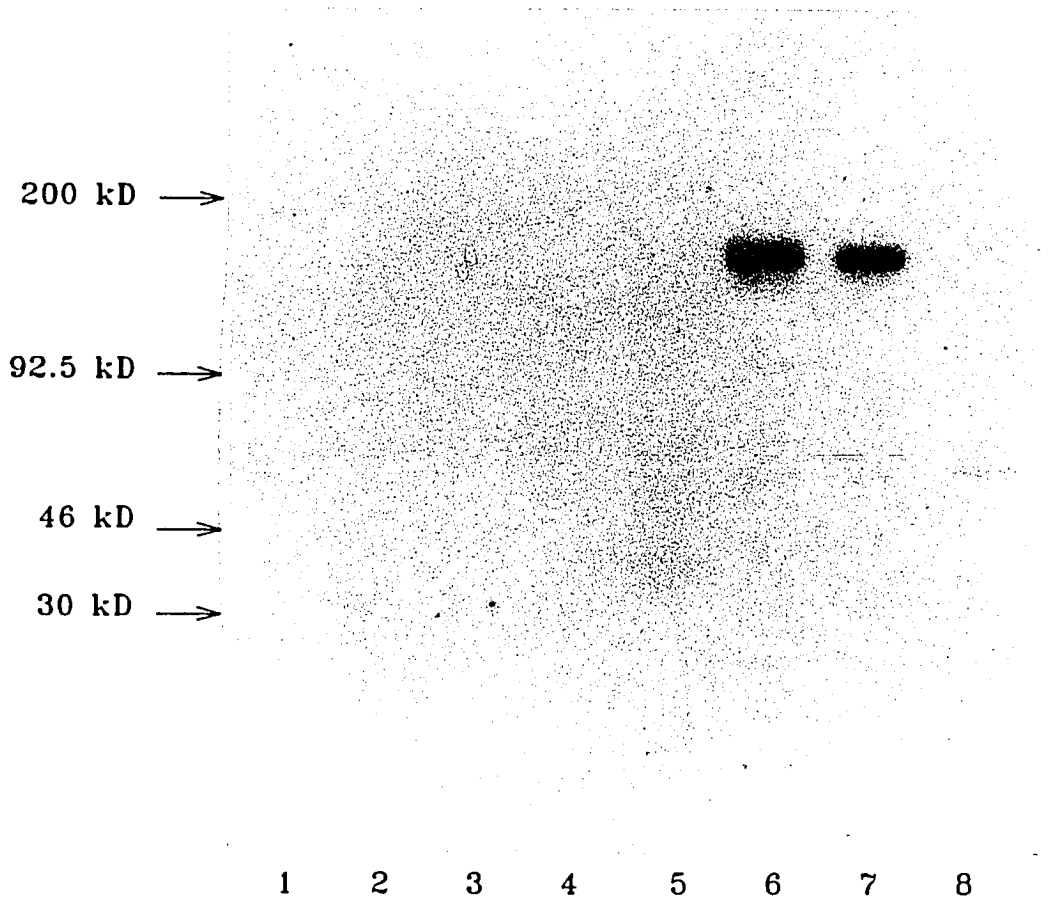

Lanes 1 and 2, human and chicken peripheral myelin, respectively; lane 3, MAG; lane 4, N-CAM; lane 5, brain; lane 6, CaP; Lane 7, BPH; and lane 8, normal prostate. Electrophoresis was a 4-15% gradient gel run under reducing conditions.

Figure 17. Western blot of prostate extracts reacted with TURP-27 or anti-N-CAM..

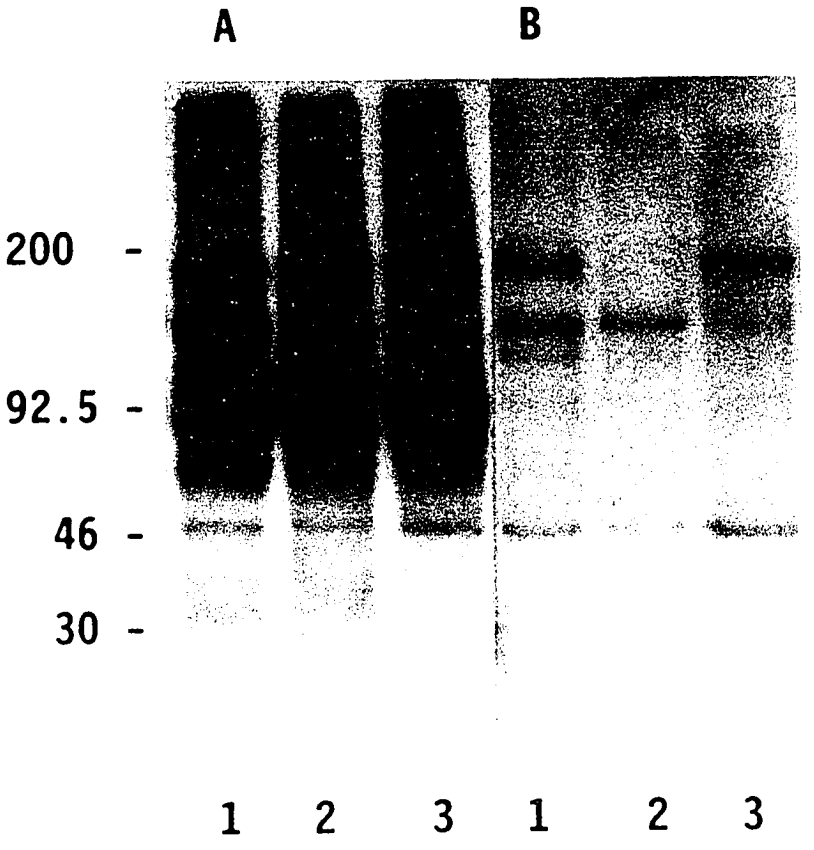

Panel A, TURP-27; panel B, anti-N-CAM. Lane 1, BPH extract; lanes 2 and 3, CaP extracts. Total protein was 75μg/lane, and electrophoresis was on a 4-15% gradient SDS-polyacrylamide gel under reducing conditions.

1). The 140 KD band was the only band detected by anti-N-CAM in one CaP extract (lane 2), while a second CaP extract (lane 3) showed the 180 KD band and a faint 140 KD band.

The anti-MAG immunoblot of prostate extracts was essentially negative. Figure 18 shows MAb B11F7 staining a 100 KD band in the positive control human peripheral nerve myelin, lane 1, and human brain extract, lane 8. Also seen in the brain extract is a 90 KD band just below the major 100 KD band. A band at approximately 50 KD is detected within myelin and all other tissues except brain. The possible light staining of a 90 KD band in the prostate extracts as well as the breast extract is lightly visible but must be taken as inconclusive. The nonspecific endogenous antibody band at 55 KD is apparent most intense one of the normal prostates and both CaPs, lane 4,7 and 8 respectively.

Turp-27 and HNK-1 Positive Glycolipids

Because it is a well established observation that the HNK-1 epitope occurs as the sulfated termini of at least two peripheral nerve system glycolipids (27,28,29) and TURP-27 is cross-reactive with this tissue, it was determined if TURP-27 binds to PNS, CNS or BPH glycolipids. In isolating the glycolipids from tissue samples three fractions were obtained (see Methods and Materials). These fractions are

Figure 18. Western blot analysis of several tissues with MAb B11F7 (anti-MAG). Lane 1, Rainbow molecular weight markers; lane 2, peripheral nerve myelin, lane 3 and 4, normal prostate extracts; lanes 5 and 6, BPH; lanes 7 and 8, CaP; lane 9, human brain; and lane 10 breast carcinoma. Electrophoresis was on a 4-15% gradient gell under reducing conditions with 80μg/lane total protein.

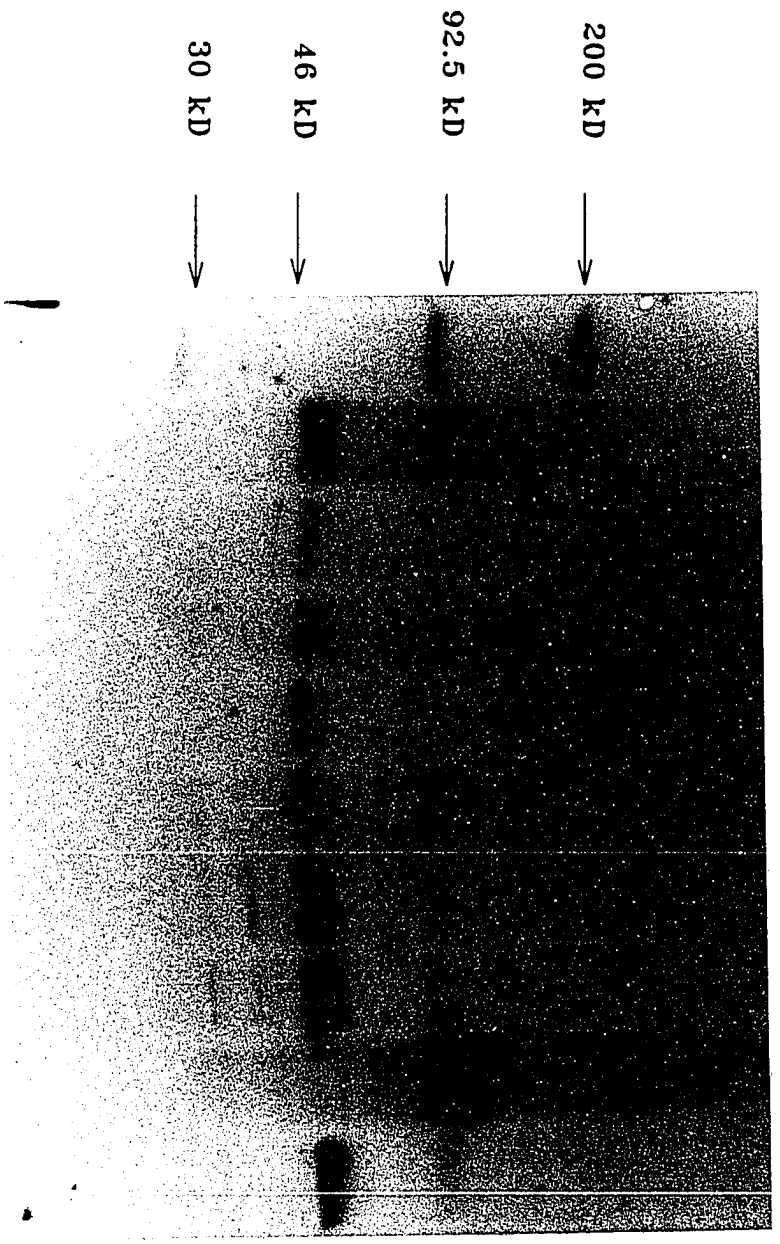

Table 3. MAb TURP-27 and MAb HNK-1 Reactivity to Fractionated Glycolipids

		MAB TURP-27
BRAIN	Upper Layer Organic	247
	Upper Layer Aqueous	284
	Lower Layer	406
PNS	Upper Layer Organic	2,380
	Upper Layer Aqueous	366
	Lower Layer	333
BPH	Upper Layer Organic	894
	Upper Layer Aqueous	614
	Lower Layer	386

Values are the average of duplicates expressed in CPM
MAb P3 served as the negetive control and values were approximately 300 CPM

termed upper layer organic, upper layer aqueous, and lower layer and are the result of the different partitioning character of glycolipids within the lipid extract mixture. Table 3 shows the results of an RIA performed on each fraction from PNS, CNS and BPH reacted with MAbs TURP-27 and HNK-1. Reactivity to HNK-1 is found within both the upper layer organic and lower layer of all three tissues. Reactivity to MAb TURP-27 is only clear within PNS and BPH upper layer glycolipids. The variation between wells was less than 10% and the result are representative of two experiments.

The investigation was extended to include immunooverlay with TURP-27 and HNK-1 of TLC separated upper layer organic glycolipids. Initial TLC separation and overlays of crude upper layer organic glycolipids were not informative due to rocketing (caused most likely by glycopeptide contaminants) within the lanes. Because the TURP-27 and HNK-1 epitopes are negatively charged, sialic acid and sulfate respectively, a DEAE column binding and elution of the upper layer organic fraction was performed and followed by immunooverlay of the wash and elution fractions. Figure 19, lane 5, reveals that MAb HNK-1 stains the two previously reported glycolipids from PNS. The heavier band running between the standards M_1 and D_{1a} is sulfate-3-glucoronyl paragloboside and the lower band is sulfate-3-glucoronyl neolactohexaosyl ceramide. A faint band appears in lane 4, CNS, running slightly higher than these bands. This position is not unexpected in light

Fig. 19. MAb HNK-1 immuno-overlay of brain PNS and BPH glycolipids. Upper layer organic glycolipids were run on a DEAE column and split into wash and elution fractions. Lanes 1-3 are wash fractions and lanes 4-6 are elution fractions. Lanes 1 and 4 are from extracted brain, lanes 2 and 5 from peripheral nerve, and lanes 3 and 6 from BPH. Glycolipid standards are noted to the right.

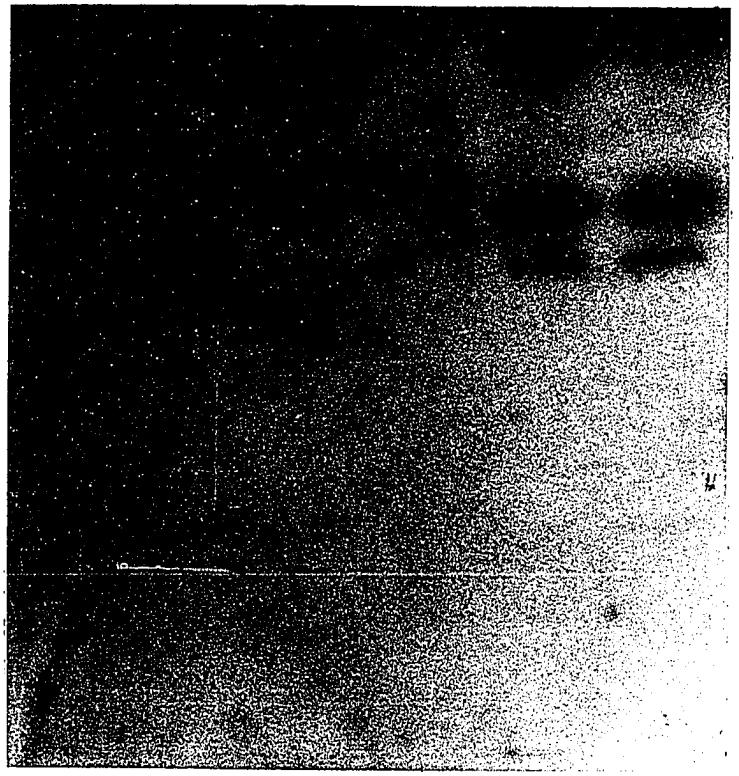

of published results showing that PNS and CNS HNK-1 positive glycolipids differ in fatty acid composition (63). Lane 6 shows that at least two glycolipids from BPH are MAb HNK-1 positive and that their mobility is comparable to the identified glycolipids from PNS. Faint banding is also seen in the wash fractions implying some bleed through from the DEAE column. What may be important to note is banding in the upper portion of the plate. These bands remain unidentified and may represent specific and/or artifactual staining.

Figure 20 shows the same samples as used in figure 19 except the overlay was conducted with MAb TURP-27. The plate was run in a separate chamber so the mobility of the glycolipids appeared slightly retarded relative to figure 19. TURP-27 does not react with any glycolipids within the same range as the known HNK-1 positive lipids. However, banding is seen in the upper portion of the plate. Lanes 1 and 4, CNS, show no staining in this area which correlates with the negative TURP-27 RIA results for this tissue (see Table 3). PNS shows strong staining in the DEAE retained fraction, lane 5, while BPH is somewhat lighter, also correlating with RIA data. It can not be ruled out that the staining at the upper area of the plate is artifact except to say that qualitatively, the staining pattern observed observed with TURP-27 differs from that with HNK-1.

Fig. 20. MAb TURP-27 immuno-overlay of brain PNS and BPH glycolipids. Upper layer organic glycolipids were run on a DEAE column and split into wash and elution fractions. Lanes 1-3 are wash fractions and lanes 4-6 are elution fractions. Lanes 1 and 4 are from extracted brain, lanes 2 and 5 from peripheral nerve, and lanes 3 and 6 from BPH. Glycolipid standards are noted to the right.

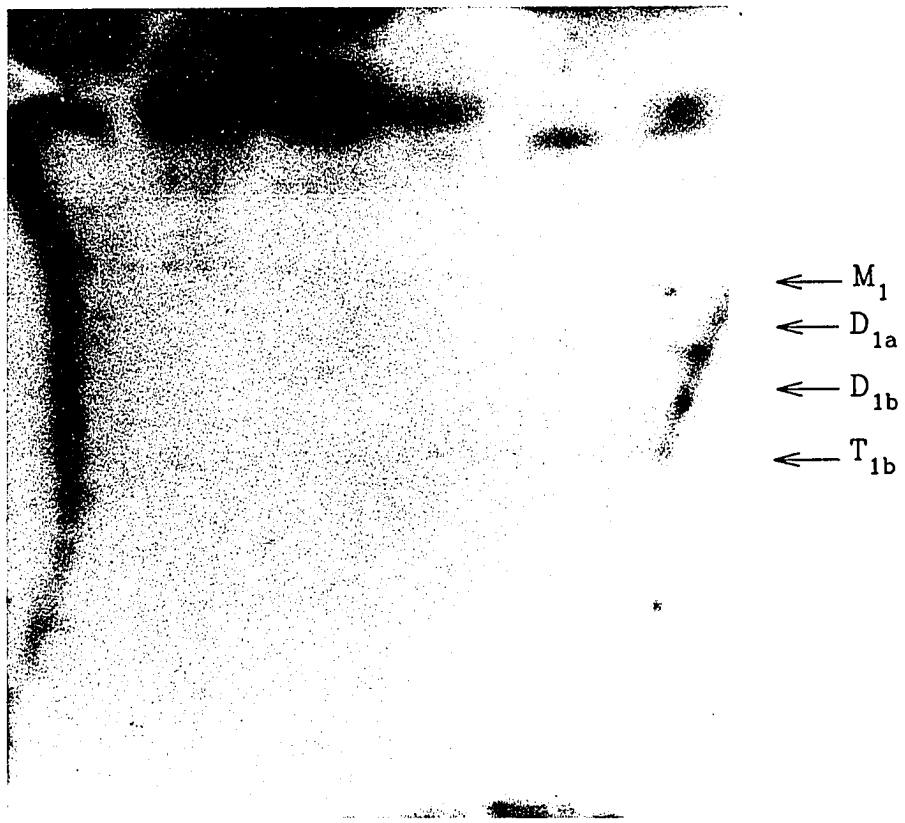

1 2 3 4 5 6

TURP-27 Purification Efforts

An attempt was made to further characterize the chromatographic behavior of the TURP-27 antigen. No prostate cell lines existed which were TURP-27 positive, greatly limiting feasible techniques. Only human prostate gland tissue taken at the time of tumor surgery or autopsy and seminal plasma from normal healthy donors were available. Autopsy material was not always reliable in its quality due to uncontrolled exposure times to proteolytic breakdown. These facts resulted in a reduced availability to the quantities of antigen necessary for analysis. Pooling of samples was avoided where possible due to the heterogeneity of protein species between individuals (see Western blots above).

Antigen Solubilization

Table 4 shows the results of a solubilization study conducted using a membrane extract from a CaP. An important observation was that protein was released into the PBS in which these extracts were stored, most likely by freeze thaw. If prostate membrane preparations were made as described in Materials and Methods, followed by freezing at -70° C, as is customary, then thawed, protein could be measured in the PBS supernatant following a 15,000 x g spin for 15 min. This quantity was substantial, amounting to 33%

Table 4. Membrane Extract Detergent Solubilization

	Supernatants			Pellets		
Solution	Protein Conc. (μg/ml)	Total Protein (mg)	% Total Protein	Protein Conc. (μg/ml)	Total Protein (mg)	% Total Protein
PBS	0.55	0.55	33			
4mM CHAPS [a]	0.541	0.271	16 (d)	1.55	0.775	46
0.5% NP-40 [b]	0.878	0.439	26 (e)	1.48	0.740	44
1.0% NP-40 [c]	0.972	0.486	29 (f)	1.31	0.655	39

Total Protein Recovery (triplicate determinations)
a. 95%
b. 103%
c. 101%

Percent Protein Solubilization from First Spin Pellet
d. 26%
e. 37%
f. 43%

Table 5. MAb TURP-27 Binding Activity to Detergent Solubilized CaP Membrane Extract

Sample	Fraction	Counts/Min	Percent Original	Activity/ μg protein *
CaP Extract	original	8,061	100	1,607
PBS	supernatant	2,497	31	1,513
4mM CHAPS	supernatant	4,042	50	2,490
	pellet	1,579	20	340
0.5% NP-40	supernatant	4,086	51	1,551
	pellet	1,254	16	282
1.0% NP-40	supernatant	4,155	52	1,424
	pellet	1,575	20	396

* Expressed as CPM/μg protein

of the total starting protein (Table 4). When this fraction was analyzed for the TURP-27 antigen it represented 31% of the initial sample's activity as measured by cpms/μg protein, Table 5.

The remaining 67% of the protein and activity remained in the membrane bound state. Two detergents were tested for their ability to solubilize the antigen, CHAPS and NP-40 at 0.5% and 1.0%. Table 4 shows that NP-40 at both concentrations was more effective than CHAPS, 37% and 43% versus 26% total protein solubilized, respectively. However, table 5 shows that CHAPS released higher activity/μg protein than either concentration of NP-40, 2,490 cpm versus 1,551 or 1,424 cpm, respectively. The insoluble pellet remaining after detergent treatment represented between 39% and 46% of the total starting protein (table 4). Table 5, however, shows that for all three detergents the activity/μg protein in the insoluble pellet was small.

Seminal Plasma

Size Exclusion Chromatography

On RIA whole seminal plasma gave low but reproducibly positive results. Seminal plasma, 28 mg, was loaded onto a Sephadex G-200 column preequilibrated with PBS, 0.5 M NaCl and eluted at a flow rate of 1.5 ml/min. One min fractions were collected and analyzed for protein and MAb TURP-27

Fig. 21. Sephadex G–200 size exclution column run after loading a soluble seminal plasma fraction. The elution buffer was PBS with 1.0 M NaCl.

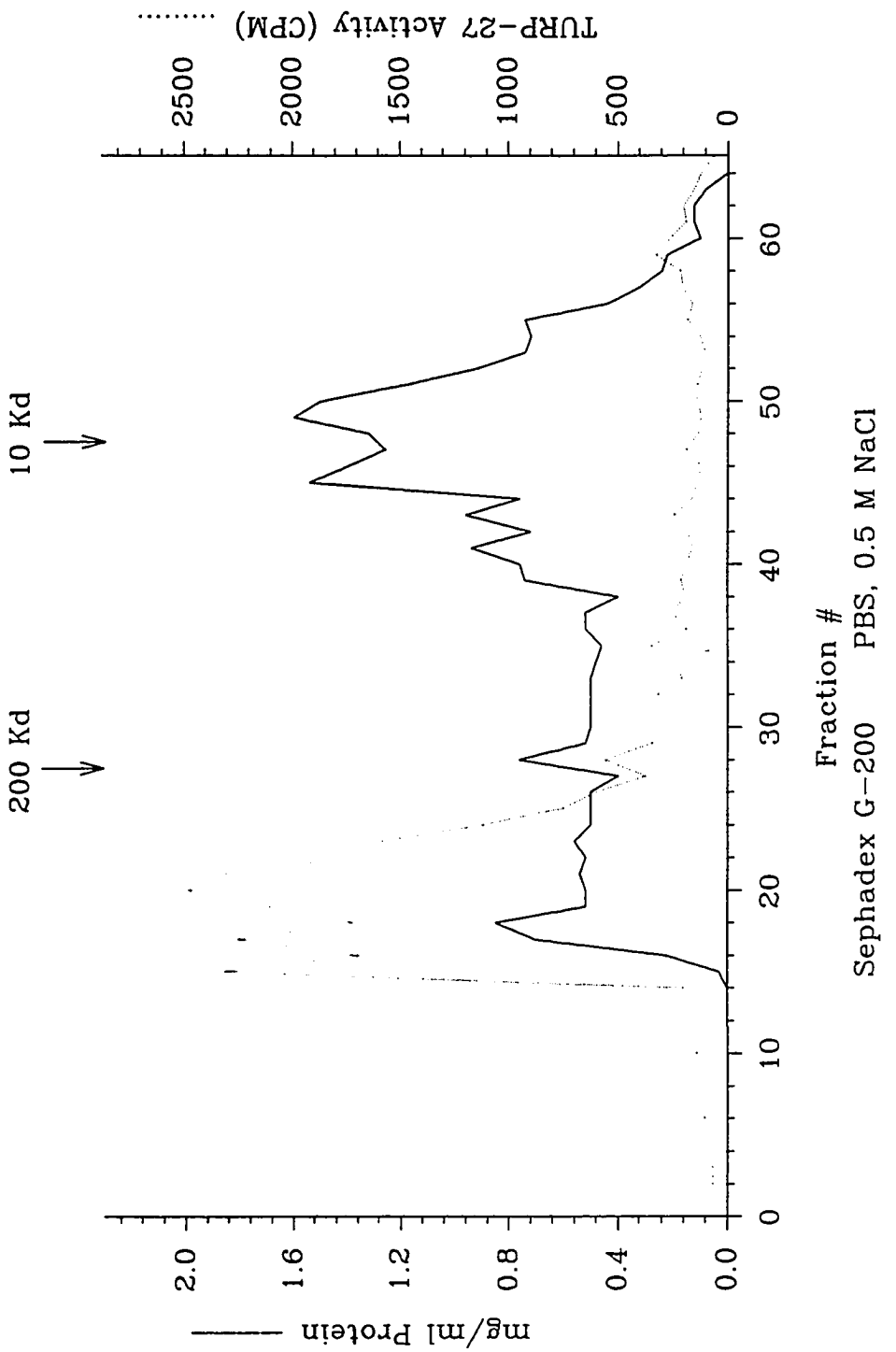

binding activity in RIA. The chromatograph is depicted in figure 21. The majority of protein within seminal plasma is in the >200 Kd range, however, the TURP-27 activity is almost exclusively in the <200 Kd range. No clear separation of the multiple protein species which are demonstrated by Western blot was evident. NaCl was included to reduce protein aggregation. A similar column run using 1.0 M guanidine HCl, a more active chaotropic agent, yielded no appreciable change in the chromatograph (not shown).

Ion Exchange Chromatography

A 30-70% ammonium sulfate fraction of seminal plasma was loaded onto a DEAE column equilibrated with 10 mM Tris-HCl, pH 7.8 and eluted with a combination step and linear NaCl gradient. Two ml fraction were collected and analyzed for protein content and TURP-27 activity. The chromatograph is depicted in figure 22. Protein peaks are evident after incremental increases in NaCl but fine resolution is absent. The TURP-27 antigen eluted with greatest activity in the void volume and 1.0 M NaCl striping peaks. All other fractions show a relatively low activity with the exception of fraction 65 eluting at the initiation of 0.08 M NaCl. Other known prostate antigens were also followed in RIA, these include; prostate specific antigen (PSA), prostatic acid phosphatase (PAP) and prostate secretory protein (PSP). PSA eluted with a major peak at fraction 70, PAP at fraction

Fig. 22. Seminal plasma resolved on a DEAE-CL-6b column eluted with a combination step and linear salt gradient. Total protein was monitored by 280 nm absorbance and the filled circles represent MAb Turp-27 activity in RIA.

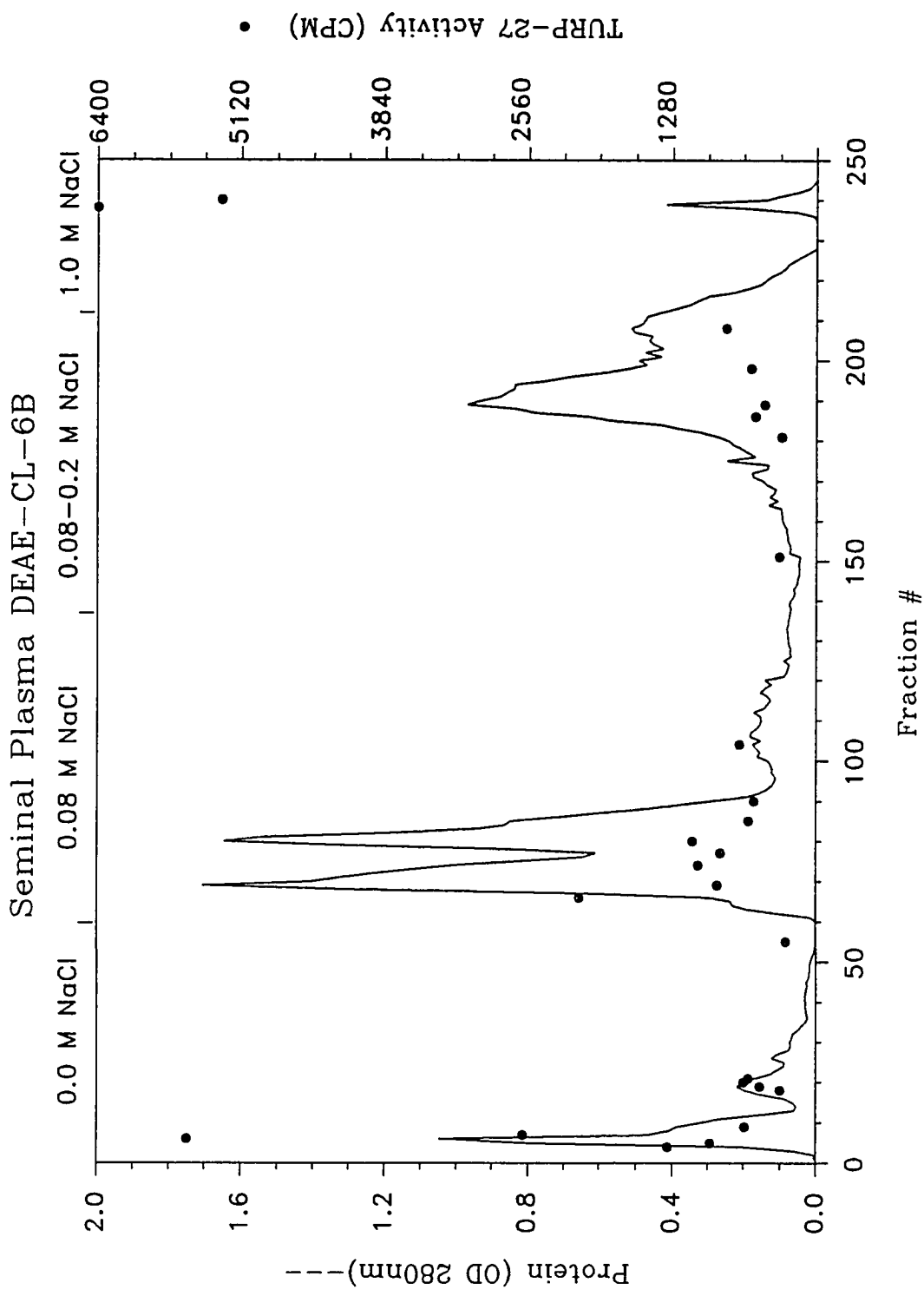

190 and PSP at fraction 85 (not shown). All three antigens were represented in the void volume.

It was noted that after the 30-70% ammonium sulfate precipitate was pelleted, resuspended and dialysed that a substantial quantity of insoluble protein was present. A different approach to processing was tried. A straight 70% precipitation was made, pelleted and solubilized in 0.5% NP-40. This was followed by dialysis and a clearing centrifugation step. The sample was then applied to a DEAE column as decribed in figure 22. Figure 23 shows the resulting chromatograph. The TURP-27 activity is represented most greatly in the higher salt elution fractions. But, less activity is found in the void volume peak relative to figure 22.

For further analysis, the 1.0 M NaCl fraction 595 from figure 23 was buffer exchanged and 50 μl were loaded onto a Bio-Sil SEC-250 column. The column was eluted with 0.1 M Na_2SO_4, 0.02 M NaH_2PO_4 at 1 ml/min. Fractions were collected and assayed for TURP-27 activity. The chromatograph is depicted in figure 24. A large part of the protein eluted in the void volume implying high molecular weight components or complexes. The highest representation of TURP-27 binding activity is also located in the high molecular weight fraction similar to what was found by size exclusion chromatography of whole seminal plasma (figure 21). Under these conditions, however, some activity is found in lower molecular weight fractions in the 60-160 Kd range.

Fig. 23. A detergent soluble fraction of seminal plasma resolved on a DEAE–CL–6B column eluted with a combination step and linear salt gradient. Total protein was monitored by 280 nm absorbance and the filled triangles represent MAb TURP–27 activity in RIA.

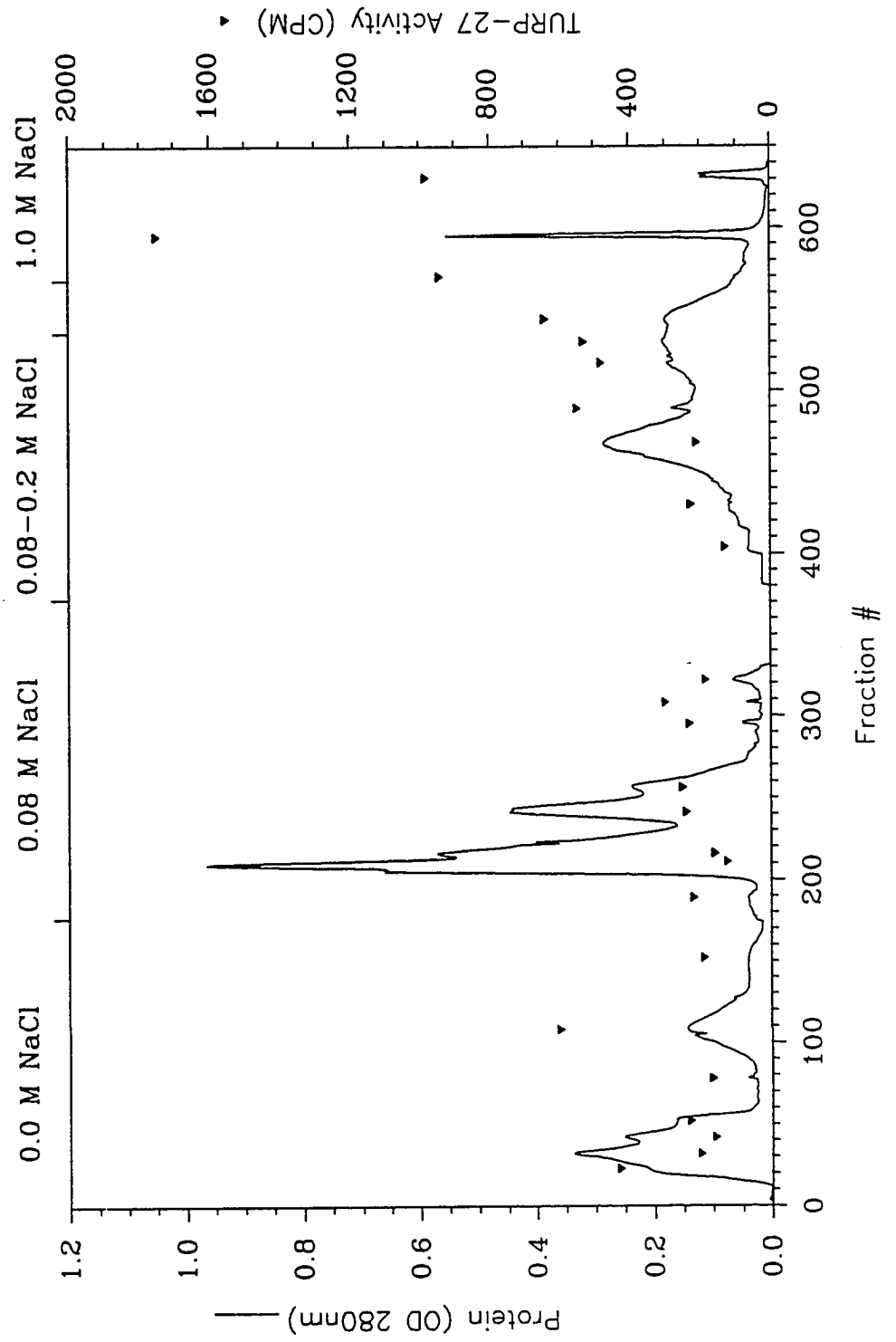

Fig. 24. Fraction 595 from the DEAE column run depicted in figure 23 resolved on a Bio-Sil 250 size exclusion column. Total protein was monitored by 280 nm absorbance and the filled triangles represent MAb TURP-27 activity in RIA.

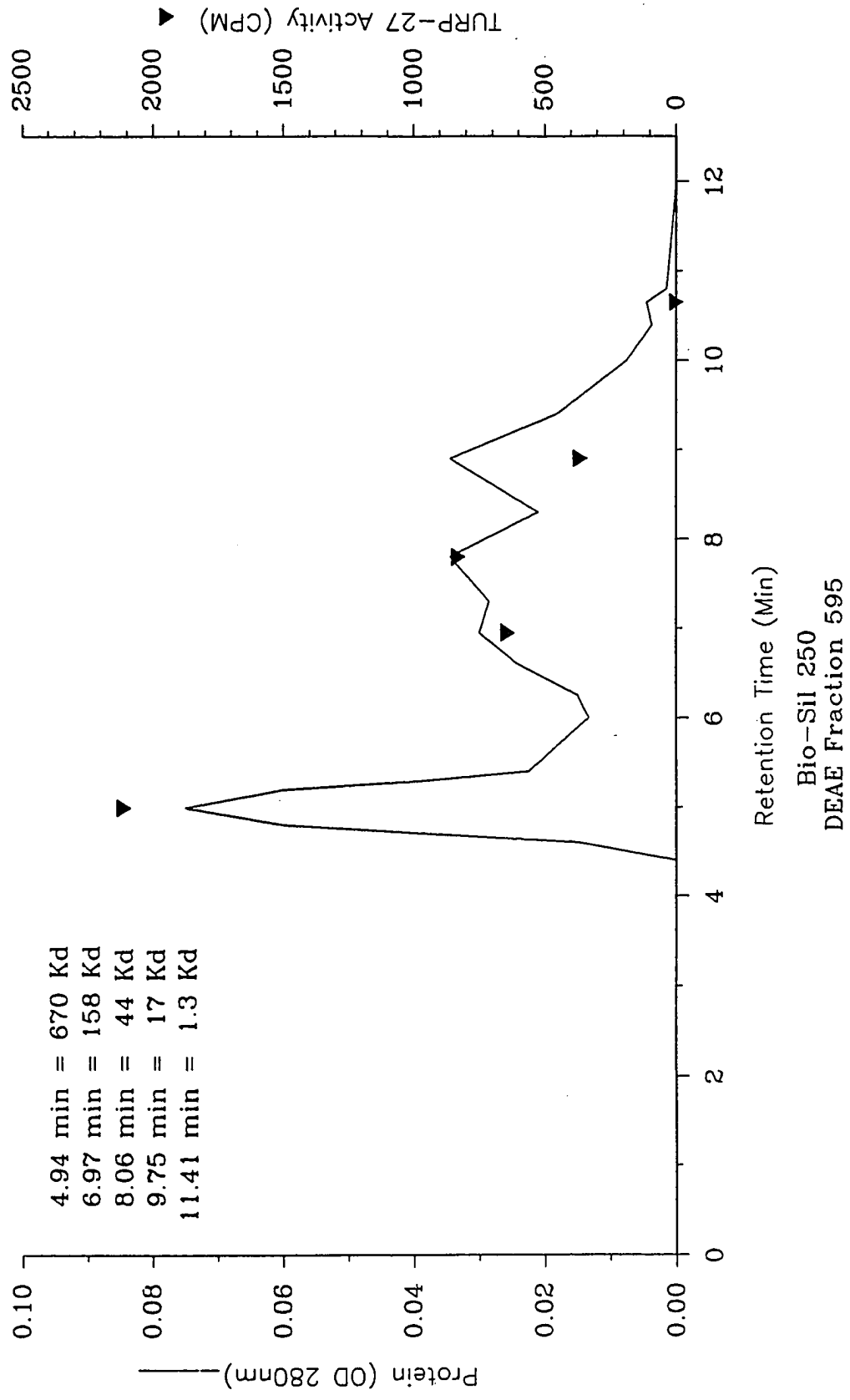

Fig. 25. Seminal plasma resolved on a HPLC DEAE column eluted with linear salt gradient. Total protein was monitored by 280 nm absorbance and the hollow circles represent MAb TURP-27 activity in RIA while the filled circles represent anti-PSA activity.

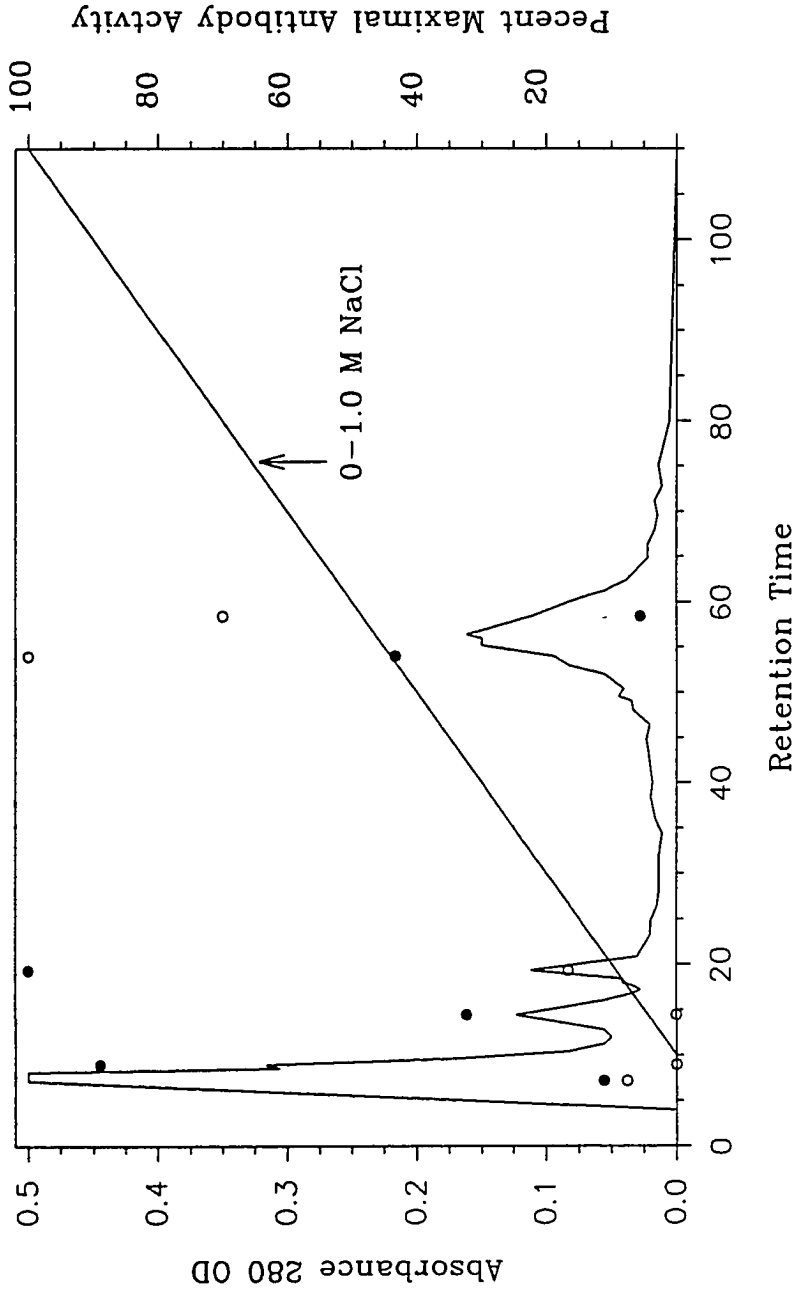

In order to more closely establish the elution condition for the TURP-27 antigen from a DEAE column, a sample of seminal plasma was loaded onto a HPLC DEAE column and eluted with a 0 to 1.0 M NaCl linear gradient. The fractions were collected and assayed for TURP-27 and PSA activity (figure 25). There were only 4 distinctive protein peaks. The TURP-27 activity eluted at 0.45 M NaCl, fraction 55. The PSA eluted primarily in the void volume peak, fraction 10, and 0.1 M NaCl peak, fraction 20. The data parallel the result shown in figure 22 and 23, but more precisely gives the salt concentration for elution of the TURP-27 antigen.

Affinity Chromatography

Affinity Column and Elution Conditions

Attempts were made to link the MAb TURP-27 to Affi-gel 10 and to the Immunopure matrix manufactured by Pierce. However, both were unsuccessful. When the Affi-gel Hz matrix was used to couple MAb TURP-27, 77% of the antibody was retained on the column and it was capable of binding antigen. In order to efficiently and safely elute the TURP-27 antigen from the Affi-gel Hz column, an assay was devised to test eluants using an RIA format (see Materials and Methods). The results are graphically depicted in figure 26. The open bars represent the effect of the eluants on the

Fig. 26. An elution and epitope resistance profile for the MAb TURP-27 antibody antigen interaction.

TURP-27 antigen relative to MAb TURP-27 binding. No eluant had a significant effect on the antigen relative to the PBS control. The hatched bars represent the eluant's ability to disrupt antibody-antigen binding. The various eluants have a range of elution capability. High NaCl and guanidine HCl were the most effective while pH extremes were less effective. The PBS, 1.0 M NaCl elution buffer was used because it is easier to handle than guanidine HCl. In subsequent experiments it was found that 0.5 M NaCl would suffice (not shown).

Affi-gel Hz TURP-27 Chromatography

A PBS soluble fraction from a BPH membrane extract was loaded on the Affi-gel HZ TURP-27 affinity column that had been equilibrated with PBS and was eluted with 1.0 M NaCl. Figure 27 shows the protein absorbance (solid line no points), and the binding activity of MAb TURP-27 and the iso-typed matched control antibody P3. The majority of the protein was eluted in the wash. The TURP-27 activity was the same in the retained and non-retained fractions while the P3 control also has a activity peak in the wash fractions as well as a small peak in the elution peak.

Figure 28 depicts the Affi-gel HZ TURP-27 chromatograph of the an NP-40 solubilized pellet from a BPH membrane extract. All steps were conducted the same as in figure 27 except that 0.5% NP-40 was included in the buffer and the

Fig. 27. Affi-gel HZ TURP-27 column loaded with PBS soluble proteins from a BPH extract. Total protein was monitored by 280 nm absorbance and the filled circles represent MAb TURP-27 activity in RIA while the open circles represent the activity of the negative control antibody. The eluent was 1.0 M NaCl.

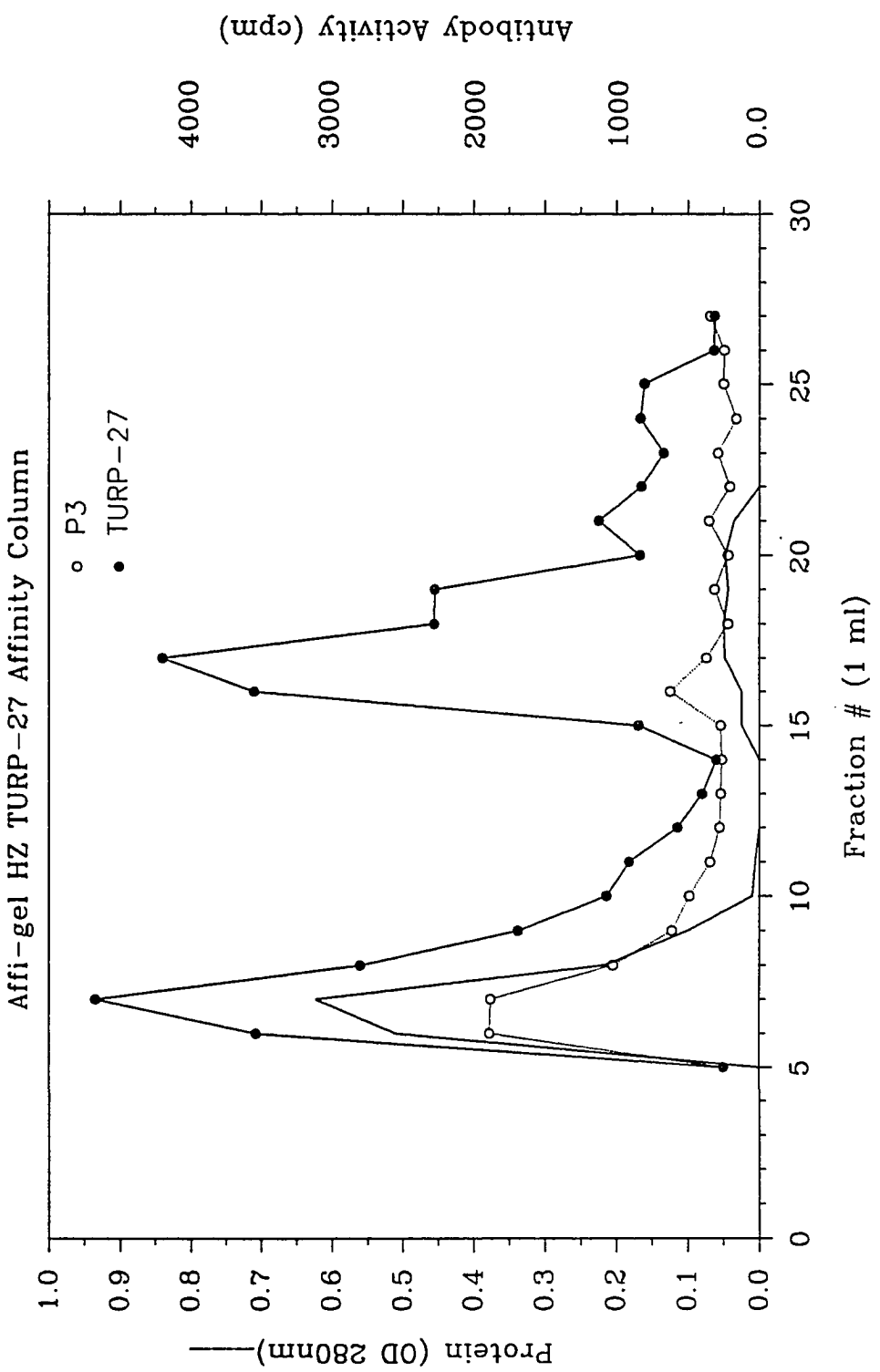

Fig. 28. Affi-gel HZ TURP-27 column loaded with NP-40 soluble proteins from a BPH extract. The filled circles represent MAb TURP-27 activity in RIA while the open circles represent the activity of the negative control antibody. The eluent was 1.0 M NaCl.

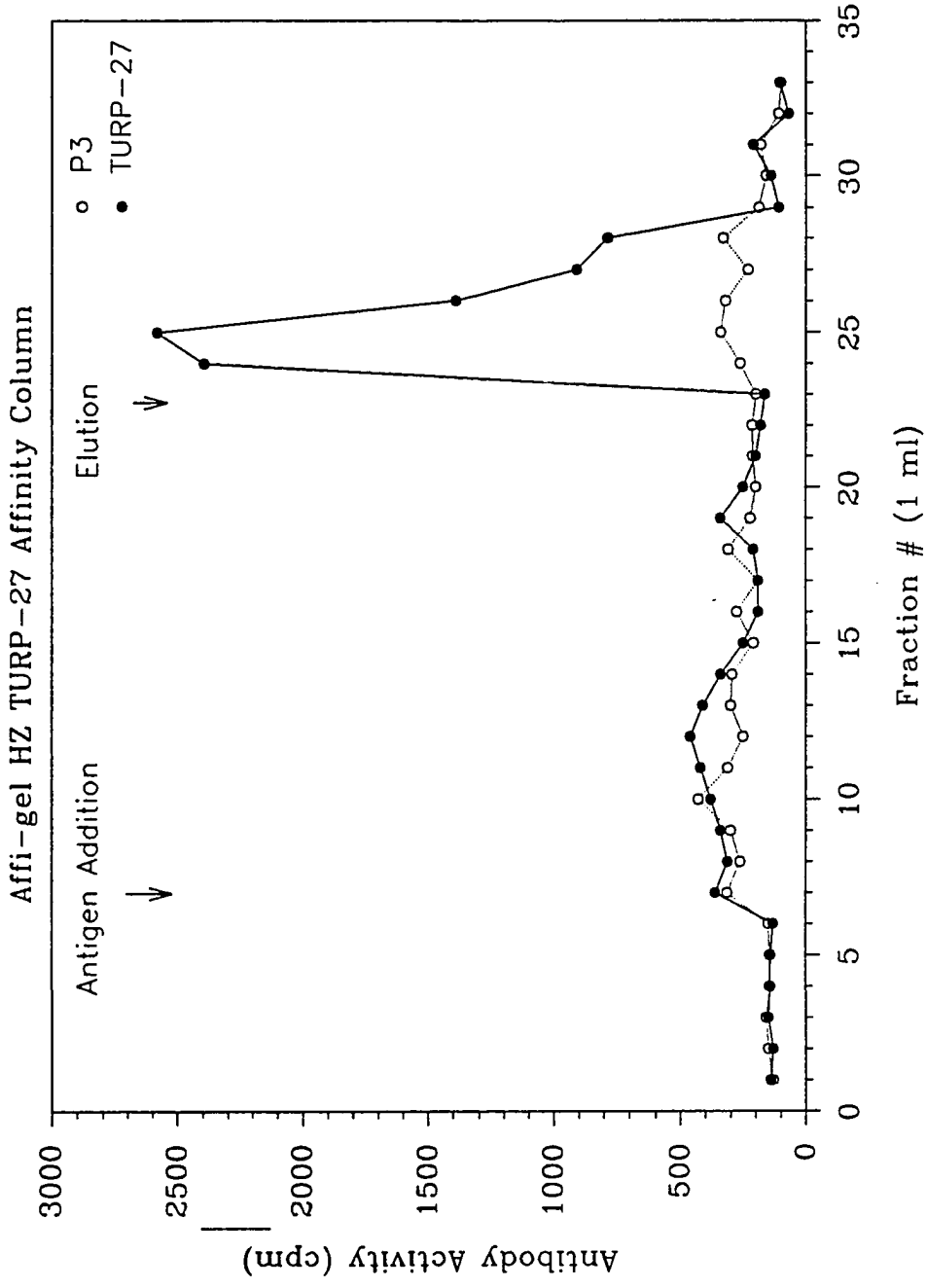

absorbance at 280 nm was not monitored due to strong UV absorbance by NP-40. In this sample there was very little activity of TURP-27 or P3 in the wash fractions. A TURP-27 activity peak was evident in the elution peak with only background P3 activity. Attempts were made to analyze the TURP-27 fractions on SDS-PAGE followed by Coomassie blue or silver staining but no bands were detected (not shown).

The Turp-27 positive fractions were further analyzed for reactivity to several other antibodies. Table 6 shows that the Affi-gel HZ TURP-27 column eluant was positive for MAb TURP-27, MAb HNK-1, polyclonal anti-N-CAM and HSP-2 (HSP-2 is an anti N-CAM antibody, but of low affinity in this study). The MAb PD-41, developed in our laboratory (60), recognizes another high molecular weight prostate antigen but was negative to pure TURP-27 antigen. All antibodies were negative to another common prostate antigen PSA.

Table 6. Affinity Purified TURP-27 Antigen in Radioimmunoassy

Antibody	TURP-27	HNK-1	N-CAM	HSP-2	PD-41
Anti-TURP-27 Column Eluent	9,969	3,675	12,498	1,753	182
Prostate Specific Antigen	244	354	220	250	371

Values are expressed as a mean of triplicate determinations minus background in terms of counts per minute

Chapter IV

Discussion and Conclusion

The goals of this study were to characterize the biochemical nature of the TURP-27 antigen and to determine its relationship to the HNK-1 antigen. The MAb TURP-27 was produced by hyperimmunization of a Balb/c mouse with a pool of transuretheral resection tissue, the pool including one prostate adenocarcinoma and three BPH tissue samples (25). An extensive study of the tissue expression patterns of the TURP-27 antigen in both fixed and frozen tissues has been conducted (25,26). Within prostate, the antigen was found within the cell membrane of normal, benign and malignant ductal epithelial cells. Approximately 10% of normal prostatic ductal cells stained with the antibody and the pattern was diffuse. However, 75-100% of ductal cells and 20-100% of tumor cells stained within BPH and CaP, respectively. The antigen was also found in fetal prostate, perhaps implying the antigen is an oncofetal developmental antigen (26). In radioimaging studies, the MAb Turp-27 was found to specifically target human prostate tumor tissue in a murine subrenal capsule model, implying a potential clinical use (63). Until the current study no information was known as to the biochemical nature of the TURP-27 antigen or epitope.

Antigen Characterization

Initial characterization of the TURP-27 antigen was by Western blot analysis using prostate membrane preparations. It was discovered that a multi-banding pattern was common to all preparations tested (note figs. 1,3,4). Concern about the quality of the Western blot bands and integrity of the proteins led to several modifications of blotting and the membrane preparation procedure. It was found that using gradient gels and slow rates of transblot in the absence of methanol considerably enhanced the amount of material retained on the PVDF membrane and the clarity of the bands (not shown). To ensure, to the best of our ability, that the multiple banding was not due to protease activity, a panel of protease inhibitors was incorporated into the membrane preparation procedure. Membrane solutions were also monitored for protease activity and found to be negative. However, degradation of the antigens can not be ruled out. Degradation may have occurred before the tissue was received. Although the tissue was frozen to -70°C shortly after surgery, proteolytic degradation may occur in-vivo and/or in-vitro prior to freezing. Also freeze thaw and/or the membrane extraction procedure itself could have conceivably damaged the antigen. Proteolytic degradation, however, is not believed to be the best explanation for the multi-banding pattern.

Western blot analysis revealed that a minimum of four specific bands can be expected from BPH membrane preparations, with approximate molecular weights of 180, 140, 120, and 90 KD (figs. 1,3,4). Within BPH there was also the less consistent 69 KD band (figs. 3,4). CaPs revealed a similar pattern, however, bands of greater than 200 KD and occasionally 40 KD were observed. Among CaPs the mobility of the 180, 140, and 120 KD bands shifted somewhat from sample to sample and on occasion additional bands were evident. Normal prostate yielded variable results, as it did in RIA and immunohistochemistry (25,26). The bands, if apparent at all, were similar to BPH but less intense (figs. 3,4). Normal seminal plasma was also positive in Western blot, reflecting the pattern of normal prostate tissue, with the typical exception that the 180 KD band was absent (fig. 4). If antigen degradation is not responsible for multiple banding, a possible explanation is that the TURP-27 epitope is a carbohydrate structure present on several different proteins. Similar glycoprotein antigen complexes have been described for breast carcinoma (64), small-cell lung carcinoma (48), and melanoma (65). Also, a series of 8 different glycoproteins bearing the epitope for the Leu-7/HNK-1 MAb have been described (66).

Two other bands, a 55 KD and less frequently a 25 KD band, appeared throughout the study in some tissues. Figure 1 and 5 demonstrate that these bands were non-specific and probably the result of binding by the secondary radiolabeled

antibody. When the isotype-matched negative control antibody J606 was used to stain blotted membranes, only these bands were visible (fig. 1,5 and not shown). Because of their relative molecular weight they were presumed to be human antibody endogenous to some of the membrane preparations (fig. 1) and detected by the labeled rabbit anti-mouse secondary antibody. This observation is strengthened by the banding pattern observed in the membrane extracts of the in-vivo mouse model of primary prostate carcinoma tumors (fig. 5). Only bands at 55 and 25 KD were present on the TURP-27 and J606 stained PVDF membranes. Also in support of this conclusion, all brain tissues blotted never showed bands at 55 or 25 KD, presumably due to the blood brain barrier excluding antibody from these tissues. Endogenous antibody background reactivity in some preparations was also noted in column purification runs (fig. 27).

Western blot results of prostate extracts under non-reducing conditions yielded non-specifc protein bands (fig. 2). Only the bands of endogenous antibody were visible with the possible exception of a 75 KD band and a band at the origin of the running gel for the BPH sample. This result was representative of three attempts. A possible explanation was that in the non-reduced state the antigen was part of a complex or aggregate that does not move into the gel and/or transblot well due to size, or, the net charge of the antigens was not conducive to transblotting procedures. The native size of the TURP-27 antigen was found to be in excess

of 200 KD by size exclusion chromatography under several elution conditions (see fig. 21,24), implying a multimeric structure or aggregation. Since the non-specific bands are strongly present and in a position suggestive of non-reduced antibodies (160 KD), the overall treatment, electrophoresis and blot must have been successful.

Two-dimensional Western blots were attempted several times. The results were always faint and difficult to interpret. Figure 6 was representative and shows that the antigens have an acidic isoelectric point, although the exact pH was not determined. This observation alone is insignificant. However, an approximate isoelectric point can assist in the design of a purification protocol.

Although MAb TURP-27 reactivity to non-prostate tissues was not noted in the primary report by Starling et al. (25), concurrent with this study it was reported that MAb TURP-27 cross-reacted with some normal cells by Wright et al. (26). The most consistent staining was to peripheral nerve and brain in 100% of the frozen tissues tested. However, less consistent staining was also noted in some neuroendocrine-like cells, such as adrenal medullary cells and chief cells of the stomach. Also, staining of large granular lymphocytes, possibly NK cells, was noted. Because of these observations, human brain membrane extracts were Western blotted to extend the scope of the TURP-27 antigen characterization. Figures 3 and 4 show that MAb TURP-27 staining of brain extracts gave a multiple banding pattern

in Western blot similar to prostate extracts. Figure 4 shows that some of the protein bands from brain have very similar mobilities to the proteins previously observed in prostate extracts. These are the 180, 140 and 120 KD bands primarily, although brain also gives bands in the >200 KD range similar to CaPs.

A relationship emerged that implied the TURP-27 antigen may be the same or similar to the HNK-1 antigen. It was known that the MAb HNK-1 stained prostate tumors by immunohistochemistry (24), and the pattern of reactivity was not unlike that of MAb TURP-27 as reported by Wright et al. (26). Wahab and Wright reported that MAb HNK-1 stained peripheral nerve and cells of neuroendocrine origin as well as natural killer cells (24). This pattern of reactivity is also similar to MAb TURP-27. However, the extensive staining of neuroendocrine cells and tumors of neuroendocrine origin seen with MAb HNK-1 was not a characteristic of the TURP-27 antibody (22,23,26). A previously described Western blot using MAb HNK-1 to stain brain proteins had been published by Noronha et al.(67). The pattern was multi-banded with relative molecular weights nearly identical to the MAb TURP-27 pattern against brain extracts as depicted in figure 4.

Upon direct comparison of MAb TURP-27 and MAb HNK-1 staining of various tissue membrane extracts run in Western blot, it became obvious that the two antigens were very closely related if not identical (figs. 7,8). When the two antibodies were used to stain seminal plasma proteins of

both normal individuals and prostate cancer patients, the multi-banding patterns were identical (fig 7). This observation was corroborated by using prostate and brain membrane extracts. Figure 8 shows that the multi-banding pattern, discussed above, for MAb TURP-27 within normal prostate, BPH, CaP and brain was exactly the same as blots using MAb HNK-1. The only exception was within brain extracts, where more bands can be detected with MAb HNK-1 (more apparent in figs. 13,14). The MAb HNK-1 was raised against the lymphoblastoid cell line HSB-2, while the MAb TURP-27 was raised against a pool of prostate tumor membrane extracts (21,25). These tissues as well as brain appeared to have antigens that were strikingly similar.

Purification Efforts

In order to assist in TURP-27 antigen characterization and potentially supply antigen to use in immunizations for second generation antibodies, attempts were made to define the criteria necessary for purification. As a first step solubilization studies were conducted. Table 4 demonstrates that antigen can be found in the PBS supernatant from membrane preparations, and accounts for approximately 33% of the total protein. When CHAPS or NP-40 were used to solubilize the remaining pellet only about 1/3 of the protein was released with the remainder in the pellet (see table 4). Table 5 demonstrates, however, that 50 % of the

total antibody reactive protein is released into the detergent resulting in an enrichment of 3 fold. The PBS soluble fraction contained 31% of the activity indicating it as a potential source, although no enrichment occurred.

Because of the limited availablity of large quantities of prostate tumors, seminal plasma was used to identify the chromatographic characteristics of the TURP-27 antigens. When seminal plasma was subjected to size exclusion chromatography in the presence of PBS it became obvious that the antigen runs as a multimeric entity or an aggregate with a relative molecular weight of >200 KD (not shown). In order to reduce the possiblity of aggregation as a problem, the salt level in the elution buffer was increased to 0.5 M NaCl. This did not appreciably change the outcome (see fig. 21). Figure 21 also shows that the majority of seminal plasma proteins are in the <100 KD range. In data not shown, no change in the antigens relative molecular weight was detected when 1.0 M guandidine HCl, a strong denaturing chaotropic agent, was included in the elution buffer. Therefore, it is concluded that the molecular weight of the TURP-27 antigen under native and/or denatured conditions is in excess of 200 KD.

When the PBS soluble seminal plasma proteins were subjected to ion exchange chromatography, the TURP-27 activity was primarily in the void volume and 1.0 M NaCl elution peaks (fig. 22). The DEAE matrix utilized is a weak ion exchanger and non-retension could be a consequence of

the antigen having a positive net charge at neutral pH or poor interaction with the column because of complex formation. When the PBS insoluble material of seminal plasma was detergent solubilized and run on a DEAE column the results were similar. However, much more of the relative activity was in the 1.0 M NaCl wash peak (fig. 23). In order to more accurately determine the DEAE elution conditions for the TURP-27 antigen, a seminal plasma sample was run on an HPLC DEAE column and eluted with a linear salt gradient. The major antigen activity was eluted at 0.45 M NaCl. These results imply that the TURP-27, at near neutral pH, has a high net negative charge and indirectly confirms the acidic isoelectric point determined by two-dimensional gel analysis (fig. 6). When the high salt eluted material was subjected to size exclusion chromatography on an HPLC column, the TURP-27 activity primarily eluted with the >200 KD peak, again indicating large relative molecular size.

Because of the scarcity of tissue and the inefficient utilization of material in the bench top columns thus far described, an attempt was made to build a TURP-27 affinity column. The greatest success was in cross-linking MAb TURP-27 to Affi-gel Hz with approximately 77% of the antibody coupled to the matrix. From a panel of eluants it was determined that high salt, reduced pH and guanidine HCl were the most effective in disrupting the antigen-antibody interaction (table 6). High salt was used in the subsequent

column runs because of its mild, less denaturing treatment of the antigen.

When the PBS soluble fraction of a BPH membrane extract was run on the TURP-27 Affi-gel HZ column sucessful binding and release of the antigen was acheived (fig. 28). What should be noted is that substantial activity was present in the void volume. This may be due to overloading the capacity of the column. However, part of this activity was because proteins reactive with the secondary antibody. Note the high isotyped matched negative control antibody reactivity. This background activity could be due to endogenous human antibody, similar to results seen in some of the Western blots.

When a detergent solublilized BPH membrane extract was used to load the Affi-gel Hz TURP-27 column, the result was as expected for antibody affinity columns (fig. 27). Attempts to analyze the eluant by SDS-PAGE followed by Coomassie blue or silver staining failed; only blank lanes were apparent. This was because the sensitivity of these techniques was too low to detect the small quantities of antigen eluted. However, when the eluant was Western blotted, the characteristic bands of 180, 140, 120, and 90 KD protein species could be seen (not shown).

Epitope Characterization

Further evidence of a close link between the HNK-1 and TURP-27 epitopes was obtained by a reciprocal blocking assay (Table 1). TURP-27 does not effectively block HNK-1 activity since only 9.7% of the binding was blocked. In constrast, HNK-1 partially blocked TURP-27 activity (61.6%). Therefore, MAb HNK-1 (IgM, ~950 KD) may be able to partially block the TURP-27 epitope by masking it through steric hindrance. By comparison, MAb TURP-27 (IgG_3, 160 KD) being a smaller molecule, is unable to block the HNK-1 epitope by steric hindrance. This evidence implied that the two epitopes were not the same but may be in close physical proximity on the same proteins.

It was known that the HNK-1 epitope was carbohydrate in nature, therefore a series of experiments was conducted to establish the biochemical nature of the TURP-27 epitope. By using a panel of lectins in a blocking assay it could be demonstrated that the MAb TURP-27 can be blocked by prior binding of sialic acid residues with lectin (fig. 9). All lectins failed to block MAb TURP-27 binding with the exception of wheat germ agglutinin (WGA). WGA binds to N-acetyl-glucosamine and sialic acid residues while succinylated WGA binds only to N-acetyl-glucosamine. Because WGA was capable of blocking and s-WGA was not, it can be concluded that lectin binding to sialic acid residues blocked or masked the TURP-27 epitope. This was confirmed by

a competition assay in which free mono- and disaccharides were used to compete for MAb TURP-27 binding (fig. 10). Only sialic acid was effective in competing for MAb TURP-27 binding activity.

A more direct analysis of the TURP-27 epitope was achieved by enzymatic and chemical modification of the antigen followed by monitoring epitope destruction with MAb TURP-27. Figure 11 shows that acetic acid and neuraminidase reduce antibody binding to 5.0%, strongly implying a sialic acid residue component to the epitope (47,48). Mixed glycosidases and periodate treatment also diminished antibody binding, suggesting a carbohydrate structure was important to the epitope (48). Heat was not destructive implying that a native protein conformation was not important to epitope integrity. However, pronase treatment did reduce antibody binding. This suggested that the epitope integrity may depend on structures adjacent to the carbohydrate structure, which were not affected by heat denaturation, but were altered by enzymatic degradation.

The TURP-27 epitope, therefore, was shown to be carbohydrate or carbohydrate dependent with a strong dependency on the integrity of sialic acid residues. This epitope is apparently a modification of multiple protein antigens within prostate and brain. The absolute need for the epitope to contain sialic acid is shown in figure 12. When BPH membrane extracts were treated with neuraminidase and run on Western blot, complete disappearance of the

banding occurred. This was not due to the incubation conditions, because a mock treatment lane contained all the bands seen in the control lane (see fig. 12, lane 2,3).

Although the co-expression of the TURP-27 and HNK-1 reactivity appeared tightly linked in the extracts examined, chemical data as well as tissue distribution of the antigens implied that the HNK-1 and TURP-27 epitopes are not the same. The HNK-1 epitope, at least as carried by glycolipids, has been shown to be a sulfated glucuronic acid residue (27,28). Enzymatic or chemical desialylation removed 90% of MAb TURP-27 reactivity, while MAb HNK-1 reactivity was enhanced approximately 25% (table 2). Regardless of the tissue extract used, TURP-27 reactivity was always destroyed by desialylation; however, enhancement of HNK-1 reactivity varied from very little to as much as two fold (data not shown). Desulfation, which eliminates HNK-1 reactivity in glycolipids, was essentially without effect on glycoproteins under our assay conditions. Conditions were too mild. In fact, if the reaction was allowed to proceed for longer than 5 hrs, effective de-sialylation began to occur; i.e., loss of TURP-27 reactivity and enhancement of HNK-1 reactivity (data not shown). It appears that this chemical treatment was either ineffective against carbohydrates supported by protein or that the HNK-1 epitope found on glycoproteins is not dependent on a sulfate group. The presence of sulfate within the HNK-1 epitope supported by protein has only been speculated and not conclusively determined (68). Thus, it

can be summarized that the TURP-27 epitope is dependent on sialic acid integrity while MAb HNK-1 activity is enhanced by desialylation. However desulfation could not be demonstrated to effect either epitope.

TURP-27 Epitope Carriers

When TURP-27 and HNK-1 were compared by Western blot analysis, again a strikingly similar pattern of reactivity emerged (fig. 7,8,13,14 and 15). Both TURP-27 and HNK-1 revealed near identical immunoblots with several matching protein components in prostate, brain and peripheral nerve myelin. The multi-banding pattern displayed on HNK-1 immunoblots, although unique for prostate, was not unexpected and was not the result of proteolytic breakdown. Similar patterns have been demonstrated in a number of HNK-1 positive tissues, including brain and peripheral blood mononuclear cells (66,67,69). The unique feature of the HNK-1 epitope is that it appears to be involved in cell adhesion and is expressed on several adhesion related proteins (30,34,36). Because of the close co-expression of the TURP-27 and HNK-1 epitopes it would seem likely that TURP-27 may be carried on these same proteins.

A well characterized HNK-1 positive series of adhesion proteins are the N-CAMs (37). N-CAM isoforms of 180, 140 and 120 KD are expressed by cells of the central and peripheral nervous system, as well as other cells of neural crest

origin, NK cells (CD-56) and some tumors (70). These different N-CAM isoforms are derived from a single gene by alternative splicing (71), are believed to be developmentally regulated, and have a pivotal role in tissue morphogenesis, cell migration and cellular differentiation (37,72). When anti-N-CAM, MAb HNK-1 and MAb TURP-27 were compared by Western blot analysis for reactivity to brain extracts, the results indicated that TURP-27 may recognize an epitope expressed on N-CAM (Fig. 13). All three brain N-CAM isoforms were detected by anti-N-CAM, HNK-1 and TURP-27 (lanes 1,2 and 3). The conclusion that TURP-27 recognizes a N-CAM associated determinant is strengthened by the reactivity of MAb TURP-27 to purified N-CAM (Fig. 14, lane 3 and fig. 15 lane 1A), reacting to all three isoforms, similar to the pattern obtained with HNK-1 (Fig. 14, lane 6 and fig. 15, lane 1B).

The relationship between TURP-27, HNK-1 and N-CAMs also may account for some of the bands detected on Western blots of prostate tissue extracts. When eluant from the Affi-gel Hz TURP-27 column was tested by RIA with MAb TURP-27, MAb HNK-1 or anti-N-CAM, all three antibodies gave strong positive results (table 6). Also, when prostate extracts were immunoblotted with anti-N-CAM, bands of 180 and 140 KD were observed in the immunoblot of BPH extracts while the expression of these bands was variable in the CaP extracts (fig. 17). This evidence supports the conclusion that the prostate is expressing N-CAMs or N-CAM like proteins and

that some heterogeneity of expression occurs in the malignant prostate. Zuber et al. have reported that the 140 and 120 KD isoforms of N-CAM are expressed within the mesodermally derived blastemal and epidermal tumor elements of Wilms' tumors (73). They also reported a N-CAM isoform variation inherently expressed by Wilms' tumors of different histological types. Thus, tumors of non-neural crest origin can express N-CAM with isoforms that may vary between tumors.

A MAb UJ-13, which was developed by using fetal brain as the immunogen, was reported to bind some isoforms of N-CAM. In the initial report, UJ-13 was shown to react to neuroblastoma, astrocytoma, retinoblastoma and oat-cell cell lines and tissues of neuroectodermal origin (74). It was subsequently reported that MAb UJ-13 reacted to the small-cell lung carcinoma cluster-1 antigen which has been shown to be identical or closely related to the muscle isoforms of N-CAM, 125 and 145 KD (75). UJ-13 was used in Western blot to determine if prostate membrane extracts were positive for these N-CAM isoforms. Figure 14 (panel C) shows that a BPH extract was positive with UJ-13 yielding a 145 KD band. However, brain, pure adult brain N-CAM and MAG were negative. The 145 KD band is clearly not a protein that is stained by MAb TURP-27 or MAb HNK-1; it resolves to a distance between the 140 and 180 KD bands stained by these antibodies in panels A and B, respectively. In a second blot, peripheral nerve myelin, MAG, N-CAM, brain, normal

prostate, BPH and CaP were tested for UJ-13 reactivity (fig. 16). Only CaP and BPH stained, showing a 145 KD band (lanes 6 and 7 respectively). The Cluster-1 positive antibodies have been shown to detect antigens expressed on numerous neuroendocrine tumors. As expressed by cell lines, the Cluster-1 antigen has a molecular weight of 145 and 185 KD, the 145 KD species being predominate (76). The present data imply that an epitope is expressed on the 145 KD N-CAM protein that is not present on brain N-CAM of 180, 140 and 120 KD. This is most likely due to the alternative splicing which differentiates muscle and neural N-CAMs. Alternative exons not found in the brain N-CAMs are used to generate the 145 KD isoform (77). The original report describing UJ-13 reactivity counted normal prostate as a negative tissue. This is tentatively supported by the negative staining of normal prostate in figure 16. However, the data imply that BPH and CaP are positive for the 145 KD isoform of N-CAM or, at the least, for what is defined as the neuroendocrine tumor associated marker, Cluster-1 antigen.

Figure 14 (panel C) and figure 16 can also serve as a negative control for the MAb TURP-27 and MAb HNK-1 blots, figure 14 (panels A and B) and figure 17 (panels A and B), respectively. It should be noted that although blotting with MAb TURP-27 or MAb HNK-1 resulted in multiple banding within myelin, N-CAM, brain, prostate and prostate tumor extracts, when staining with a antibody of different specificity only one strong band was seen. The band seen in the UJ-13 blots

was of the expected molecular weight implying that at least this isoform of N-CAM is not subject to proteolytic degradation prior to blotting.

To extend our search for likely TURP-27 positive proteins we tested known HNK-1 positive proteins common to peripheral nerve, such as MAG and P_o. TURP-27 was found to be reactive to purified MAG in RIA (data not shown) and by an ELISA performed at the University of Heidelberg (personal communication, Dr. M. Schachner and Dr. B. Schmitz). TURP-27 was also found to react with purified MAG by Western blot analysis (fig. 14, lane 4 and fig. 15, lane 2A). The band detected by both TURP-27 and HNK-1 was approximately 90 KD. This band is most likely dMAG, and represents MAG that has lost a small fragment during purification (78). The 100 KD band appearing in the myelin preparations and detected by both antibodies (fig. 15, lanes 3,4), represents intact MAG. MAb Turp-27 also showed reactivity to the 28 KD P_o protein present in the two myelin preparations (fig. 3, lanes 3,4). The P_o protein is one of the most abundant proteins found in myelin. It carries the HNK-1 carbohydrate and is thought to be involved in myelin wrapping (79). Therefore, TURP-27 reacts to an antigenic determinant on both the glycoproteins MAG and P_o in a fashion similar to what has been reported for HNK-1 (30,31).

To test if MAG could be detected in prostate, the MAb B11F7 (gift of Dr R. Quarles) was used in Western blot (Fig. 18). The positive control tissues, peripheral nerve myelin

and brain, clearly showed a band of approximately 100 KD, lanes 2 and 9 respectively. Within the brain extract there appeared to be staining of a 90 KD band, presumably dMAG, as discussed above. All other tissues appeared to be negative for MAG or dMAG. All tissues except brain appear to have a band at approximately 50 KD. This band is unidentified and because MAb B11F7 has not previously been used in Western blot against non-myelin preparations, has not been previously reported. One of the normal prostate and the two CaP extracts appear to have the 55 KD band believed to be the endogenous antibody band. In summary, prostate appeared negative for MAG, however, a previously unidentified protein of 50 KD, present within prostate and breast carcinoma was detected. This 50 KD protein could be a degradation product of MAG or contain a cross-reactive epitope from MAG. MAb B11F7 detects a protein epitope within MAG, and MAG is a member of the N-CAM like sub-family of the immunoglobulin gene family (39). It is conceivable that the 50 KD protein is an unreported member of this family detected by B11F7.

Because MAb HNK-1 has been shown to detect two species of sulfated glycolipids, it was of interest to determine if MAb TURP-27 was reactive with glycolipids. Lipid preparations were made from peripheral nerve and brain, known sources of HNK-1 positive lipids, as well as a BPH tissue specimen. The preparations were made according to a method developed by Dr. G. Clark, Eastern Virginia Medical School (personal communication, unpublished results) and

yielded three fractions. When the fractions were tested in RIA with MAb TURP-27 and MAb HNK-1, only the upper layer organic of peripheral nerve and possibly the upper layer organic and aqueous fractions of BPH were positive for TURP-27 activity. The MAb HNK-1 appeared positive to several fractions within nervous tissue and prostate (table 3). When the preparations were resolved by thin layer chromatography and immuno-overlayed with MAb HNK-1 or MAb TURP-27, positive bands were visible (figs. 19 and 20). The expected doublet banding for a peripheral nerve immuno-overlayed with MAb HNK-1 is shown in figure 19 lane 6. The bands ran as expected and were sulfate-3-glucuronyl paragloboside and sulfate-3-glucuronyl neolactohexaosyl ceramide (27,28,29). It was clearly evident that BPH upper layer glycolipids yields two bands of the same relative mobility. These glycolipid species must be considered the same as those present in peripheral nerve and represent the only demonstration of this association to date. Also seen in the immuno-overlay was a banding in the upper areas of the plate well beyond the position of the standard M_1. These species are unidentified and may be an artifact since they have not been reported in the numerous studies conducted using this technique and the MAb HNK-1. The immuno-overlay using MAb TURP-27 was negative in the area of the sulfated ceramides, and the only bands visible were at the upper area of the overlay beyond the M_1 standard (fig. 20). The fact that MAb TURP-27 was negative for these glycolipids is not unexpected

because these glycolipid species do not contain a sialic acid residue (27,28,29). Sialic acid has been shown to be an integral part of the TURP-27 epitope (see above). However, the MAb TURP-27 was positive in the RIA (table 3) for upper layer glycolipids from PNS. This reactivity could not be documented in the immuno-overlay, except for staining above the M_1 standard. Again this staining could be due to unidentified glycolipids or artefacts. Clearly more work is necessary, but it is obvious that MAb HNK-1 positive lipids can be found in BPH.

In summary the data obtained in this study do not provide clear evidence as to whether the two epitopes are part of the same carbohydrate structure or are two independent structures. However, based on the tight link in co-expression, it seems likely that only one carbohydrate structure supports the expression of the two epitopes at least within glycoprotein antigens. It also seems likely that the TURP-27 epitope is a sialic acid modification of the HNK-1 positive carbohydrate. This conclusion is supported by the more limited expression of the TURP-27 epitope relative to the HNK-1 epitope (24,26) and could explain why the enhancement of HNK-1 binding was variable between tissues when sialic acid was removed. Additional support for this hypothesis derives from the evidence that the protein P_o has only one glycosylation site (80) and that both TURP-27 and HNK-1 bind P_o (fig. 3, lanes 3,4). Therefore, because the two MAbs bind P_o, the epitopes must

be positioned on the same carbohydrate structure or are mutually exclusive in expression by this oligosaccharide.

It has been reported that HNK-1 reactivity to glycoproteins is linked to multi-antennary oligosaccharides (68,81). Burger et al. reported that the HNK-1 reactive epitope on P_o is supported by tri- and tetraantennary oligosaccharides of approximately 12 sugar units. These structures may allow for simultaneous or independent expression of sialic acid and/or sulfate moieties at their termini. It has been shown that brain proteoglycans express multi-antennary oligosaccharides containing terminal sulfate and sialic acid moieties simultaneously (82). A subset of brain proteoglycans are HNK-1 positive and appear on Western blots as a smear in the >200 KD range (83). Figure 2 shows that both TURP-27 and HNK-1 reveal a positive signal in this molecular weight range for Western blot analysis of brain extracts. Thus the TURP-27/HNK-1 antigenic structure may be a tri- or tetraantennary oligosaccharide with TURP-27 and HNK-1 positive termini.

We conclude that the TURP-27 epitope may be a sialic acid modification of the HNK-1 positive oligosaccharide and is expressed on at least some N-CAM, MAG and P_o glycoproteins. We were able to also demonstrate that immunoreactivity for N-CAM or N-CAM like proteins is expressed in both benign prostatic hyperplasia and carcinoma of the prostate. More work will be required to identify the proteins carrying the anti-N-CAM activity and to determine

the nature of the carriers for the TURP-27 and HNK-1 epitopes. Provided the HNK-1 oligosaccharide is only associated with adhesion proteins (30), it is possible that adhesion proteins other than N-CAMs are being detected in prostate. If proteins involved in cell adhesion events are altered in their expression or functional capacity during prostate carcinogenesis, it would be significant in our understanding of the natural history of prostatic malignancies and may lead to improved diagnosis of the aggressive tumor phenotype. For example, perineural invasion and growth along the nerve fiber is a means of prostate capsular penetration in a large percentage of prostate carcinomas (38). In view of the data presented in this study, nerve involvement in BPH and CaP may represent an aberrant adhesion event, representing more than just passive egress along planes of least resistance as has been suggested.

Another intriguing observation is that the neuroendocrine tumor-associated Cluster-1 antigen detected by MAb UJ-13, among others, can be detected in BPH and CaP membrane extracts by Western blot. As described in the Introduction section of this thesis, several observations imply that prostate epithelial cells are capable of neuroendocrine differentiation and that this alternative path may be enhanced during tumor progression (16). The staining seen with MAb UJ-13 within BPH and CaP but not

normal prostate may be indicative of enhanced neuroendocrine marker expression in prostate tumors.

This observation is at the heart of a semantic confusion that exists when discussing neuroendocrine cell differentiation. Although stains conducted with antibodies to traditional neuroendocrine markers such as neuron specific enolase, chromogranin A, calcitonin or bombesin, are positive with prostate, the number of cells positive are low and variable. However, antibodies to cell surface markers such as UJ-13 and HNK-1 are positive to much greater number of cells, which both have the traditional neuroendocrine phenotype as well as either differentiated or undifferentiated epithelial cell phenotypes. The most plausible explanation for this dichotomy is that there is a continuum of cell differentiation phenotypes and that within prostate and perhaps other epithelial tissues with partial neuroendocrine character two or more end point cells exist arising from a omnipotential stem cell. The observation that prostate epithelia take on the expression of neuroendocrine cell surface markers without the full expression of neuroendocrine enzymes may be explained by this hypothesis. If markers such as UJ-13, HNK-1 and possibly TURP-27 are expressed transiently by cells on their differentiation pathway to mature fully differentiated epithelial or neuroendocrine cells, then the detection of these antigens on the cell surface may mark cells at a less than fully differentiated point. This cell population may become the

predominant cell population in the rapidly growing tumor and may reflect a proliferative state similar to that occuring during tissue morphogenesis. It is striking that all three antibodies detect isoforms of N-CAM. N-CAMs are becoming well recognized for their roles in tissue morphogenesis, cell migration and cellular differentiation (37,72). The data discussed showed that this family of cell adhesion molecules is expressed by BPH and CaP. One could postulate that these antigens are harbingers of altered states of cellular and tissue arrangement. Recognition and understanding of this phenomena could be important in diagnosing the aggressive potential of a tumor by having a finer scale on which to compare individual tumors through the use of a panel of differentiation markers.

References

1. National Center for Health Statistics: "Vital and Health Statisics." Series 13, No. 96. 1986 Annual Summary. Public Health Service, 1988. DHHS Pub. No. (PHS) 88-1757.

2. Carter, H.B., and D.S. Coffey. The prostate: an increasing medical problem. Prostate, 16:39-48, 1990.

3. Ca-A Cancer Journal for Clinicians. 40:9-26, 1990.

4. Division of Cancer Prevention and Control: "1987 Annual Cancer Statistics Review." National Cancer Institue, 1988. NIH pub. No. 88-2789.

5. Carter,H.S. and Coffey, D.S., Prostate Cancer: The Magnitude of the Problem in the United States. In: A Multidisciplinary Analysis of Controversies in the Managment of Prostate Cancer. Ed. by J.P. Karr. New York: Plenum Press, 1-7, 1988.

6. Carter, B.S., Carter, H.S., and Issacs, J.T., Epidemiologic evidence regarding predisposing factors to prostate cancer. Prostate 16:187-197, 1990.

7. Carter H.S., Piantadosi, S., and Isaccs, J.T., Clinical evidence for and implications of the multistepdevelopment of prstate cancer. J. Urol. 143:742-746, 1990.

8. Drago, J.R., CA-A Cancer Journal for Clinicians. 39(6) :326-336, 1990.

9. Chodak, G.W. Screening for prostate cancer. Role of ultrasound. "Advances in Urologic Ultrasound". Urol Clin. of N.A., 16:657-662. 1989.

10. Abrahmsson, P.A., and Wadstrom, L.B. Peptide-hormone- and sertonin-immunoreactive cells in normal and hyperplastic prostate glands. Path. Res. Pract. 181:675-683, 1986.

11. DiSant'Agnese, P.A., and DeMesyJensen, K.L. Neuroendocrine differentiation in prostate carcinoma. Human Path. 18:849-856, 1987.

12. Bonkhoff, H., Wernert, N., Dhom, G., and Remberger, K. Relationship of endocrine-paracrine cells to cell

proliferation in normal, hyperplastic, and neoplastic human prostate. Prostate 19:91-98, 1991.

13. Feyter, F. Z. Uber das urogenitale helle-zellen-system des menschen. Mikrosk. Anat. Forsch. 57:324-326, 1951.

14. Pearse, G.B. Neuroendocrine cell. PNAS. 170:71-80, 1968.

15. Johnson, D.E. and Georgieff, M.K. Pulmonary neuroendocrine cells. Their secretory products and their potential roles in health and chronic lung disease in infancy. Am. Rev. Respir. Dis. 140:1807-1812, 1989.

16. Abrahamsson, P.A., Falkmer, S., Falt, K., Grimelius, L. The course of neuroendocrine differentiation in prostatic carcinoma. An immunohistochemical study testing chromagranin A as an "endocrine marker". Path. Res. Pract. 185:373-380, 1989.

17. Azumi, N., Shibuya, H., Ishibura, M. Primary prostatic carcinoid tumor with intracytoplasmic prostatic acid phosphatase and prostate-specific antigen. Am. J. Surg. Path. 8:545-550, 1984.

18. LeDoriarin, N.M. On the origin of pancreatic endocrine cells. Cell 53:169-171, 1988.

19. DeLellis, R.A., Tischler, A.S., Wolfe, H.J. J. Multidirectional differentiation in neuroendocrine neoplasias. Histochem. Cytochem. 32:899-904, 1984.

20. Stratton, M. Evans, D.J. Lampert, I.A. Prostatic adenocarcinoma evolving into carcinoid: selective effect of hormonal treatment. J. Clin. Path. 39:750-756, 1986.

21. Abo, T., and C.M. Blach. A differentiation antigen of human NK and K cells identified by a monoclonal antibody (HNK-1). J. Immunol., 127:1024-1029, 1981.

22. Lipinski, M., Braham, K., Caillaud, J. Carlu, C., Tursz, T. HNK-1 antibody detects an antigen expressed on neuroendocrine cells. J. Exp. Med. 158:1775-1780, 1983.

23. Caillaud, J., Benjelloun, S. Bosg, J., Braham, K., Lipinski, M. HNK-1-defined antigen detected in paraffin-embedded neuroectoderm tumors and those derived from cells of the amine precusor uptake and decarboxylation system. Cancer Research 44:4432-4439, 1984.

24. Wahab, Z.A., and G.L. Wright, Jr. Monoclonal antibody (anti-Leu-7) directed against natural killer cells reacts with normal, benign and malignant prostate tissues.Int. J. Cancer., 36:677-683, 1985.

25. Starling, J.J., Sieg, S.M., Beckett, M.L., Wirth, P.R.,Wahab, Z.A., Schellhammer, P.F., Ladaga, L.E., Poleskic, S., and G.L. Wright, Jr. Human prostate tissue antigens defined by murine monoclonal antibodies. Cancer Res., 46:367-374, 1986.

26. Wright, G.L., Jr., Beckett, M.L., Lipford, G.B., Haley, C.L., and P.F. Schellhammer. A novel prostate carcinoma-associated glycoprotein complex (PAC) recognized by monoclonal antibody TURP-27. Int. J. Cancer., 47:717-725, 1991.

27. Chou, D.K.H., Ilyas, A.A., Evans, J.E., Quarles, R.H., and F.B. Jungalwala. Structure of a glycolipid reacting with monoclonal IgM in neuropathy and HNK-1. Biochem. Biophys. Res. Commun., 128:383-388, 1985.

28. Chou, D.K.H., Ilyas, A.A., Evans, J.E., Costello, C., Quarles, R.H., and F.B. Jungalwala. Structure of sulfated glucoronyl glycolipids in the nervous system reacting with HNK-1 antibody and some IgM paraproteins in neuropathy. J. Biol. Chem., 261:11717-11725, 1986.27.Chou, D.K.H., Ilyas, A.A., Evans, J.E., Quarles, R.H., and F.B. Jungalwala. Biochem. Biophys. Res. Commun., 128:383-388, 1985.

29. Ilyas, A.A., Dalakas, M.C., Brady, R.O., and Quarles, R.H. Sulfated glucoronyl glycolipids reacting with anti-myelin-associated glycoprotein monoclonal antibodies including IgM paraproteins in neuropathy: species distribution and partial characterization of epitopes. Brain Res., 385: 1-9, 1986.

30. Kruse, J., Mailhammer, R., Wernecke, H., Faissner,A., Sommer, I., Gordis, C., and M. Schachner. Neural cell adhesion molecules and myelin-associated glycoprotein share a common carbohydrate moiety recognized by monoclonal antibodies L2 and HNK-1. Nature, 311:153-155, 1984.

31. Bollensen, E., and M. Schachner. The peripheral myelin glycoprotein P_o expresses the HNK-1 and L3 carbohydrate structure shared by neural adhesion molecules. Neuroscience Letters, 82:77-82, 1987.

32. Grumet, M., Hoffman, S., Crossin, K.L., and G.M. Edelman. Cytotactin, an extracellular matrix protein of neural and non-neural tissues that mediates glia-neuron interaction. Proc. Nat. Acad. Sci. USA, 82:8075-8079, 1985.

33. Riopelle, R.J., McGarry, R.C., and J.C. Roder. Adhesion properties of a neuronal epitope recognized by the monoclonal antibody HNK-1. Brain Res., 367:20-25, 1986.

34. Keilhauer, G., Faissner, A., and M. Schachner. Differential inhibition of neurone-neurone, neurone-astrocyte and astrocyte-astrocyte adhesion by L1, L2 and N-CAM antibodies. Nature, 316:728-730, 1985.

35. Künemund, V., Jungalwala, F.B., Fischer, G., Chou, D.K.H., Keilhauer, G., and M. Schachner. The L2/HNK-1 carbohydrate of neural cell adhesion molecules is involved in cell interactions. J. Cell Biol., 106:213-223, 1988.

36. Kruse, J., Keilhauer, G., Faissner, A., Timpl, R., and M. Schachner. The J1 glycoprotein a novel nervous system cell adhesion molecule of the L2/HNK-1 family. Nature, 316:146-148, 1985.

37. Edelman, G. Cell adhesion molecules in the regulation of animal form and tissue pattern. Annual Review of Biochemistry, 54:135-169, 1985.

38. Villers, A., McNeal, J.E., Redwine, E.A., Freiha, F.S., and T.S Stamey. The role of perineural space invasion in the local spread of prostatic carcinoma. J. Urol., 142:763-768, 1989.

39. Dobersen, M.J., Hammer, J.A., Noronha, A.B., MacIntosh, T.D., Trapp, B.O., Brady, R.O., and Quarles, R.H. Generation and characterization of mouse monoclonal antibodies to the myelin-associated glycoprotein (MAG). Neurochem. Res., 10:423-428, 1985.

40. Greenwood, F.C., Hunter, W.M., and Glover, J.S. The preparation of 131-I-labelled human growth hormone of high specific radioactivity. Biochem. J. 89:114-123, 1963.

41. Lee, D.S.C., and Griffiths, B.W. Comparative studies of iodo-bead and chloramine-T methods for the radioiodination of human alpha-fetoprotein. J. Immunol. Methods, 74:181-189, 1984.

42. Lipford, G.B., Feng, Q., and G.L. Wright, Jr. A method for separating bound versus unbound label during radioiodination. Anal. Biochem., 187:133-135, 1990.

43. Laemmli, U.K. Cleavage of structural proteins during the assembly of the head of bacteriophage T4. Nature, 227:680-685, 1970.

44. Morrissey, J.H. Silver stain for proteins in polyacrylamide gels: A modified procedure with enhanced uniform sensitivity. Anal. Biochem. 117:307-310, 1981.

45. Towbin, H., Staehelin, T., and J. Gordon. Electrophoretic transfer of proteins from polyacrylamide gels to nitrocellulose sheets: procedure and some applications. Proc. Nat. Acd. Sci. USA, 76:4350-4354, 1979.

46. Mangnani, J.L., Spitalnik, S.L. and Ginsburg, V. Antibodies against cell surface carbohydrates. In: Ginsburg (ed.), Methods in enzymology, Vol. 138, Complex carbohydrates, Part E. pp. 195-207, Academic Press, Orlando, FL, 1987.

47. Varki, A., and S. Diaz. The release and purification of sialic acid from glycoconjugates: method to minimize the loss and migration of O-acetyl groups. Anal. Biochem., 137:236-247, 1984.

48. Waibel, R., O'Hara, C.J., and R.A. Stahel. Characterization of an epithelial and tumor-associated human small cell lung carcinoma glycoprotein. Cancer Res., 47:3766-3770, 1987.

49. Wasman, L. Calcium activated proteases in mammalian tissues. In: V. Ginsburg (ed) Methods in enzymology, Vol. 80, pp. 664-680, Academic Press, Orlando, FL, 1987.

50. Starling, J.J., Sieg, S.M., Beckett, M.L., Schellhammer, P.F., Ladaga, L.E., and G.L. Wright, Jr. Monoclonal antibodies to human prostate and bladder tumor-associated antigens. Cancer Res., 42:3084-3089, 1982.

51. Svennerholm, L. and Fredman, P. Biochim. A procedure for the quantitative isolation of brain gangliosides. Biophys. Acta. 617:97-109, 1980.

52. Williams, M.A., and McCluer, R.H. The use fo sep-pak C18 cartridges during the isolation of gangliosides. J. Neurochem. 35:266-269, 1980.

53. Ilyas, A.A., Chou, D.K.H., Jungawala, F.B., Costello, C., and Quarles, R.H. Variability in the structural requirements for binding of human monoclonal anti-MAG IgM antibodies and HNK-1 to sphingoglycolipid antigens. J. Neurcohem 45:204-210, 1990

54. Hjelmeland, L.M., and Charmbach, A. "Membrane, Detergents and Recptor Solubilization". Receptor Biochemistry and Methodology. Vol. 1:35-46. Eds. J.C. Venter and L.C. Harrison. Alan R. Liss, Inc. New York. 1983.

55. Wright, G.L., Jr., Huang, C.L., Lipford, G., Beckett, M.L., Liang, H.M., Haley, C., Newhall, K., and Morningstar, M.Generation and characterization of

monoclonal antibodies to prostate secretory protein. Int. J. Cancer, 46:39-49, 1990.

56. Dubé, J.Y., Frenette, G., Panquin, R., Chapdelaine, P., Trembaly, R.R., Lazure, C., Seidah, N., and Chrétien, M. Isolation from human seminal plasma an abundant 16-kd protein originating from the prostate, it's identification with a 94-residue peptide originally described as beta-inhibin. J. Androl. 8:182-189, 1987.

57. Wahab, Z., Wright, Jr., G.L. Monoclonal antibody against natural killer cells reacts with normal,benign, and malignant prostate tissues. Fifth annual Seminar of Cancer Research in Virginia. March, 1985.

58. Waibel, R., O'Hara, C.L. and Stahel, R.A. Characterization of an epithelial and tumor-associated human small cell lung carcinoma glycoprotein. Cancer Res., 47:3766-3770, 1987.

59. Patel, K., Rossell, R.J., Pemberton, L.F., Cheung, N-K.V., Walsh, F.S., Moore, S.E., Sugimoto, T., and Kempshead, J.T. Monoclonal antibody 3F8 recognizes the neural cell adhesion molecule (NCAM) in addition to the ganglioside GD2. Brit. J. Cancer. 60:861-866, 1989.

60. Beckett, M.L., Lipford, G.B., Haley, C., Newhall, K, Schellhammer, P.L. and Wright, Jr, G.L. Monoclonal antibody PD41 recognizes an antigen restricted to prostate adenocarcinomas. Cancer Res. 51:2296-2301, 1991.

61. Feng, Q., Wright, G.L., Jr., Lipford, G.B., Beckett, M.L., Lopes, D., and Gillman, S.C. Characterization of a new prostate carcinoma-associated marker: 7E11-C5. Tenth Annual Seminar of Cancer Researchers in Virginia, Blacksburg, Va, March 17, 1990.

62. Wright, Jr., G.L., Feng, Q., Lipford, G.B., Lopes, D., and Gillman, S.C. Charaterization of a new prostate carcinoma-associated marker: 7E11-C5. Fifth International Conference on Monoclonal Antibody Immunoconjugates for Cancer, San Diego, March 16, 1990.

63. Wright, G.L., Jr., Wilson, E., Klinger, M., Roland, W., Beckett, M.L., and Daddona, P.E. Radiolocalization of human prostate tumor in a mouse subrenal capsule model by monoclonal antibody TURP-27. Prostate 16:81-89, 1990.

64. Burchell, J., Durbin, H. and Taylor-Papadimitriou, J. Complexity of expression of the antigenic determinants recognized by monoclonal antibodies HMFG-1 and HMFG-2 in normal and malignant human mammary epithelial cells. J. Immunol. 131:508-513, (1983).

65. Spiro, R.C., Casteel, H.E., Luafer, D.M., Reisfeld, R.A. and Harper, J.R. Post-Translational addition of chondroitin sulfate glycosaminoglycans. Role of N-linked oligosaccharide addition, trimming, and processing. J. Biol. Chem. 264:1779-1786, (1989).

66. Arai, M., Nishizawa, M., Inuzuka, T., Tanaka, M., Baba, H., Sato, S., and T. Miyatake. Murine monoclonal antibodies to the myelin-associated glycoprotein (MAG) recognize Leu-7 reactive molecules on human mononuclear cells. J. Immunol., 138:3259-3263, 1987.

67. Noronha, A.B, Ilyas, A., Antonicek, H., Schachner, M. and R.H. Quarles. Molecular specificity of L2 monoclonal antibodies that bind to carbohydrate determinants of neural cell adhesion molecules and their resemblance to other monoclonal antibodies recognizing the myelin-associated glycoprotein. Brain Res., 385:237-244, 1986.

68. Shashoua, V.E., Daniel, P.F., Moore, M.E., and F.B. Jungalwala. Demonstration of glucoronic acid on brain glycoproteins which react with HNK-1 antibody. Biochem. Biophys. Res. Comm., 138:902-909, 1986.

69. O'Shannessy, D.J., Wilson, H.J., Inuzuka, T., Dobersen, M.J, and R.H. Quarles. The species distribution of nervous system antigens that react with anti-myelin-associated glycoprotein antibodies. J. Neuroimmuno., 9:255-268, 1985.

70. Brackenbury, R. Expression of neural cell adhesion molecules in normal and pathologic tissues. Ann. N.Y. Acad. Sci., 540:39-46, 1988.

71. Cunningham, B.A., Hemperly, J.J., Murray, B.A., Prediger, E.A., Brackenbury, R., and G.M. Edelman. Neural cell adhesion molecule: structure, immunoglobulin-like domains, cell surface modulation and alternative RNA splicing. Science, 236:799-806, 1987.

72. Crossin, K.L. Cell and substrate adhesion molecules in embryonic and neural development. Clin. Chem., 35:738-747, 1989.

73. Zuber, C., and J. Roth. The relationship of polysialic acid and the neural cell adhesion molecule N-CAM in Wlims tumor and their subcellular distributions. Eur. J. Cell Biol., 51:313-321, 1990.

74. Allan, P.M., Garson, J.A., Harper, E.I., Asser, U., Coakham, H.B., Brownell, B., and J.T. Kempshead. Biological characterization and clinical applications of a monoclonal antibody recognizing an antigen restricted

to neuroendocrine tissues. Int. J. Cancer, 31:591-598, 1983.

75. Patel, K., Moore, S.E., Dickerson, G., Rossell, R.J., Beverley, P.C., Kempshead, J.T., and F.S. Walsh. Neural cell Adhesion Molecule (N-CAM) is the antigen recognized by monoclonal antibodies of the similar specificity in small-cell lung carcinoma and neuroblastoma. Int. J. Cancer, 44:573-578, 1988.

76. Moolenaar, C.E.C.K., Muller, E.J., Schol, D.J., Figdor, C.G., Bock, E., Bitter-Suermann, D., and R.J.A.M. Milchalides. Expression of neural cell adhesion molecule-related sialoglycoprotein in small cell lung cancer and neuroblastoma cell lines H69 and CHP-212. Cancer Res., 50:1102-1106, 1990.

77. Gower, H.J., Barton, C.H., Elsom, V.L., Thompson, J., Moore, S.E., Dickson, G., and F.S. Walsh. Alternative splicing generates a secreted form of N-CAM in muscle and brain. Cell, 55:955-964, 1988.

78. Sato, S., Quarles, R.H., and R.O. Brady. Susceptibility of the myelin-associated glycoprotein and basic protein to a neural protease in highly purified myelin from human and rat brain. J. Neurochem., 39:97-105, 1982.

79. Filbin, M.T., and Tennekoon, G.I. The role of complex carbohydrates in adhesion of the myelin protein, P_o. Neuron 7:845-855, 1991

80. Lemke, G., and R. Axel. Isolation and sequence of a cDNA encoding the major structural protein of peripheral myelin. Cell., 40:501-508, 1985.

81. Burger D., Simon, M., Perruisseau, G., and A.J. Steck. The epitope(s) recognized by HNK-1 antibody and IgM paraproteins in neuropathy is present on several N-linked oligosaccharide structures on human P_o and myelin-associated glycoprotein. J. Neurochem., 54:1569-1575, 1990.

82. Krusius, T., Reinhold, V.N., Margolis, R.K., and R.U. Margolis. Structural studies on sialylated and sulfated O-glycosidic mannose-linked oligosaccharides in the chondroitin sulfate proteoglycan of brain. Biochem. J., 245:229-234, 1987.

83. Gowda, D.C., Margolis, R.U., and R.K. Margolis. Presence of the HNK-1 epitope on poly(N-acetyllactosaminyl) oligosaccharides and identification of multiple core proteins in the chondroitin sulfate proteoglycans of brain. Biochem., 28:4468-4474, 1989.